GEOGRAPHIC VARIATION IN SKULL MORPHOLOGY OF THE BONE CRACKING HYENAS, *CROCUTA CROCUTA* AND *HYAENA HYAENA*

By

Cybil Nicole Cavalieri

A DISSERTATION

Submitted to
Michigan State University
in partial fulfillment of the requirements
for the degree of

Zoology-Doctor of Philosophy
Ecology, Evolutionary Biology, and Behavior-Dual Major

2021

ABSTRACT

GEOGRAPHIC VARIATION IN SKULL MORPHOLOGY OF THE BONE CRACKING HYENAS, *CROCUTA CROCUTA* AND *HYAENA HYAENA*

By

Cybil Nicole Cavalieri

My dissertation focuses on identifying geographic patterns in the size and shape of spotted hyena and striped hyena skulls and determining if bioclimatic and social variables explain observed patterns. Within the subsequent chapters of this dissertation I investigate geographic variation in spotted hyena and striped hyena skulls using geometric morphometrics and spatial statistics.

In chapter one, I examined the relationship between bioclimatic factors, social factors, and spotted hyena skull size to better understand the forces that might underlie geographic patterns of size. Spotted hyenas exhibit slight female-biased sexual size dimorphism. Skull size co-varies with temperature, precipitation, and landcover but more strongly co-varies with population density. The highest densities are associated with the smallest skull size, possibly reflecting a relationship between high population density and access to resources. These findings support the idea that the underlying driver of geographical and ecological rules is access to resources, providing further empirical evidence for the energetic equivalence rule.

In chapter two, I investigated the influence of climatic variables and food resources on observed geographic patterns in striped hyenas. Striped hyenas exhibit slight male-biased sexual size dimorphism. There is a strong geographic pattern of size variation in striped hyena skulls with larger individuals found at higher latitudes, as predicted by Bergmann's rule. I found

evidence that seasonal climatic variables are better predictors of hyena skull size than annual climatic variables. We did not find evidence to support our prediction that striped hyenas would be larger in areas with higher net primary productivity or increased access to human-provided foods. These findings support the notion that geographic variation in body size is primarily driven by seasonal climatic variables, which is consistent with the seasonality hypothesis.

In chapter three, I investigated whether striped hyena skull shape is sexually dimorphic and whether the geographic pattern of skull shape variation supports the historic delineation of subspecies proposed by Pocock (1934). I found no evidence for sexual shape dimorphism in the skull of striped hyenas. While we found considerable morphological overlap between historic subspecies, some parts of morphological shape space were occupied by a single subspecies, suggesting that striped hyenas vary in morphology across geography, but that historic subspecies are not effectively capturing this variation.

ACKNOWLEDGMENTS

This work would not have been possible without the support, love, and mentorship of many people. I would particularly like to thank Vince Cavalieri who supported me in countless ways during this dissertation, including assisting in data collection, editing manuscripts and providing emotional support. I would like to thank Barbara Lundrigan for this opportunity and for all her support throughout my doctoral research, especially given the challenges of the pandemic. I would like to thank Dustin Lynch, Ani Hristova, Connie Rojas, Courtney Larson, Rachel Osborn, Robert Mobley, and Laura Abraczinskas, without their encouragement and wisdom, this dissertation would not have been completed.

I would like to thank the following undergraduate assistance for their help in digitizing and organizing the data for this project E. Gauci, K. Heffernan, C. Hughes, K. John, K. Markiewicz, A. Richardson, N. VanAcker, K. Fenner, D. Fortin, A. Lazzari, E. Oja, L. Podolski, M. Schlis, D. C. Druskins, M. Watson, S. Hule, A. Langfeldt, E. Marquardt, A. O'Toole, M. Ratzenberger, C. A. Winters, E. Zimmer, S. Kelley, and S. L. Lamb. I particularly want to thank Tony Beals, Jackie Heikkila, Rebekka Winklepleck, and Delany Morris for their work on this project. It was an honor to be your mentor and to see you progress in your own careers and lives.

I would like to thank my other committee members Kay Holekamp, Feng Wei and Miriam Zelditch who generously offered me their support and expertise during my doctoral program. I would like to thank Robin Bolig, Kasey Wilson, Ashton Shortridge, Andrew Dennhardt, Pat Bills, Teresa McElhinny, Matthew Rupp, Tim Schmidt, Jory Schossau, Arend

Hintze, Andrea Taylor Morrow, Taylor Rupp, and Lauren Koenig for their assistance, guidance and insight.

I would like to thank the curators and collection managers at the Michigan State University Museum, Tel Aviv University Zoological Museum, British Natural History Museum, University, Museum of Zoology Cambridge, The Odontological Collection The Royal College of Surgeons, Oklahoma State University Collection of Vertebrates, the Smithsonian Museum of Natural History, The Field Museum of Natural History, and the National Museums of Kenya for facilitating the use of their collections.

Funding for this dissertation and my professional development came from the Department of Integrative Biology, Ecology, Evolutionary Biology, and Behavior Program, and BEACON. Specific funding sources that made this work possible are Research Enhancement Award, Michigan State University Graduate School, Natural Science Collections 2019 Summer Intern Stipend, Michigan State University Enrichment Fellowship (UEF), Joseph G. Schotthoefer Memorial Student Award, John R. Shaver Research Fellowships for Graduate Students in the Department of Integrative Biology, Travel fellowship, Department of Integrative Biology, Conference award, Council of Graduate Students, Travel fellowship, Ecology, Evolutionary Biology and Behavior Program, Travel fellowship, BEACON, Travel fellowship, International studies and programs and NSF grants IBN0113170 & IOB0618022(to KEH and BLL).

For all this, I am appreciative and grateful.

TABLE OF CONTENTS

LIST OF TABLES viii

LIST OF FIGURES xi

Introduction 1
WORKS CITED 8

Chapter 1: Geographic variation in spotted hyena skull size; empirical evidence for the energetic equivalence rule 14
ABSTRACT 14
1 | INTRODUCTION 15
2 | MATERIALS AND METHODS 21
2.1 | Specimens 21
2.2 | Morphological Data 21
2.3 | Bioclimatic Variables 22
2.4 | Hyena Density Data 23
2.5 | Statistical Analysis 23
3 | RESULTS 26
3.1 | Sexual Dimorphism 26
3.2 | Geography 26
3.3 | Bioclimatic variables 27
3.4 | Hyena Density 28
4 | DISCUSSION (overview) 29
4.1 | Sexual Dimorphism 29
4.2 | Geography and Bioclimatic factors 31
4.3 | Hyena density 33
APPENDICES 36
APPENDIX A FIGURES AND TABLES 37
APPENDIX B SPECIMENS LIST 47
APPENDIX C LANDMARK DEFINITIONS 73
WORKS CITED 77

Chapter 2: Geographic variation in striped hyena skull size supports Bergmann's rule and the seasonality hypothesis 87
ABSTRACT 87
1 | INTRODUCTION 88
2 | MATERIALS AND METHODS 94
2.1 | Specimens 94
2.2 | Morphological Data 94
2.3 | Climatic Variables 95
2.4 | Resource Variables 96
2.5 | Statistical Analysis 97
3 | RESULTS 100
3.1| Model performance 100

3. 2| Sexual dimorphism 100
3.3| Geographic variables 100
3.4| Climatic variables 101
3.5| Resource variables 101
4| DISCUSSION 102
4.1| Geographic pattern 102
4.2| Sexual Dimorphism 103
4.3| Climatic variables 104
4.4| Resource availability 107
APPENDICES 109
APPENDIX A FIGURES AND TABLES 110
APPENDIX B SPECIMENS LIST 121
APPENDIX C LANDMARK DEFINITIONS 126
WORKS CITED 130

Chapter 3: Cranial shape variation among proposed subspecies of the striped hyena, *Hyaena hyaena* 139
ABSTRACT 139
1| INTRODUCTION 140
2 | MATERIALS AND METHODS 145
2.1 | Specimens 145
2.2 | Morphological Data 145
2.3 | Subspecies Designation 146
2.4 | Statistical Analysis 147
3 | RESULTS 149
3.1 | Sexual Dimorphism 149
3.2 | Procrustes ANOVA 149
3.3 | Allometry 150
3.4 | Principal Components Analysis 151
3.5 | Cross validation and overall classification accuracy 152
4 | DISCUSSION 154
4.1 | Sexual Dimorphism 154
4.2 | Allometry and Subspecies designation 155
4.3 | Reiger's hunting hypothesis 157
APPENDICES 160
APPENDIX A FIGURES AND TABLES 161
APPENDIX B SPECIMENS LIST 173
APPENDIX C LANDMARK DEFINITIONS 185
WORKS CITED 189

LIST OF TABLES

Table 1.1: Locality, country, population density estimate (hyenas/ km2), years(s) of study, and source for spotted hyena (*Crocuta crocuta*) densities used in this analysis (see Fig 3 for map). NP = National Park; GR = Game Reserve. 41

Table 1.2: Regression of *Crocuta crocuta* ventral cranium size onto geographic, environmental and social variables: Estimate, Standard Error, t value, and p-values. Residual standard error: 13.61 on 295 degrees of freedom, Multiple R-squared: 0.4476, Adjusted R-squared: 0.4026, F-statistic: 9.958 on 24 and 295 DF, p-value: < 0.001 for full model. X represents longitude and Y represents latitude. For factor variables sex female, density low and vegetation type forest were set at reference levels. 43

Table 1.3: Regression of *Crocuta crocuta* lateral cranium size onto geography, environmental and social variables: Estimate, Standard Error, t value, and p-values. Residual standard error: 39.75 on 299 degrees of freedom, Multiple R-squared: 0.5758, Adjusted R-squared: 0.5488, F-statistic: 21.36 on 19 and 299 DF, p-value: < 0.001 for full model. X represents longitude and Y represents latitude. For factor variables sex female, density low and vegetation type forest were set at reference levels. 44

Table 1.4: Regression of *Crocuta crocuta* lateral mandible size onto geography, environmental and social variables: Estimate, Standard Error, t value, and p-values. Residual standard error: 19.15 on 307 degrees of freedom, Multiple R-squared: 0.5254, Adjusted R-squared: 0.4883, F-statistic: 14.16 on 24 and 307 DF, p-value: < 0.001 for full model. X represents longitude and Y represents latitude. For factor variables sex female, density low and vegetation type forest were set at reference levels. 45

Table 1.5: *Crocuta crocuta* mean centroid size, standard deviation and sample size for different regions of Africa for three skull views. eastern (east of the Nile and the east African lake system), western (west of the Nile and the east African lake system); and southern (south of the east African lake system). Mean female/mean male centroid size, and sample sizes (Female n; Male n). 46

Table 1.6: *Crocuta crocuta* specimens ventral cranium 48

Table 1.7: *Crocuta crocuta* specimens lateral cranium 56

Table 1.8: *Crocuta crocuta* specimens mandible 64

Table 1.9: Ventral landmarks definitions 74

Table 1.10 Lateral Landmarks defination 75

Table 1.11 Mandible landmarks definitions 76

Table 2.1: Comparison of general linear model performance assessing effects of geographic and environmental variables on ventral cranium size in *Hyaena hyaena*: Estimate, Standard Error, t value, p-values, adjusted R squared, root mean square error and accuracy. For factor variables, reference levels were set as female for sex and barren or sparsely vegetated for landcover. Significant values are noted with an asterisk and significant main covariates are noted in bold. 118

Table 2.2: *Hyaena hyaena* specimens ventral cranium 122

Table 2.3: Ventral landmarks definitions 127

Table 2.4: Lateral Landmarks definations 128

Table 2.5: Mandible landmarks definitions 129

Table 3.1: Procrustes ANOVAs of shape and sex for the ventral cranium, lateral cranium, and mandible views of *Hyaena hyaena*. The fit of the linear model was evaluated using RRPP. df, degrees of freedom; SS, sums of squares; MS mean square; R2, coefficient of determination; F, F statistic; Z, effect sizes; p, associated probability level. Significance was based on 999 permutations. Significant values indicated with an asterisk, 0 '***' 0.001 '**' 0.01 '*' 0.05 '.' 0.1 ' ' 1. 170

Table 3.2: Procrustes ANOVAs of shape, log size and subspecies for subspecies of *Hyaena hyaena* described by Pocock (1934) for the ventral cranium, lateral cranium, and mandible views. The fit of the linear model was evaluated using RRPP. The two fixed factors (log size and subspecies) were allowed to interact with each other. df, degrees of freedom; SS, sums of squares; MS mean square; R2, coefficient of determination; F, F statistic; Z, effect sizes; p, associated probability level. Significance was based on 999 permutations. Significant values indicated with an asterisk, 0 '***' 0.001 '**' 0.01 '*' 0.05 '.' 0.1 ' ' 1. 171

Table 3.3: Cross validation results and overall classification accuracy as percentages for the between group principal component analysis for subspecies of *Hyaena hyaena* described by Pocock (1934). 172

Table 3.4: *Hyaena hyaena* specimens ventral cranium 174

Table 3.5: *Hyaena hyaena* specimens lateral cranium 178

Table 3.6: *Hyaena hyaena* specimens mandible 181

Table 3.7: Ventral landmarks definitions 186

Table 3.8: Lateral Landmarks definations 187

Table 3.9: Mandible landmarks definitions 188

LIST OF FIGURES

Figure 1.1: Specimen collecting localities (points) for *Crocuta crocuta* skulls used in this study. Point color represents centroid sizes: 315-360 light grayish blue; 361-382 slightly desaturated blue; 383-422 dark moderate violet. The Rift valley (grey) and the Albertine rift (black) are indicated by heavy lines. A region of especially dense sampling that encompasses the Aberdare National Park (pink) is enclosed by a red box and enlarged. The area with the cluster of the smallest individuals is labeled Small Cluster and shaded in 50% transparent yellow. East Africa is shaded in dark green and Eastern Africa is shaded in medium green. The current geographical range for *Crocuta crocuta* is shaded in grey. 38

Figure 1.2: Position of landmarks and semilandmarks on a skull of spotted hyena (*Crocuta crocuta*) for the ventral cranium, lateral cranium, and lateral mandible. Landmarks and semilandmarks are numbered and represented by red points. 39

Figure 1.3: Locations for spotted hyena (*Crocuta crocuta*) density estimates listed in Table 1 (green stars) and interpolated density estimates corresponding with specimen collecting sites (dots): blue low density (0.0045 – 0.02 spotted hyena/km2; n=60) and red high density (0.03-1.65 spotted hyena/km2; n=260) high density. 40

Figure 2.1: A: Specimen localities for *Hyaena hyaena* skulls used in this study. Point color indicates ventral view centroid size class delineated using Jenks natural breaks: small (green), medium (yellow), large (orange). The current geographical range for the species is highlighted in blue. Latitude and longitude in decimal degrees are labeled on the axes. The red square indicates the area magnified in the lower map. B: Diagram comparing median centroid sizes for representatives from each of the three size classes, drawn to scale. Green (CS = 305, USNM 182047), Yellow (CS = 337, NMK 3474), and Orange (CS = 357, TAU 7238). The blue bar represents the species' range. 111

Figure 2.2: Position of landmarks on a skull of striped hyena (*Hyaena hyaena*) for the ventral cranium. 113

Figure 2.3: Boxplots of *Hyaena hyaena* centroid size for female (red) and male (blue) ventral view of skull (N = 48 females and 50 males). Boxplots illustrate the means (black dots) and medians (horizontal lines) for each sex. The lower and upper hinges correspond to the 25th and 75th percentiles, respectively. The upper and lower whiskers extends from the hinge to the largest value no further than 1.5 * interquartile range from the hinge. 114

Figure 2.4: Regression of ventral centroid size of the skull of *Hyaena hyaena* on absolute latitude. The red dashed line shows the regression of model lm(CS~Abslat,data=Data). 115

Figure 2.5: Regressions of centroid size and Isothermality for ventral view of the skull for *Hyaena hyaena*. The red dashed line shows the regression of model lm(CS ~ 1 + BIO10M_03_, data = Data). 116

Figure 2.6: Regressions of centroid size and Precipitation of Driest Quarter for ventral view of the skull for *Hyaena hyaena*. The red dashed line shows the regression of model lm(CS~1+BIO10M_17_, data=Data). 117

Figure 3.1: Specimen localities for *Hyaena hyaena* skulls used in this study. Point color indicates subspecies designations by Pocock (1932) (*H. h. barbara*,- green, *H. h. syriaca* - blue , *H. h. hyaena* - red , *H. h. dubbah* - orange, and *H. h. sultana* - pink). The current geographical range for the species is highlighted in gray. Decimal latitude and longitude are labeled on the axes.162

Figure 3.2: Position of landmarks and semilandmarks on a skull of striped hyena (*Hyaena hyaena*) for the ventral cranium, lateral cranium, and mandible.....163

Figure 3.3: Regression of shape onto size. Standardized shape scores from the regression as a function of log centroid size illustrating allometric growth of striped hyena (*Hyaena hyaena*) for the ventral cranium view. Point color and shape indicates subspecies designations by Pocock (1932) (*H. h. barbara*,- green filled square, *H. h. syriaca* – blue open diamond, *H. h. hyaena* – red cross, *H. h. dubbah* – orange open triangle, and *H. h. sultana* – pink filled circle). Photographs of skulls represent shapes at the opposite extremes of the range of allometric variation. Symbols filled with black indicate individual from photograph 164

Figure 3.4: Plot of the first two principal components of the PCA based on Procrustes shape coordinates for the ventral cranium of striped hyena (*Hyaena hyaena*). Point color indicates subspecies designations by Pocock (1932) (*H. h. barbara*,- green, *H. h. syriaca* - blue , *H. h. hyaena* - red , *H. h. dubbah* - orange, and *H. h. sultana* - pink). The areas are the convex hulls of the subspecies. The wireframe figures illustrate shape at the minimum and maximum PC scores. 165

Figure 3.5: Regression of shape onto size. Standardized shape scores from the regression as a function of log centroid size illustrating allometric growth of striped hyena (*Hyaena hyaena*) for the lateral cranium view. Point color and shape indicates subspecies designations by Pocock (1932) (*H. h. barbara*,- green filled square, *H. h. syriaca* – blue open diamond, *H. h. hyaena* – red cross, *H. h. dubbah* – orange open triangle, and *H. h. sultana* – pink filled circle).

Photographs of skulls represent shapes at the opposite extremes of the range of allometric variation. Symbols filled with black indicate individual from photograph.....166

Figure 3.6: Plot of the first two principal components of the PCA based on Procrustes shape coordinates for the lateral cranium of striped hyena (*Hyaena hyaena*). Point color indicates subspecies designations by Pocock (1932) (*H. h. barbara*,- green, *H. h. syriaca* - blue, *H. h. hyaena* - red , *H. h. dubbah* - orange, and *H. h. sultana* - pink). The areas are the convex hulls of the subspecies. The wireframe figures illustrate shape at the minimum and maximum PC scores.....167

Figure 3.7: Regression of shape onto size. Standardized shape scores from the regression as a function of log centroid size illustrating allometric growth of striped hyena (Hyaena hyaena) for the mandible view. Point color and shape indicates subspecies designations by Pocock (1932) (*H. h. barbara*,- green filled square, *H. h. syriaca* – blue open diamond, *H. h. hyaena* – red cross, *H. h. dubbah* – orange open triangle, and *H. h. sultana* – pink filled circle). Photographs of skulls represent shapes at the opposite extremes of the range of allometric variation. Symbols filled with black indicate individual from photograph. 168

Figure 3.8: Plot of the first two principal components of the PCA based on Procrustes shape coordinates for the mandible of striped hyena (Hyaena hyaena). Point color indicates subspecies designations by Pocock (1932) (*H. h. barbara*,- green, *H. h. syriaca* - blue, *H. h. hyaena* - red, *H. h. dubbah* - orange, and *H. h. sultana* – pink. The areas are the convex hulls of the subspecies. The wireframe figures illustrate shape at the minimum and maximum PC scores.....169

Introduction

The natural world varies predictably over space and time. The human desire to document and make sense of these patterns is at least 35,500 years old (Aubert et al., 2014). Our documentation of the types, numbers, and locations of plants and animals encountered has progressed from rock art (Guagnin et al., 2016; Mohana, Deo, & Sundara, 2017) to a network of international databases (Robertson et al., 2014). Our understanding of the geographic patterns in nature and the processes responsible for these patterns constitutes the field of biogeography.

Not only do the type and number of plants and animals vary predictably across geography, but so do biological traits, which tend to form spatial patterns that can be explained by ecogeographical rules. Numerous ecogeographical rules have been proposed to explain geographic patterns in morphology. For instance, the 'Island Rule' suggests that smaller species become larger and larger species become smaller on islands than on continental land masses (Foster, 1964). The proposed explanation for this is smaller animals become larger because predation pressure on islands is less intense than continental land masses due to the absence of some predators on islands, and that larger animals become smaller on islands due to constrained resources on islands compared to continental land masses (Foster, 1964). 'Allen's Rule' suggests that endotherms in cooler climates have reduced limb and appendage length relative to body size than individuals from warmer climates, to reduce heat loss (Allen, 1877; Nudds & Oswald, 2007). 'Bergmann's rule' suggests that endotherms found at higher latitudes or in cooler climates are larger than close relatives from warmer climates (Bergmann, 1847; Mayr, 1956; Meiri & Thomas, 2007; Watt, Mitchell, & Salewski, 2010). The historic proposed

explanation for Bergmann's rule is that larger bodies are more efficient at conserving heat than smaller bodies. McNab (2010) argued that the availability of resources was the root cause of all geographical and ecological 'rules' germane to size. Two proposed explanations for how size is influenced by access to resources are density and seasonality. Damuth (1981) noted that there is an inverse relationship between the body size of an animal and its species population density, and reasoned that reduced access to resources per capita at higher density resulted in smaller body sizes; he called this the energetic equivalence rule. Boyce (1979), asserted that larger body size should be favored in areas with greater seasonality, as seasonal high mortality leads to reduced density-dependent competition and larger individuals are more resistant to starvation during periods of resource shortages. Both heat conservation and access to resources are compelling explanations for patterns of size across geography. To further understand whether body size is better explained by heat conservation or access to resources, I identify geographic patterns in size and shape of hyena skulls and investigate the relationship between bioclimatic variables, social variables, and observed patterns in size.

The mammalian skull is a complex multipurpose structure that is critically involved in respiration, vision, olfaction, mastication, and information storage and processing. As the skull serves as a feeding apparatus and houses the brain and sensory organs, it is under strong selective pressure from the environment, making it valuable for exploring species' ecology and evolution (Cheverud, 1982; Machado, Zahn, & Marroig, 2018).

There is a long history of studying the relationship between the environment and the mammalian skull (Cuvier, 1827; Darwin, 1840), particularly skull size (Calder, 1984; Gittleman,

1991; Gittleman & Valkenburgh, 1997). Body size affects abundance of individuals (Peters & Wassenberg, 1983), community composition (Smith & Lyons, 2013), competition (Calder, 1996), energy balance (Alexander, 2005; Zhao et al., 2017), metabolism (Speakman, 2005), fecundity (Honěk, 1993; Shine, 1988), generation time (Martin & Palumbi, 1993), longevity (Yu et al., 2018), strength (Christiansen & Adolfssen, 2005; van Gelder, Poorter, & Sterck, 2006), and complexity of anatomical structures (Bonner, 2004; Heim et al., 2017). Size is the foremost determinant of all biological processes and is integral to almost every aspect of biology (Bonner, 2004; Peters & Peters, 1986). Examining patterns in size across geography can illuminate how different climates, habitats, and biotic communities influence the evolution of mammals. Skull size was chosen for this study as it is a good proxy for overall body size in hyenas (McElhinny, 2009) and natural history collections contain more skulls than post-cranial skeletons.

Changes in size are often associated with changes in shape (Bonner, 2004). Allometry, shape change associated with change in size, has been well documented in mammals and usually accounts for a large proportion of morphological variation (Cardini, 2019; Cardini & Polly, 2013; Klingenberg, 2016; Mitteroecker, Gunz, Windhager, & Schaefer, 2013). Historically our understanding of the diversity of biological life and taxonomic classification of organisms was based on the description of morphological form (Cuvier, 1827; Darwin, 1859; Thompson, 1917). As morphology and associated function are the direct objects of selection (Arnold, 1983), we can elucidate what factors drive the evolution of species by investigating patterns of morphological form across different environmental conditions.

To study morphological variation and identify its causes, we must be able to quantify shape. Shape is difficult to quantify using linear measurements; a teardrop and an oval can have

the same maximum length and maximum width but are very different shapes (Adams, Rohlf, & Slice, 2004). Thus, we use geometric morphometric methods to quantify shape and to study the evolution of morphological variation. Geometric morphometrics quantifies shape using Cartesian coordinates for homologous structures, after the effects of non-shape variation have been mathematically held constant (Bookstein, 1997). Once variation due to scale, position, and orientation are removed, only information about shape remains (Zelditch et al., 2012). Another advantage to using geometric morphometrics is the ability to graphically depict shape and shape changes (Adams et al., 2004). In the past, variation in skull morphology could only be subjectively described but; now we can quantify morphological differences with precision and create visualizations of the differences in shape that are comprehensible to non-specialists. This allows for rigorous morphological comparisons within a species where variation in morphology may be subtle but biologically important.

Spotted hyenas (*Crocuta crocuta*) are highly social, pack-hunting carnivores, with clan size reaching over 100 individuals (Green, Johnson-Ulrich, Couraud, & Holekamp, 2018; Holekamp, Smale, Berg, & Cooper, 1997; Mills & Hofer, 1998). They have a fission-fusion social structure with a linear dominance hierarchy in which females and their offspring are dominant to breeding males (Frank, 1986; Smale, Frank, & Holekamp, 1993). Female dominance over males is rare in mammals (Bidau & Martinez, 2016; Gittleman & Valkenburgh, 1997; Meiri, Dayan, & Simberloff, 2005; Ralls, 1976). This social structure may have important consequences for patterns of morphology between the sexes. Spotted hyenas typically feed on the most abundant medium-sized ungulate in their habitats, but their diet is remarkably flexible and; they have been documented foraging on everything from caterpillars to scavenged elephant

carcasses (Holekamp & Dloniak, 2010; Mills, 1990). They occur throughout sub-Saharan Africa and occupy a diverse array of habitats, including savannas, deserts, swamps, woodlands, and forests up to 4000 m of elevation, although they are absent or at very low densities in dense rain forest (Mills & Hofer, 1998; Sillero-Zubiri & Gottelli, 1992).

In contrast to spotted hyenas, striped hyenas (*Hyaena hyaena*) are often considered to be solitary (AbiSaid & Dloniak, 2015), although recent research in Kenya suggests a more complex and variable social structure (Califf et al 2020: Wagner et al 2008). Two populations in Kenya approximately 300 km apart exhibit markedly different space-use patterns. The Laikipia population formed stable polyandrous social groups composed of multiple males and a single female, with male home ranges overlapping considerably with those of other males, whereas the Shompole population exhibited less male home range overlap and a high degree of female home range overlap (Califf et al., 2019; Wagner, Frank, & Creel, 2008). Additional studies are needed to determine the extent to which social structure in striped hyenas varies across geography. Striped hyenas usually forage alone, scavenging or taking prey smaller than themselves (Mills & Hofer, 1998). The striped hyena's diet is opportunistic and extraordinarily flexible, including insects, small mammals, birds, fish, tortoises, crocodiles, dogs, wild ungulates, primates, livestock, human remains, seeds, leaves, and fruits (Bhandari, Morley, Aryal, & Shrestha, 2020; Kruuk, 1976; Leakey et al., 1999; Wagner, 2006). Striped hyenas have the largest range of any extant hyena, spanning three continents. Their range extends from the Atlantic coast of western Africa, to far eastern India, north along the foothills of the Himalayas in Nepal and the Caspian Sea to Turkey and south to Tanzania (AbiSaid & Dloniak, 2015).

Spotted hyenas and striped hyenas are *bone-cracking members* of the family Hyaenidae. They have robust skulls and reduced dentition adapted to access the nutritious marrow in the bones of large ungulates. As a consequence of durophagy (i.e., feeding on hard objects), the skulls and teeth of *bone-cracking* hyenas fossilize well. Hyenas are well represented in the fossil record of the Old World since the Miocene (Coca-Ortega & Pérez-Claros, 2019; Werdelin, Solounias, & strata, 1991). This continual appearance in the fossil record has led paleontologists to use hyenas as indicators of historic climatic conditions (Klein, 1986; Kurten, 1957). Not only are modern hyenas important dominant carnivores in their own communities, but our understanding of the relationship between morphology and climate of modern hyenas is pivotal for making inferences about communities and climatic conditions in the past.

In this dissertation, I identify geographic patterns in skull size and morphology of two extant *bone-cracking* hyenas and determine if climatic and social variables explain these observed patterns in the context of ecogeographical rules. In Chapter 1, I investigate geographic variation in spotted hyena skull size to determine if sex, climatic variables, or access to resources better explains skull size. I determine whether spotted hyenas conform to the heat conservation hypothesis proposed by Bergmann or if geographic patterns in skull size are better explained by ecogeographical rules driven by the availability of resources as proposed by the energetic equivalence rule. In Chapter 2, I examine geographic variation in striped hyena skull size to determine whether skull size is better explained by sex, latitude, annual climatic or seasonal climatic variables. I establish whether striped hyenas exhibit a latitudinal size increase as predicted by Bergmann's rule and whether geographic variation in size is better explained by ecogeographical rules pertaining to annual or seasonal conditions. Finally, in Chapter 3, I

scrutinize whether geographic patterns of skull shape variation in striped hyenas are in accord with historic subspecies designations, proposed by Pocock (1934) and whether patterns of shape correspond to morphological expectations based on dietary differences across their range.

WORKS CITED

WORKS CITED

AbiSaid, M., & Dloniak, S. (2015). Hyaena hyaena. *The IUCN Red List of Threatened Species*, 2015-2012.

Adams, D. C., Rohlf, F. J., & Slice, D. E. (2004). Geometric morphometrics: Ten years of progress following the 'revolution'. *Italian Journal of Zoology,* 71(1), 5-16.

Alexander, R. M. (2005). Models and the scaling of energy costs for locomotion. *The Journal of Experimental Biology, 208*(Pt 9), 1645-1652.

Arnold, S. J. (1983). Morphology, Performance and Fitness. *American Zoologist, 23*, 347-361.

Aubert, M., Brumm, A., Ramli, M., Sutikna, T., Saptomo, E. W., Hakim, B., Morwood, M. J., van den Bergh G.D., Kinsley l.,&Dosseto, A. (2014). Pleistocene cave art from Sulawesi, Indonesia. *Nature, 514*(7521), 223-227.

Bhandari, S., Morley, C., Aryal, A., & Shrestha, U. B. (2020). The diet of the striped hyena in Nepal's lowland regions. *Ecology and Evolution, 10*(15), 7953-7962.

Bidau, C. J., & Martinez, P. A. (2016). Sexual size dimorphism and Rensch's rule in Canidae. *Biological Journal of the Linnean Society, 119*(4), 816-830.

Bonner, J. T. (2004). Perspective: the size-complexity rule. *Evolution, 58*(9), 1883-1890.

Bookstein, F. L. (1997). *Morphometric Tools for landmark data: geometry and biology*: Cambridge University Press.

Calder, W. (1984). *Size, Function, and Life History*. Cambridge, Massachusetts: Harvard University Press.

Calder, W. A. (1996). *Size, function, and life history*: Courier Corporation.

Califf, K. J., Green, D. S., Wagner, A. P., Scribner, K. T., Beatty, K., Wagner, M. E., & Holekamp, K. E. (2019). Genetic relatedness and space use in two populations of striped hyenas (Hyaena hyaena). *Journal of Mammalogy*.

Cardini, A. (2019). Craniofacial Allometry is a Rule in Evolutionary Radiations of Placentals. *Evolutionary Biology*.

Cardini, A., & Polly, P. D. (2013). Larger mammals have longer faces because of size-related constraints on skull form. *Nature communications, 4*(1), 1-7.

Cheverud, J. M. (1982). Phenotypic, genetic, and environmental morphological integration in the cranium. *Evolution*, 499-516.

Christiansen, P., & Adolfssen, J. S. (2005). Bite forces, canine strength and skull allometry in carnivores (Mammalia, Carnivora). *Journal of Zoology, 266*(2), 133-151.

Coca-Ortega, C., & Pérez-Claros, J. A. (2019). Characterizing ecomorphological patterns in hyenids: a multivariate approach using postcanine dentition. *PeerJ, 6*, e6238.

Cuvier, G. (1827-1835). The animal kingdom : arranged in conformity with its organization In. London Printed for Whittaker and Co.

Darwin, C. (1840). *The Zoology of the Voyage of H. M. S. Beagle: Under the Command of Captain Fitzroy, R. N., During the Years 1832 to 1836*: Smith, Elder and Co.

Darwin, C. (1859). *On the origin of species by means of natural selection, or preservation of favoured races in the struggle for life*: London :John Murray.

Frank, L. G. (1986). Social organization of the spotted hyaena (*Crocuta crocuta*). I. Demography. *Animal Behaviour, 34*(5), 1500-1509.

Gittleman, J. L. (1991). Carnivore olfactory bulb size: allometry, phylogeny and ecology. *Journal of Zoology, 225*(2), 253-272.

Gittleman, J. L., & Valkenburgh, B. V. (1997). Sexual dimorphism in the canines and skulls of carnivores: effects of size, phylogency, and behavioural ecology. *Journal of Zoology, 242*(1), 97-117.

Green, D., Johnson-Ulrich, L., Couraud, H., & Holekamp, K. (2018). Anthropogenic disturbance induces opposing population trends in spotted hyenas and African lions. *Biodiversity and Conservation, 27*(4), 871-889.

Guagnin, M., Jennings, R., Eager, H., Parton, A., Stimpson, C., Stepanek, C., Madlene P., Huw S.G., Drake N. A., Alsharekh A., & Petraglia M.D, (2016). Rock art imagery as a proxy for Holocene environmental change: A view from Shuwaymis, NW Saudi Arabia. *The Holocene, 26*(11), 1822-1834.

Heim, N. A., Payne, J. L., Finnegan, S., Knope, M. L., Kowalewski, M., Lyons, S. K., McShea D.W., Novack-Gottshall P. M., Smith F. A., Wang, S. C. (2017). Hierarchical complexity and the size limits of life. *Proceedings of the Royal Society B: Biological Sciences, 284*(1857), 20171039.

Holekamp, K. E., & Dloniak, S. M. (2010). Chapter 6 - Intraspecific Variation in the Behavioral Ecology of a Tropical Carnivore, the Spotted Hyena. In R. Macedo (Ed.), *Advances in the Study of Behavior* (Vol. 42, pp. 189-229): Academic Press.

Holekamp, K. E., Smale, L., Berg, R., & Cooper, S. M. (1997). Hunting rates and hunting success in the spotted hyena (*Crocuta crocuta*). *Journal of Zoology, 242*(1), 1-15.

Honěk, A. (1993). Intraspecific Variation in Body Size and Fecundity in Insects: A General Relationship. *Oikos, 66*(3), 483-492.

Klein, R. G. (1986). Carnivore size and quaternary climatic change in southern Africa. *Quaternary Research, 26*(1), 153-170.

Klingenberg, C. P. (2016). Size, shape, and form: concepts of allometry in geometric morphometrics. *Development genes and evolution, 226*(3), 113-137.

Kruuk, H. (1976). Feeding and social behaviour of the striped hyaena (*Hyaena vulgaris* Desmarest). *African Journal of Ecology 14*, 91-111.

Kurten, B. (1957). The bears and hyenas of the interglacials. *Quaternaria, 4*, 69-81.

Leakey, L., Milledge, S., Leakey, S., Edung, J., Haynes, P., Kiptoo, D., & McGeorge, A. (1999). Diet of striped hyaena in northern Kenya. *African Journal of Ecology, 37*(3), 314-326.

Machado, F. A., Zahn, T. M. G., & Marroig, G. (2018). Evolution of morphological integration in the skull of Carnivora (Mammalia): Changes in Canidae lead to increased evolutionary potential of facial traits. *Evolution, 72*(7), 1399-1419.

Martin, A. P., & Palumbi, S. R. (1993). Body size, metabolic rate, generation time, and the molecular clock. *Proceedings of the National Academy of Sciences, 90*(9), 4087.

McElhinny, T. L. (2009). *Morphological Variation in a Durophagous Carnivore, the Spotted Hyena, Crocuta Crocuta*: Michigan State University. East Lansing, Michigan.

Meiri, S., Dayan, T., & Simberloff, D. (2005). Variability and sexual size dimorphism in carnivores: testing the niche variation hypothesis. *Ecology, 86*(6), 1432-1440.

Mills, M. (1990). Kalahari hyaenas: the behavioural ecology of two species. London. *UK: Unwin Hyman*.

Mills, M., & Hofer, H. (1998). Status survey and conservation action plan. Hyaenas. *IUCN/SSC Hyaena Specialist Group, IUCN, Switzerland*.

Mitteroecker, P., Gunz, P., Windhager, S., & Schaefer, K. J. H., the Italian Journal of Mammalogy. (2013). A brief review of shape, form, and allometry in geometric morphometrics, with applications to human facial morphology. *Hystrix, the Italian Journal of Mammalogy, 24*(1), 59-66.

Mohana, R., Deo, S. G., & Sundara, A. (2017). Newly Discovered Rock Art Sites in the Malaprabha Basin, North Karnataka: A Report. *Heritage: Journal of Multidisciplinary Studies in Archaeology*.

Peters, R. H., & Peters, R. H. (1986). *The ecological implications of body size* (Vol. 2): Cambridge university press.

Peters, R. H., & Wassenberg, K. (1983). The effect of body size on animal abundance. *Oecologia, 60*(1), 89-96.

Ralls, K. (1976). Mammals in Which Females are Larger Than Males. *The Quarterly Review of Biology, 51*(2), 245-276.

Rios, N. (2019). GEOLocate - Software for Georeferencing Natural History Data. [Web application software]. Retrieved from http://www.geo-locate.org

Robertson, T., Döring, M., Guralnick, R., Bloom, D., Wieczorek, J., Braak, K., . . . Desmet, P. (2014). The GBIF integrated publishing toolkit: facilitating the efficient publishing of biodiversity data on the internet. *PloS one, 9*(8), e102623.

Shine, R. (1988). The evolution of large body size in females: a critique of Darwin's" fecundity advantage" model. *The American Naturalist, 131*(1), 124-131.

Sillero-Zubiri, C., & Gottelli, D. (1992). Population ecology of spotted hyaena in an equatorial mountain forest. *African Journal of Ecology, 30*, 292-300.

Smale, L., Frank, L. G., & Holekamp, K. E. (1993). Ontogeny of dominance in free-living spotted hyaenas: juvenile rank relations with adult females and immigrant males. *Animal Behaviour, 46*(3), 467-477.

Smith, F. A., & Lyons, S. K. (2013). *Animal body size: linking pattern and process across space, time, and taxonomic group*: University of Chicago Press.

Speakman, J. R. (2005). Body size, energy metabolism and lifespan. *J Exp Biol, 208*(Pt 9), 1717-1730.

Thompson, D. A. W. (1917). *On growth and form*. Cambridge [Eng.]: University press.

van Gelder, H. A., Poorter, L., & Sterck, F. J. (2006). Wood mechanics, allometry, and life-history variation in a tropical rain forest tree community. *New Phytol, 171*(2), 367-378.

Wagner, A. P. (2006). Behavioral ecology of the striped hyena (*Hyaena hyaena*). Montana State University Bozeman, Montana.

Wagner, A. P., Frank, L. G., & Creel, S. (2008). Spatial grouping in behaviourally solitary striped hyaenas, Hyaena hyaena. *Animal Behaviour, 75*(3), 1131-1142.

Werdelin, L., Solounias, N. J. F., & strata. (1991). The Hyaenidae: taxonomy, systematics and evolution. *Fossils and strata, 30*, 1-104.

Yu, X., Zhong, M. J., Li, D. Y., Jin, L., Liao, W. B., & Kotrschal, A. (2018). Large-brained frogs mature later and live longer. *Evolution, 72*(5), 1174-1183.

Zelditch, M. L., Swiderski, D. L., & Sheets, H. D. (2012). Geometric morphometrics for biologists: a primer. academic press.

Zhao, M., Christie, M., Coleman, J., Hassell, C., Gosbell, K., Lisovski, S., Minton, C., Klaassen, M. (2017). Time versus energy minimization migration strategy varies with body size and season in long-distance migratory shorebirds. *Mov Ecol, 5*, 23.

Chapter 1: Geographic variation in spotted hyena skull size; empirical evidence for the energetic equivalence rule

ABSTRACT

Size is the most important aspect of morphology. In many mammals, size varies intraspecifically across geography. Much historic work has focused on establishing geographical and ecological rules that broadly explain patterns in size. One such ecological rule is the "energetic equivalence rule" which states that there is an inverse relationship between the body size of an animal species and its population density, such that reduced access to resources per capita at higher densities results in smaller body sizes. Geographic variation in spotted hyena skulls was investigated using geometric morphometrics and spatial statistics. Sexual size dimorphism of the skull was quantified and the influence of temperature, precipitation, land cover types, and population density on skull size was evaluated. We tested the hypothesis that sexual size dimorphism is greatest where population density is highest. Female spotted hyenas are slightly larger on average than males. There was no evidence for geographic variation in sexual size dimorphism. The smallest individuals of both sexes occur between -5.00^{o} and 10.00^{o} latitude and east of 28.50^{o} longitude, with larger individuals found elsewhere. Spotted hyena skull size co-varies with temperature, precipitation, and landcover, but more strongly co-varies with population density. The highest densities are associated with the smallest skull size, possibly reflecting a relationship between high population density and access to resources. These findings provide empirical evidence for the energetic equivalence rule.

1 | INTRODUCTION

Size is the most important aspect of physical form. Body size influences the composition of biological assemblages, the abundance of individuals, their spatial and temporal distribution, and their interactions (Brown & West, 2000; Calder, 1996; Smith & Lyons, 2013). Strength varies with size (Christiansen & Adolfssen, 2005; van Gelder, Poorter, & Sterck, 2006), as does the complexity of anatomical structures and their functions (Bonner, 2004; Heim et al., 2017). Body size affects metabolism (Speakman, 2005), fecundity (Honěk, 1993; Shine, 1988), generation time (Martin & Palumbi, 1993), longevity (Yu et al., 2018), and regulation of energy balance (Alexander, 2005; Zhao et al., 2017).

Unsurprisingly, there is an extensive history of research aimed at identifying factors that influence mammalian body size. Much of this work focuses on establishing geographical and ecological rules that can be applied broadly to explain patterns in size, such as size differences between island and continental species ("The Island Rule", (Foster, 1964)), the relative size of body extremities in warm versus colder environments ("Allen's Rule", (Allen, 1877)) and variation in size across latitudes ("Bergmann's rule",(Bergmann, 1847). Bergmann's rule is a well studied phenomenon in which endotherms found at higher latitudes or in cooler climates are larger than close relatives from warmer climates (Mayr, 1956; Meiri & Thomas, 2007; Watt, Mitchell, & Salewski, 2010). The premise underlying this rule is that in cooler climates larger individuals have a thermoregulatory advantage over smaller ones because (other things being equal) they have a more favorable surface area to volume ratio for retaining heat. In a review of intraspecific body size variation in mammals, Ashton, Tracy, and Queiroz (2000) found broad support for Bergmann's rule (78 of 110 species), but not for heat conservation as the primary

mechanism. A subsequent compilation of research on geographic size variation in mammalian carnivorans found that only 22 of 44 species (i.e., 50%) conformed to Bergmann's Rule (Meiri, Dayan, & Simberloff, 2004).

McNab (2010), proposed that all geographical and ecological 'rules' germane to size are aspects of the same phenomenon, the availability of resources. Thus, they could be lumped together as a single concept, "the resource rule," such that species become larger or smaller depending on the size, abundance, and availability of resources (McNab, 2010). One proposed explanation for the resource rule phenomenon is the "energetic equivalence rule", which states that there is an inverse relationship between the body size of an animal species and its population density (Damuth, 1981). Several authors have attributed this pattern to reduced access to resources per capita at higher densities, such that more smaller individuals can be supported on limited resources (Damuth, 1981; Loeuille & Loreau, 2006; R. H. Peters & Karen, 1983; Silva, Brimacombe, Downing, & Biogeography, 2001). Larger bodies require more resources to maintain (Damuth, 1981; Silva et al., 2001) and thus we expected density to affect body size. Few studies have directly examined the relationship between body size and food resources because the availability of food resources is often difficult to measure (Dobson & Kjelgaard, 1985; Jones, Waldschmidt, & Potvin, 1987; Li et al., 2016). Most studies evaluate proxies for food availability using large-scale environmental parameters like temperature, rainfall, and vegetation (Ferger, Schleuning, Hemp, Howell, & Böhning-Gaese, 2014; Olalla-Tárraga et al., 2006; Yom-Tov & Geffen, 2006).

Access to food is influenced not only by food abundance, but also by intraspecific competition. There are finite nutrients in an ecosystem and large individuals use more

resources per capita per unit time, therefore limited resources will support more smaller individuals than larger ones (Loeuille & Loreau, 2006; R. H. Peters & Karen, 1983; Silva et al., 2001). There is empirical evidence for an inverse relationship between body size and population density within a number of large-bodied mammal species. This pattern of small body size associated with higher density is well documented in artiodactyls (moose: Sand et al., 1995; e.g., white-tailed deer: Simard, Côté, Weladji, & Huot, 2008; reindeer: Skogland, 1983), probably due to interest in body size management for harvest purposes. Clutton-Brock and Harvey (1977) compared 100 species of primates and found that intraspecific population density is negatively related to body weight. Some carnivorans also show a decrease in body size at high population densities. Carbone and Gittleman (2002) found that the number of carnivores supported on a given biomass of prey increases with decreasing body size. In brown bears, females exhibit smaller head circumference, a common proxy for bear body size, at higher densities (Zedrosser, Dahle, & Swenson, 2006), and in red foxes, males and females have shorter body lengths at higher densities (Cavallini, 1995), and males are also lighter at higher densities (Cavallini, 1995).

The influence of interspecific competition on adult body size is not as well understood. African carnivores may have to share food resources with up to 22 other carnivore species (Caro & Stoner, 2003), and competition for food resources with lions has profound effects on the lives of smaller carnivores (Hayward & Slotow, 2009). Indeed, spotted hyenas living at lower lion densities enjoy greater lifetime reproductive success, likely as a result of higher rates of food intake (Watts & Holekamp, 2008).

Here we investigate intraspecific size variation in a wide-ranging, large-bodied carnivore,

the spotted hyena, *Crocuta crocuta* (Erxleben 1777) (Wilson & Reeder, 2005). We focus on the cranium and mandible as they are central to the feeding biology of this species and have been found to be good proxies for overall body size (McElhinny, 2009). Spotted hyenas occur throughout most of sub-Saharan Africa and are found in a diverse array of habitats, including savannas, deserts, swamps, woodlands, and forests up to 4000 m of elevation (Mills, 1990; Mills & Hofer, 1998); they occur at very low densities or are absent from dense low-elevation rainforest (Mills & Hofer, 1998). Spotted hyenas are highly social pack-hunting carnivores (Mills & Hofer, 1998). They typically hunt the most abundant medium size ungulate present (Kay E. Holekamp & Dloniak, 2010) and are known for their ability to crack open large bones to access the nutritious marrow within (Tanner, Dumont, Sakai, Lundrigan, & Holekamp, 2008). Although ungulates are an important food source for this species, the diet is remarkably flexible; spotted hyenas have been documented foraging on everything from caterpillars to scavenged elephant carcasses (Kay E. Holekamp & Dloniak, 2010; Mills, 1990). This flexibility facilitates local adaptation to heterogeneous habitats.

Previous studies of spotted hyenas have described marked intraspecific variation with geography (H. Kruuk, 1972; Mills, 1990). Indeed, although the species is currently considered monotypic (Wilson & Reeder, 2005), variation in skeletal morphology and pelage color have led to the naming of as many as 21 distinct subspecies (Allen, Lang, & Chapin, 1924; Heller, 1914; Matthews, 1939; Meester, 1986). Two geographic clines in body size have been described. The first is based on carnassial length of recent specimens from Africa, as well as fossils from the late Pleistocene of Africa, Asia, and Europe. This cline is characterized by smaller individuals at the equator and larger individuals to the north and south (Klein & Scott, 1989; Kurten, 1957;

Mills, 1990). The second cline, based on body mass, extends from southern to eastern Africa, with spotted hyenas in the (eastern) Aberdare forest of Kenya being the lightest (Sillero-Zubiri & Gottelli, 1992). Some authors (Klein & Scott, 1989; Kurten, 1957) have argued that these clines in body size largely reflect the influence of temperature (an example of Bergmann's rule). But another plausible explanation for these observed relationships between body size measures and locality is that they reflect variation across the species range in resource availability. Northern and southern Africa have more seasonal climates than equatorial Africa, causing resources to be periodically scarce in those areas. Moreover, the woodlands and savannahs of equatorial eastern Africa have predictable rainfall that drives migration of ungulates across these landscapes, making food periodically more plentiful and predictable there than elsewhere (Sinclair & Arcese, 1995; Sinclair & Norton-Griffiths, 1984; Sinclair, Packer, Mduma, & Fryxell, 2008).

Most analyses of size variation in spotted hyenas have combined the sexes, as sexual size dimorphism appears to be very low or absent in this species (Buckland-Wright, 1969; Sillero-Zubiri & Gottelli, 1992; Skinner, 1976). Spotted hyenas are especially interesting with respect to sex roles in that they have a fission-fusion social structure, with a linear dominance hierarchy in which females and their offspring are dominant to breeding males (Frank, 1986; Smale, Frank, & Holekamp, 1993). Female dominance over males is rare in mammals (Bidau & Martinez, 2016; Gittleman & Valkenburgh, 1997; Meiri, Dayan, & Simberloff, 2005; Ralls, 1976). In the most extensive study of sexual dimorphism in this species, Swanson et al. (2013) examined measurements taken from 651 live animals immobilized in the Masai Mara National Reserve, Kenya, and found that females were slightly but significantly larger for some head

dimensions important to the function of the feeding apparatus, likely reflecting differences in the musculature and bones associated with bite force (Schwenk, 2000). Like the skulls of other bone-cracking hyenas, spotted hyena skulls take a long time to mature, presumably reflecting the durophagous diet ingested by adults of these species (. Tanner, Zelditch, Lundrigan, & Holekamp, 2010; Watts, Tanner, Lundrigan, & Holekamp, 2009). These authors suggest that female social dominance in this species may reflect selection pressure on mothers to help young with immature jaws obtain access to food in a highly competitive environment. If so, the degree of skull sexual dimorphism might be expected to co-vary positively with group size or density.

In this study, we investigate geographic variation in spotted hyena skull size using a large sample from across the range of the species. We first quantify sexual size dimorphism and then evaluate the influence of temperature, precipitation, land cover types, and population density on skull size. We use temperature and precipitation indices as surrogates for thermoregulatory demands, and water availability and land cover type as proxies for habitat (Ferrer-Castán, Morales-Barbero, & Vetaas, 2016; Hillebrand, 2004; McNab, 2010; O'Donnell & Ignizio, 2012). Population density is used as an indicator of intraspecific competition; population densities of spotted hyenas are known to vary by orders of magnitude across the species range (Holekamp, Smith, Trelioff, Van horn, & Watts, 2012). We also test the hypothesis that sexual size dimorphism is greatest where population density, and thus presumably intraspecific competition, is also highest.

2 | MATERIALS AND METHODS

2.1 | Specimens

The sample comprised 332 skulls of adult spotted hyenas (121 females, 125 males, 86 sex unknown) obtained from 14 natural history collections (APPENDIX B). Full maturity was defined by complete eruption of permanent teeth, and complete, or nearly complete, closure of the lambdoid and basilar sutures. Specimens were collected from the field between 1900 and 2006 and include individuals from 21 sub-Saharan Africa countries (Figure 1.1). The distribution of collecting localities encompasses much of the current geographical range of *C. crocuta,* as well as regions in south and central Africa where *C. crocuta* appears to have been recently extirpated (IUCN, 2021). The Sahel, tropical west Africa, Angola, and western Zambia are not as well represented as East Africa. Collection data for each specimen, including date of collection, locality, and sex (determined at the time of collection), were obtained from museum records. Specimens without coordinate data were georeferenced from specimen locality data, using established guidelines from Chapman and Wieczorek (2006), and the georeferencing software GEOLocate Web Application (Rios, 2019).

2.2 | Morphological Data

Skulls were photographed using a digital camera in three views: ventral cranium, lateral cranium, and lateral mandible (Figure 1.2). Images of the cranium in ventral view were obtained by orienting specimens with the palate parallel to the photographic plane, in lateral view by orienting the mid-sagittal plane parallel to the photographic plane, and in lateral view of mandible by orienting the long axis of the dentary parallel to the photographic plane. A 10-mm scale was included in all photographs.

To quantify variation in skull size, we used 2D landmark-based geometric morphometrics. Landmarks and semi-landmarks (Figure 1.2, APPENDIX C), selected to capture overall size (Zelditch et al., 2012), were digitized by the same observer (CNC), using tpsDig2.32 (Rohlf, 2015). For each view, landmark configurations were superimposed to remove variation in scale, position, and orientation by a generalized least-squares Procrustes superimposition using the 'geomorph' package (Adams, Collyer, & Sherratt, 2015; Adams & Otárola-Castillo, 2013) in R version 3.4.1 (R Core Team, 2017). Semilandmarks contain an additional nuisance parameter (position along the curve), this was removed by sliding them to minimize bending energy (Bookstein, 1997; W. Green, 1996). We used centroid size as the size metric in all analyses. Centroid size is the square root of the summed squared distances of each landmark from the centroid of the landmark configuration; it better captures the overall size of an object than linear measurements (Zelditch et al., 2012).

2.3 | Bioclimatic Variables

Bioclimatic variables were obtained for each specimen's collection locality. Annual mean temperature and annual precipitation were extracted at a spatial resolution of 10 minutes (~340Km^2), from WorldClim global climate database (Fick & Hijmans, 2017). To represent habitat types, twenty-eight vegetation types were extracted from the land cover map of Africa, at a spatial resolution of 1 km (Mayaux, Bartholomé, Fritz, & Belward, 2004). Mayaux et al. (2004), grouped these vegetation types into six categories. We categorized our vegetation types similarly into four land cover types (forest, mixed grassland and forest, grassland, and bare ground), as the range of spotted hyena contains fewer unique vegetation types than the entire continent of Africa.

2.4 | Hyena Density Data

Spotted hyena density data (individuals/ km^2; Table 1) were obtained from a compilation in Kay E. Holekamp and Dloniak (2010) that was updated to include research subsequent to 2010. All density data are based on published field studies, PhD dissertations, or MS theses. These density estimates are geographically widespread, but correspond only roughly to the regions where our specimens were obtained (Figure 1.3). To expand coverage, the density data were interpolated across the entire geographic range of the species (including recently extirpated regions in central and southern Africa) using geographic midpoints of census sites and universal kriging in ArcGIS 10.6 (units: hyenas per km2; model: stable; nugget: 0.439; Sill: 0.2855; Major Range: 1.928; lag: 12) (Cressie, 1993; Esri, 2018). Four density categories were identified using Jenks natural breaks (Jenks, 1963). Exploratory models indicated a significant relationship between skull size and the lowest density category, but did not show significant relationships between skull size and any of the other three density categories. Consequently, the number of density categories was reduced to two, low (0.0045 – 0.02 spotted hyena/km^2; n=60) and high (0.03-1.65 spotted hyena/km^2; n=260), thereby decreasing the number of parameters in the model and simplifying interpretation.

2.5 | Statistical Analysis

To assess sexual dimorphism, the mean female to male skull centroid size ratio was calculated for the entire sample (Ralls, 1976). The sample was divided into regions based on visible geographic clusters and habitat types. Regional differences in sexual dimorphism were

evaluated by dividing the sample into three geographic regions: eastern (east of the Nile and the east African lake system- dominated by tropical and subtropical grassland, savannas and shrublands), western (west of the Nile and the east African lake system-a mix of dense tropical forest and tropical and subtropical grassland, savannas and shrublands); and southern (south of the east African lake system-dominated by deserts and xeric shrubland). The single specimen from Mali was not included in this analysis because it was geographically isolated from all others. Because sexual size dimorphism was extremely small relative to size variation related to geography, the sexes were pooled for subsequent geographic analyses (Table 1.5).

Geographic parameters (latitude and longitude) are difficult to model because ecological responses to spatial change exhibit nonlinear behavior (Peters et al., 2007), such that a small change in the driving variable (geography) can have a large but discontinuous influence on the response variable. To accommodate this, we first quantified the spatial component of skull centroid size by determining the best-fit combination of spatial variables that contributed significantly to explaining variation in size, and then incorporated the bioclimatic and density parameters into the analysis (Botes et al., 2006; Cardini, Jansson, & Elton, 2007; Legendre & Legendre, 1998). The spatial component was modeled using a fourth order polynomial, where x and y are longitude and latitude respectively (Appendix 3). A global model of centroid size was regressed onto all of the higher order polynomials for geography. We used the function pdredge from the R package 'MuMIn' to perform an automated model selection with combinations (subsets) of fixed effects terms from the global model to find the model with the most support using Akaike Information Criterion (AIC) (Sakamoto, Ishiguro, & Kitagawa, 1986). The model with the most support was used as the spatial component in subsequent analyses.

A model was built for each view of the crania or mandible by combining sex, temperature, precipitation, land cover, and density parameters with the view-specific spatial component to determine how these influence skull centroid size. Variance inflation factor analysis (vif package 'car') detected multicollinearity in all three views so, following recommendations in Zuur, Ieno, and Elphick (2010), a backward stepwise variable selection was performed using AIC to address parameters problematic enough to impact the model. All impactful parameters were higher order polynomials for geography. A reduced model for each view was constructed excluding the impactful parameters from the spatial component. The reduced models were used in all subsequent analysis. We examined residuals and fitted values to determine whether assumptions of normality (Shapiro-Wilk), equal variance, and independence (Durbain Watson) were violated (Fox & Wyrick, 2008; Royston, 1995). We also examined the data using Cook's distance (Fox & Wyrick, 2008) and the function acf in the R package 'forecast' (Venables & Ripely, 2002) to identify any influential outliers or significant autocorrelations. All model analyses were performed in R VERSION 3.4 (R CORE TEAM, 2017). To visualize size patterns across geography, centroid size was divided into 3 categories (small, medium, and large) using Jenks natural breaks, and mapped using specimen locality data.

3 | RESULTS

3.1 | Sexual Dimorphism

Sex was a predictor of skull size, with females having significantly larger ventral (P= 0.01, Table 1.2) and lateral (P=0.01, Table 1.3) crania than males. There was no significant relationship between lateral mandible size and sex (p=0.55, Table 1.4). Though statistically significant, the actual size differences between female and male crania were very small; the mean female to male size ratio for our sample was 1.011 for ventral crania (females 113, males 121), 1.011 for lateral crania (females 114, males 122), and 1.007 for lateral mandibles (females 121, males 125)(Table 1.5). Sexual dimorphism in skull size does not show significant geographic variation (Tables 1.2-1.5) and there is no evidence that degree of sexual dimorphism is positively correlated with hyena density. However, sample sizes are too small in all but the eastern geographic region to permit a firm conclusion (Table 1.5).

3.2 | Geography

We observed a considerable range in adult skull size across geography, with the smallest skull being 25% smaller than the largest skull. Geographic parameters (i.e., latitude and longitude) were strongly predictive in explaining variation in skull centroid size in our models with 75% of geographic parameters significant in ventral view ($p< 0.05$), 62.5% in lateral view ($p< 0.05$), and 100% in the lateral view of mandible ($p< 0.05$) (Tables 1.2-1.4). Individuals with small skulls are clustered between -5.00^{o} and 10.00^{o} latitude and east of 28.50^{o} longitude (Small Cluster-Figure 1.1). This eastern boundary corresponds with the Albertine Rift, the western branch of the East African rift system (Figure 1.1) (Ebinger, 1989). Specimens from near

the Aberdare National Park (Figure 1.1) had the smallest mean ventral cranium, lateral cranium, and lateral mandible, while the largest skull was from Botswana in the southern region.

3.3 | Bioclimatic variables

Annual mean temperature and annual precipitation were significant predictors of lateral cranium size in spotted hyenas, with smaller centroid sizes occurring in drier ($p<0.001$) and cooler ($p< 0.001$) regions (Table 1.3). These variables were not, however, significant predictors of the centroid size of either the ventral cranium (Table 1.2) or lateral mandible (Table 1.4).

Vegetation type was a significant predictor of lateral cranium (Table 1.3) and lateral mandible (Table 4) centroid size, but not of ventral cranium centroid size (Table 1.2). Lateral crania ($p< 0.001$) were smaller in more closed habitats with trees (i.e., forest or mixed forest and grassland) than in more open habitats (i.e., grassland and bare ground), whereas lateral mandibles were largest in mixed forests and grassland. This contrasting relationship between size and habitat variables in lateral crania versus lateral mandibles seems surprising because these structures are expected to evolve concomitantly since they function together as a feeding apparatus. However, centroid size is not a linear measurement, rather it captures distances of each landmark from the centroid of the landmark configuration. Thus, changes in mandible shape, such as in the curvature of the coronoid process or the arch of the interparietal, will affect the magnitude of this metric. Additionally, the mandible of vertebrates is very plastic and has been shown to change shape with changes in dietary hardness (Mavropoulos, Bresin, & Kiliaridis, 2004; Meyer, 1987; Renaud, Auffray, & De la Porte, 2010; Scott, McAbee, Eastman, & Ravosa, 2014). Spotted hyenas are highly durophagous, relying on bone cracking to access marrow when prey are scarce, and may experience plastic shape change in the mandible over

the course of their lifetime.

3.4 | Hyena Density

Population density was a significant predictor of ventral ($p < 0.001$) and lateral ($p < 0.001$) cranium centroid size; larger skulls came from regions where population density is lower (Tables 1.2 and 1.3). Population density was not, however, a significant predictor of lateral mandible centroid size ($p=0.288$) (Table1. 4).

4 | DISCUSSION (overview)

Studying the patterns of size across geographic regions can provide insight into the interplay of environmental and social factors that drive morphological evolution. This study examines geographic variation in the size of spotted hyena skulls, a proxy for body size. Our aim was to identify how sex, bioclimatic variables, and population density co-vary with size in nature. In accord with earlier work (Swanson et al., 2013), we found significant female biased sexual dimorphism. Females are slightly larger on average than males (Table 1.5) and there is no evidence for geographical variation in sexual size dimorphism (Table 1.5). There is a marked tendency for the smallest individuals to occur clustered between -5.00^{o} and 10.00^{o} latitude and east of 28.50^{o} longitude, with larger individuals found elsewhere (Figure 1.1). This is not simply a latitudinal gradient as previously reported (Klein & Scott, 1989; Kurten, 1957) as individuals from western populations near the equator are not particularly small. Smaller lateral cranium sizes were associated with cooler, drier habitats, with trees (Table 1.3). Larger lateral mandible sizes were associated with habitats with a heterogenous vegetation structure (Table 1.4). Skull size and population density were inversely related, such that high density populations included the smallest individuals, and both skull size and density varied dramatically with geography (Tables 1.2-1.4; Figures 1.1 and 1.3). The highest densities and smallest skull sizes occur between 15.00 N^{o} and 10.00 S^{o} latitude, east of 28.50^{o} longitude (Figure 1.1).

4.1 | Sexual Dimorphism

Our finding that female spotted hyenas have larger craniums than males is in agreement with several previous studies (Arsznov, Lundrigan, Holekamp, & Sakai, 2010; Hans Kruuk, 1972; Mann, Frank, Glickman, & Towe, 2018; Matthews, 1939; Skinner, 1976; Swanson et al., 2013).

The ratio of mean female to mean male size was slightly, but significantly, greater than 1.00 for ventral and lateral craniums. These findings are comparable to those of Ralls (1976), who reported a 1.04 female to male ratio for mean head and body length in this species. They support the hypothesis proposed by Rensch (Rensch's rule), which predicts that in species with female biased sexual size dimorphism, the size difference between the sexes will be small (Bidau & Martinez, 2016; Rensch, 1950). Our results also suggest that Swanson et al. (2013) were correct in concluding that the size difference between male and female spotted hyenas is very small and thus not consistently detected when sample sizes are small.

In contrast to previous studies, our sample allowed examination of broad geographic patterns. Although there was no significant geographical variation in sexual dimorphism, spotted hyenas in the Small Cluster (Figure 1.1 and 1.3), where the smallest size and highest population densities occur, exhibit the largest female to male ratio for all views of the skull. Spotted hyena mothers help offspring, including those that are reproductively mature, gain access to resources during feeding competitions with conspecifics (Watts et al., 2009). Morphologically immature young in high-density populations, such as those found in the Small Cluster (Figure 1.3), presumably face especially fierce competition for resources. Even a small advantage might have a positive impact on their survival. Thus, even though not statistically significant, our finding of the largest female to male size ratio in areas with the highest competition is consistent with the argument that selection on female spotted hyenas for dominance over males may reflect the need for maternal assistance during the slow morphological development of young that prepares them for durophagy in adulthood, coupled with intense competition at kills (Tanner, Zelditch, Lundrigan, & Holekamp, 2010).

4.2 | Geography and Bioclimatic factors

We found that the smallest individuals occur in equatorial East Africa. The smallest on average, are within 160 km of the Aberdare Forest Reserve (Table 1.5). Due to living at high elevation, these spotted hyenas experience cold temperatures despite being located near the equator. If patterns in size were driven by thermoregulation, we would expect spotted hyenas in the Aberdare Forest Reserve to be larger. Our data are not consistent with Bergmann's rule in that individuals are larger everywhere else, including in low elevation equatorial regions west of the Albertine Rift. The smallest spotted hyena skulls are found, between -5.00^{o} and 10.00^{o} latitude and east of 28.50^{o} longitude, with larger individuals found elsewhere (Figure 1.1). Previous researchers have described geographic clines in body size of spotted hyenas. Hans Kruuk (1972) reported a Northwest-Southeast cline with larger spotted hyena skulls in Queen Elizabeth Park in Uganda than in the Serengeti. Sillero-Zubiri and Gottelli (1992) described a south-east cline in body mass with the lightest spotted hyenas being found in the Aberdare Forest. Kurten (1957), reported a two- direction cline, extending north and south from the equator for extant African and late Pleistocene Syrian and European populations of spotted hyenas. The smallest lower carnassial lengths were in the equatorial belt, and the lower carnassial lengths increased in size gradually to the north and south (Kurten, 1957). Klein and Scott (1989), described a tendency for spotted hyena carnassial length to increase with latitude in present-day Africa, suggesting that spotted hyena body size is inversely related to temperature, as predicted by Bergmann's rule. We suggest that the Kurten (1957) and Klein and Scott (1989) plots of lower carnassial lengths against latitude for spotted hyenas may have been overly influenced by the large numbers of individuals from the east. We cannot directly

compare our results to theirs, as they did not report longitude for specimens. We would thus caution against using spotted hyena carnassial length as an independent gauge of Pleistocene temperature variation, as our large sample of modern spotted hyenas did not conform well to Bergmann's rule.

Indeed, we found that annual mean temperature and annual precipitation were significant predictors for lateral cranium size, with smaller skulls found in cooler and dryer areas (Table 1.3). We also expected to find larger skulls and, by proxy, larger individuals in drier areas, because larger bodies retain moisture better than smaller bodies, which have a higher surface area to volume ratio (Hill, Wyse, Anderson, & Anderson, 2004; Hudson, 2018). Perhaps, finding smaller individuals in drier areas can be explained because it is more important to dissipate heat than to retain moisture (Hill et al., 2004; Hudson, 2018). A greater surface area to volume ratio allows heat to dissipate. The pattern of smaller lateral crania in dry and cool areas may be an artifact of some other relationship related to geographic area that we did not measure. Other factors, such as seasonality of precipitation, temperature fluctuations or prey abundance, could potentially have a greater impact on spotted hyena size than our measurements of bioclimatic variables.

We expected land cover to influence spotted hyena size because land cover provides habitat for prey, influences prey abundance, and affects predator navigation and perception. We found smaller lateral crania in forest, mixed grassland, and forest than in grassland or bare ground. Sillero-Zubiri and Gottelli (1992), also found small spotted hyenas in the forest of the Aberdares Open grassland habitats in East Africa have higher densities of prey compared to the montane forest of the Aberdares (Massey, King, & Foufopoulos, 2014; Anthony Ronald Entrican

Sinclair & Arcese, 1995). Spotted hyena density in the Aberdares exceeds one animal per square kilometer (Sillero-Zubiri & Gottelli, 1992). Fewer prey and higher densities of spotted hyenas result in less food per capita. Thus, smaller spotted hyenas in forests may be a consequence of limited resources in forested habitats with higher densities of spotted hyenas, providing empirical evidence for the energetic equivalence rule (Damuth, 1981).

4.3 | Hyena density

Skull size, and by proxy body size, of spotted hyenas varies with geography but does not adhere to strict geographical and ecological rules such as Bergmann's rule. We found that spotted hyena crania were smaller in areas characterized by higher population densities (Table 1.2-1.3). This pattern is congruent with the energetic equivalence rule (Damuth, 1981), and is consistent with what has been seen in some other mammals (red fox: Cavallini, 1995; primates: Clutton-Brock & Harvey, 1977; moose: Sand et al., 1995; white-tailed deer: Simard et al., 2008; reindeer: Skogland, 1983; brown bear: Zedrosser et al., 2006). It suggests that intraspecific competition for resources is an important driver of cranium size in spotted hyena. The smallest skulls for all three views were from East Africa where clan sizes are known to reach over 100 (Green, Johnson-Ulrich, Couraud, & Holekamp, 2018). Not only do spotted hyenas compete with conspecifics for resources, but with other carnivores as well. Kleptoparasitism of spotted hyena kills by lions is common throughout Africa (Höner, Wachter, East, & Hofer, 2002; Watts & Holekamp, 2008). It is particularly intense in eastern Africa because, with the exception of one population in Botswana, all lion populations greater than 2000 individuals are found in eastern Africa (Riggio et al., 2013). Thus, the true effect of competition is only realized when

interspecific competition is also considered. Although we did not directly test the influence of competition with lions and other carnivores on spotted hyena size our results suggest that intense resource competition with both conspecifics and other carnivores may drive spotted hyenas to be smaller in eastern Africa as predicted by the energetic equivalence rule (Damuth, 1981).

An important limitation of this study is the sparse and incomplete sampling from western tropical Africa. We were restricted to specimens present in museum collections, and most collections contain very few individuals from western Africa. In addition, specimens in collections rarely represent systematically collected samples. Specimens in collections are often opportunistically collected and include donations from big game hunters, which could lead to biases in size and locality. Thirdly, density data for spotted hyenas were available for a few localities and we used interpolation methods to infer density for areas without density data. Fourth, skull size may be an imperfect proxy for body size.

We examined the relationship between bioclimatic factors, social factors, and spotted hyena skull size to better understand the forces that might underlie geographic patterns in size. Sexual size dimorphism, with females being larger than males, in spotted hyenas is small but significant, and there is little evidence for geographic variation in sexual size dimorphism. There is a strong tendency for the smallest individuals of both sexes to occur in the small cluster between -5.00^{o} and 10.00^{o} latitude and east of 28.50^{o} longitude, with larger individuals found elsewhere. Spotted hyena skull size co-varies with temperature, precipitation and landcover but much more strongly co-varies with population density. The highest densities are associated with the smallest skull size, possibly reflecting a relationship between high population density

and access to resources. Our findings support the idea that the underlying driver of geographical and ecological rules is access to resources, providing further empirical evidence for the energetic equivalence rule.

APPENDICES

APPENDIX A

FIGURES AND TABLES

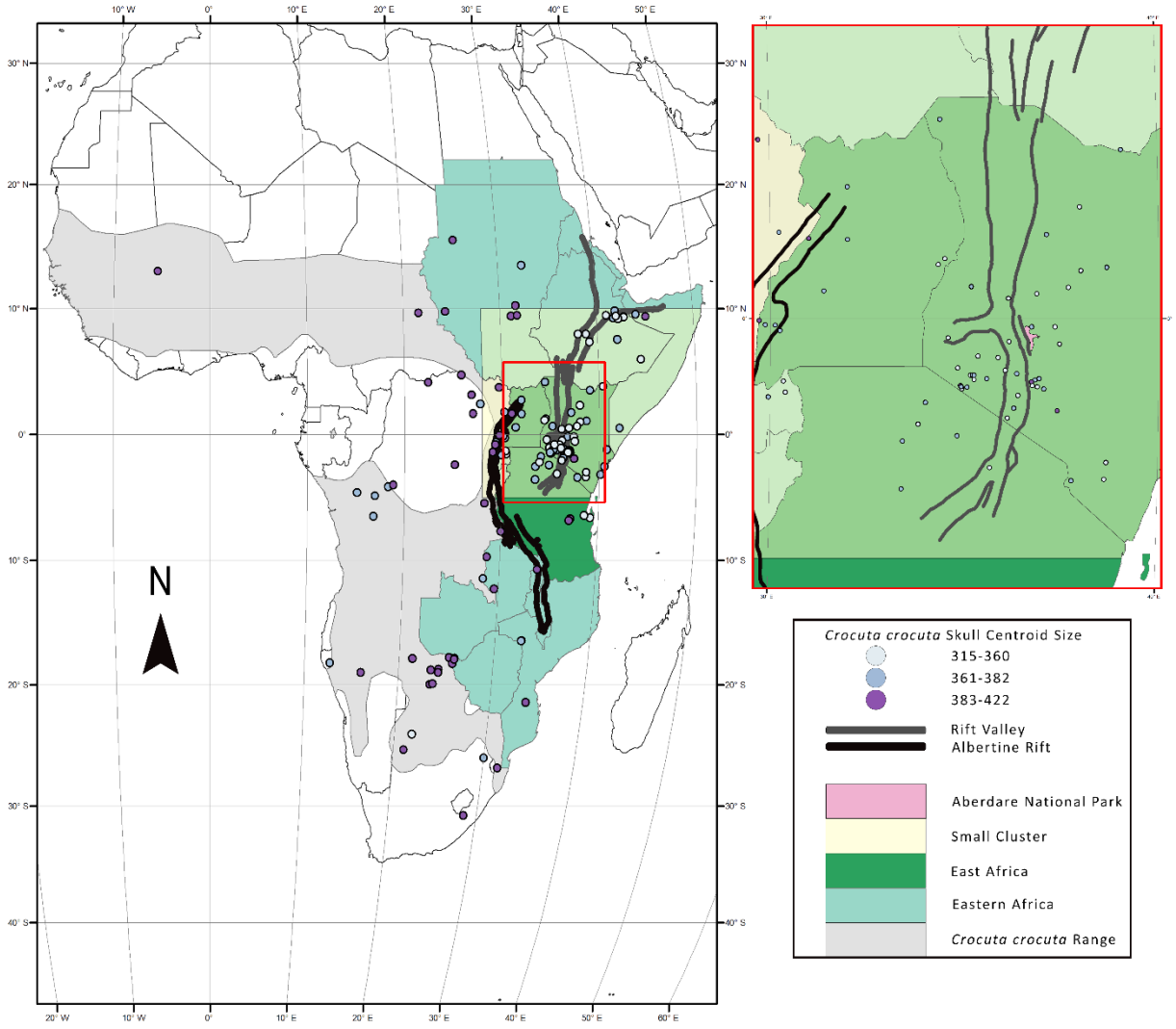

Figure 1.1: Specimen collecting localities (points) for *Crocuta crocuta* skulls used in this study. Point color represents centroid sizes: 315-360 light grayish blue; 361-382 slightly desaturated blue; 383-422 dark moderate violet. The Rift valley (grey) and the Albertine rift (black) are indicated by heavy lines. A region of especially dense sampling that encompasses the Aberdare National Park (pink) is enclosed by a red box and enlarged. The area with the cluster of the smallest individuals is labeled Small Cluster and shaded in 50% transparent yellow. East Africa is shaded in dark green and Eastern Africa is shaded in medium green. The current geographical range for *Crocuta crocuta* is shaded in grey.

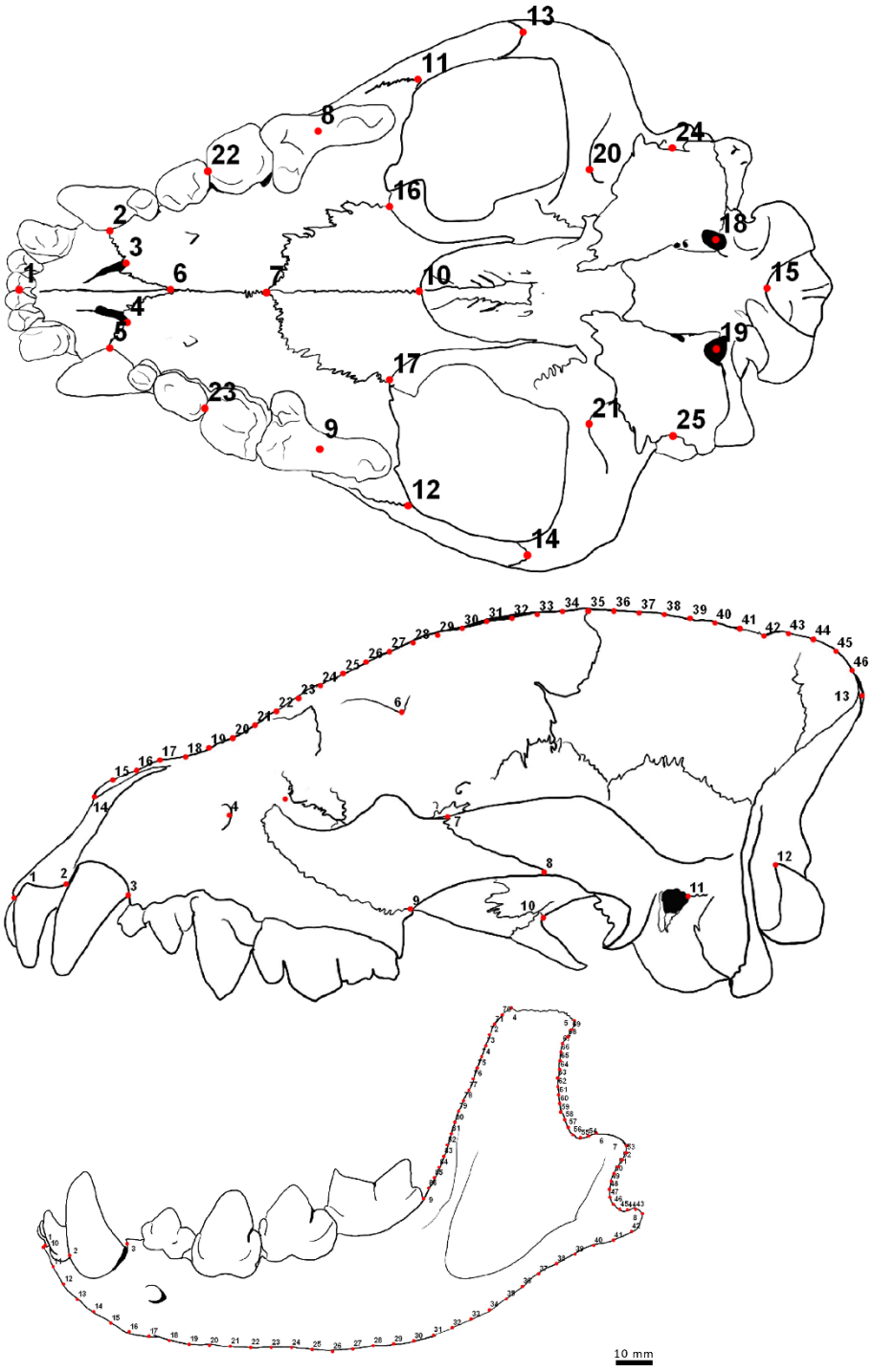

Figure 1.2: Position of landmarks and semilandmarks on a skull of spotted hyena (*Crocuta crocuta*) for the ventral cranium, lateral cranium, and lateral mandible. Landmarks and semilandmarks are numbered and represented by red points.

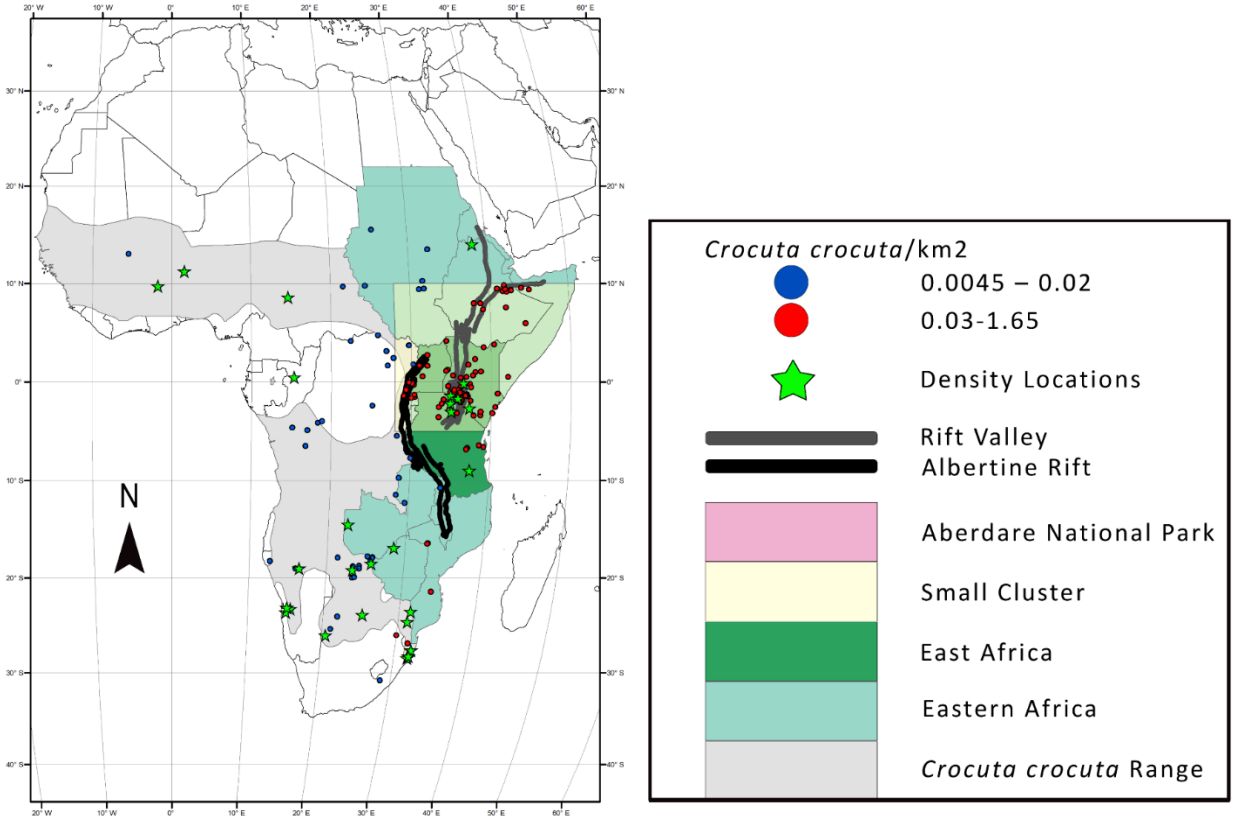

Figure 1.3: Locations for spotted hyena (*Crocuta crocuta*) density estimates listed in Table 1.1 (green stars) and interpolated density estimates corresponding with specimen collecting sites (dots): blue low density (0.0045 – 0.02 spotted hyena/km2; n=60) and red high density (0.03-1.65 spotted hyena/km2; n=260) high density.

Table 1.1: Locality, country, population density estimate (hyenas/ km2), years(s) of study, and source for spotted hyena (*Crocuta crocuta*) densities used in this analysis (see Fig 3 for map). NP = National Park; GR = Game Reserve.

Locality	Country	Density (km^2)	Year(s)	References
Pendjari NP	Benin	0.02	2001-2009	Sogbohossou & Tehou 2007
Chobe NP	Botswana	0.44	1986-1988	Cooper 1989
Moremi GR	Botswana	0.14	2007-2010	Cozzi et al. 2013
Benoue ecosystem	Cameroon	0.06	2015	Bauer et al. 2015
Tigray (Wukro Dist.)	Ethiopia	0.52	2011	Yirga et al. 2013
Tigray (Enderta Dist.)	Ethiopia	0.8	2012	Yirga et al. 2017
Mole NP	Ghana	0.14	2006-2009	Takahashi & Burton 2010
Masai Mara NR	Kenya	0.86	1979-1983	Frank 1986
Aberdares NP	Kenya	1.34	1986-1987	Sillero-Zubiri & Gottelli 1992
Masai Mara	Kenya	0.94	1988-1992	Watts & Holekamp 2008
Amboseli NP	Kenya	1.65	2003-2005	Watts & Holekamp 2008
Namib-Naukluft NP	Namibia	0.005	1976-1977	Tilson et al. 1980
Namib-Naukluft NP	Namibia	0.009	1977-1979	Tilson & Henschel 1986
Etosha NP	Namibia	0.05	1986	Gasaway et al. 1989
Etosha NP	Namibia	0.02	2008	Trinkel 2009
Odzala-Kotoua	Republic of Congo	0.46	1975-1977	Whateley & Brooks 1978
Odzala-Kotoua NP	Republic of Congo	0.16	2007	Henschel et al. 2014
Timbavati GR	South Africa	0.48	1973-1975	Bearder 1977
Kruger NP	South Africa	0.32	1974-1975	Smuts 1978
Hluhluwe NP	South Africa	0.46	1975-1977	Whateley & Brooks 1978

Table 1.1 (cont'd)

Locality	Country	Density (km^2)	Year(s)	References
Umfolozi GR	South Africa	0.36	1979-1981	Whateley 1981
Kalahari Gemsbok NP	South Africa	0.009	1979-1984	Mills 1984
Kruger NP	South Africa	0.13	1982-1984	Henschel & Skinner 1987
Kruger NP	South Africa	0.19	1984-1989	Mills et al. 2001
Mkuze GR	South Africa	0.13	1989	Skinner et al. 1992
Hluhluwe-iMfolozi	South Africa	0.36	2003-2004	Graf et al. 2009
Serengeti	Tanzania	0.17	1965-1967	Kruuk 1972
Ngorongoro	Tanzania	1.54	1965-1967	Kruuk 1972
Selous GR	Tanzania	0.31	1991-1996	Creel & Creel 2002
Ngorongoro	Tanzania	0.59	1996	Honer et al. 2005
Liuwa Plains NP	Zambia	0.33	1995-1999	Purchase 2004
Hwange NP	Zimbabwe	0.07	1999-2003	Salnicki 2004

Table 1.2: Regression of *Crocuta crocuta* ventral cranium size onto geographic, environmental and social variables: Estimate, Standard Error, t value, and p-values. Residual standard error: 13.61 on 295 degrees of freedom, Multiple R-squared: 0.4476, Adjusted R-squared: 0.4026, F-statistic: 9.958 on 24 and 295 DF, p-value: < 0.001 for full model. X represents longitude and Y represents latitude. For factor variables sex female, density low and vegetation type forest were set at reference levels.

Variables	estimate	SE	*t*	*p*
(Intercept)	-213.905	143.160	-1.494	**0.136***
X	65.994	15.527	4.250	**0.000***
X^2	-2.216	0.528	-4.195	**0.000***
X^3	0.024	0.006	4.095	**0.000***
Y	-10.380	4.158	-2.497	**0.013***
Y^2	0.843	0.737	1.144	0.254
Y^3	0.179	0.048	3.722	**0.000***
Y^4	0.010	0.004	2.218	**0.027***
$X * Y^2$	-0.066	0.050	-1.309	0.191
$X * Y^3$	-0.012	0.003	-3.804	**0.000***
$X * Y^4$	-0.001	0.000	-2.070	**0.039***
$X^2 * Y$	0.035	0.012	2.795	**0.006***
$X^2 * Y^2$	0.001	0.001	1.412	0.159
$X^2 * Y^3$	0.000	0.000	3.607	**0.000***
$X^2 * Y^4$	0.000	0.000	1.893	**0.059***
$X^3 * Y$	-0.001	0.000	-2.893	**0.004***
$X^3 * Y^4$	0.000	0.000	-1.723	0.086
Sex male	-4.766	1.829	-2.606	**0.010***
Sex unknown	-6.006	2.195	-2.736	**0.007***
Annual mean temperature	-0.028	0.032	-0.882	0.379
Annual precipitation	-0.009	0.005	-1.713	0.088
Density high	-19.787	4.888	-4.048	**0.000***
Mixed forest and grassland	2.781	2.415	1.151	0.250
Grassland	1.448	3.277	0.442	0.659
Bare ground	7.859	7.182	1.094	0.275

Table 1.3: Regression of *Crocuta crocuta* lateral cranium size onto geography, environmental and social variables: Estimate, Standard Error, t value, and p-values. Residual standard error: 39.75 on 299 degrees of freedom, Multiple R-squared: 0.5758, Adjusted R-squared: 0.5488, F-statistic: 21.36 on 19 and 299 DF, p-value: < 0.001 for full model. X represents longitude and Y represents latitude. For factor variables sex female, density low and vegetation type forest were set at reference levels.

Variables	estimate	SE	*T*	*p*
(Intercept)	837.393	30.003	27.910	**0.000***
Y	-42.045	20.725	-2.029	**0.043***
Y^3	0.230	0.112	2.042	**0.042***
$X^2 * Y$	-0.232	0.087	-2.662	**0.008***
$X^2 * Y^3$	0.001	0.001	2.241	**0.026***
$X^2 * Y^4$	0.000	0.000	3.244	**0.001***
X^3	-0.001	0.000	-1.868	0.063
$X^3 * Y$	0.003	0.001	2.528	**0.012***
$X^3 * Y^3$	0.000	0.000	-2.016	**0.045***
*X * Y*	6.044	2.361	2.560	**0.011***
$X * Y\text{^}3$	-0.034	0.015	-2.301	**0.022***
$X * Y^4$	0.000	0.000	-3.289	**0.001***
Sex male	-12.994	5.278	-2.462	**0.014***
Sex unknown	-9.635	6.269	-1.537	0.125
Annual mean temperature	-0.710	0.077	-9.255	**0.000***
Annual precipitation	-0.051	0.011	-4.535	**0.000***
Density high	-54.211	10.855	-4.994	**0.000***
Mixed forest and grassland	-34.496	6.707	-5.143	**0.000***
Grassland	-49.270	8.497	-5.798	**0.000***

Table 1.4: Regression of *Crocuta crocuta* lateral mandible size onto geography, environmental and social variables: Estimate, Standard Error, t value, and p-values. Residual standard error: 19.15 on 307 degrees of freedom, Multiple R-squared: 0.5254, Adjusted R-squared: 0.4883, F-statistic: 14.16 on 24 and 307 DF, p-value: < 0.001 for full model. X represents longitude and Y represents latitude. For factor variables sex female, density low and vegetation type forest were set at reference levels.

Variables	estimate	SE	*t*	*p*
(Intercept)	304.102	85.667	3.550	**0.000***
Y	27.247	10.142	2.686	**0.008***
Y^2	1.630	0.497	3.283	**0.001***
Y^3	-0.084	0.032	-2.667	**0.008***
Y^4	-0.006	0.002	-3.912	**0.000***
X	31.276	10.266	3.046	**0.003***
X^2	-1.105	0.374	-2.954	**0.003***
$X^2 * Y$	0.118	0.043	2.722	**0.007***
$X^2 * Y^2$	0.003	0.001	3.273	**0.001***
$X^2 * Y^3$	0.000	0.000	-2.874	**0.004***
$X^2 * Y^4$	0.000	0.000	-3.911	**0.000***
X^3	0.012	0.004	2.770	**0.006***
$X^3 * Y$	-0.001	0.001	-2.740	**0.006***
$X * Y$	-3.100	1.159	-2.674	**0.008***
$X * Y^2$	-0.125	0.040	-3.150	**0.002***
$X * Y^3$	0.006	0.002	2.671	**0.008***
$X * Y^4$	0.001	0.000	3.773	**0.000***
Sex male	-1.516	2.518	-0.602	0.548
Sex unknown	-2.283	3.005	-0.760	0.448
Annual mean temperature	0.063	0.042	1.487	0.138
Annual precipitation	0.001	0.007	0.116	0.908
Density high	-6.570	6.173	-1.064	0.288
Mixed forest and grassland	8.767	3.235	2.710	**0.007***
Grassland	-0.249	3.992	-0.062	0.950
Sex male	14.459	9.503	1.522	0.129

Table 1.5: *Crocuta crocuta* mean centroid size, standard deviation and sample size for different regions of Africa for three skull views. eastern (east of the Nile and the east African lake system), western (west of the Nile and the east African lake system); and southern (south of the east African lake system). Mean female/mean male centroid size, and sample sizes (Female n; Male n).

	Skull view	Mean	SD	n	mean female/male	female n; male n
Total Africa	Ventral Cranium	368.89	±17.30	331	1.011637	115; 122
	Lateral Cranium	539.77	±59.25	337	1.01122	114; 122
	Lateral Mandible	575.65	±26.77	332	1.007275	121; 125
Western	Ventral Cranium	385.97	±16.01	50	1.028634	10; 12
	Lateral Cranium	541.16	±24.55	52	1.005448	11; 12
	Lateral Mandible	596.05	±25.79	58	0.9970687	13 12
Eastern	Ventral Cranium	363.39	±13.38	256	1.014775	100; 102
	Lateral Cranium	539.87	±65.89	262	1.01168	96; 103
	Lateral Mandible	566.61	±19.38	248	1.009602	102; 104
Southern	Ventral Cranium	390.04	±15.58	24	0.9599159	4; 8
	Lateral Cranium	536.07	±26.76	22	1.019905	4; 8
	Lateral Mandible	616.81	±28.51	24	1.025117	4; 9
Aberdare	Ventral Cranium	362.95	±12.09	40	1.004546	12; 8
	Lateral Cranium	497.85	±42.95	36	1.011846	4; 4
	Lateral Mandible	563.99	±20.04	19	1.031449	5; 4

APPENDIX B

SPECIMENS LIST

Table 1.6: *Crocuta crocuta* specimens ventral cranium

Crocuta crocuta specimens ventral cranium	
Museum	Catalog Number
AMNH	114227
AMNH	114256
AMNH	165118
AMNH	165119
AMNH	187769
AMNH	187771
AMNH	187772
AMNH	187776
AMNH	187777
AMNH	187779
AMNH	187782
AMNH	20809
AMNH	20810
AMNH	216355
AMNH	27765
AMNH	27767
AMNH	52059
AMNH	52060
AMNH	52063
AMNH	52064
AMNH	52065
AMNH	52068
AMNH	52069
AMNH	52097
AMNH	54243
AMNH	54244
AMNH	55467
AMNH	81833
AMNH	83591
AMNH	83592
AMNH	83593
BM	3441136
BM	314113
BM	39383
BM	01031
BM	031822
BM	0862
BM	18927

Table 1.6 (cont'd)

BM	19613
BM	2854
BM	21291030
BM	233414
BM	233415
BM	233416
BM	233419
BM	25124233
BM	27299
BM	27738A
BM	27738
BM	281163
BM	291138
BM	3012182
BM	311211
BM	3441137
BM	3441138
BM	3441139
BM	3441140
BM	38101847
BM	385102
BM	385103
BM	39339
BM	39340
BM	39342
BM	39343
BM	39344
BM	39345
BM	39346
BM	39348
BM	39349
BM	39351
BM	39353
BM	39355
BM	39356
BM	39358
BM	39360
BM	39361
BM	39362
BM	39363
BM	39364

Table 1.6 (cont'd)

BM	39366
BM	39368
BM	39369
BM	39370
BM	39373
BM	39375
BM	39376
BM	39378
BM	39381
BM	39382
BM	39387
BM	39388
BM	39389
BM	39390
BM	39391
BM	39394
BM	39395
BM	39396
BM	39397
BM	39399
BM	39400
BM	39401
BM	39402
BM	39403
BM	39404
BM	39407
BM	39408
BM	39409
BM	39410
BM	39411
BM	39412
BM	39413
BM	39414
BM	39416
BM	39417
BM	39419
BM	39420
BM	39421
BM	39422
BM	39423
BM	39424

Table 1.6 (cont'd)

BM	39425
BM	39427
BM	39428
BM	39429
BM	39430
BM	39431
BM	39432
BM	39433
BM	39435
BM	39437
BM	58208
BM	62706
BM	62707
BM	96114
BM	9 6 1 14
BM	92 8 1 4
Cambridge	K4062
Cambridge	K4065
Cambridge	K4067
CM	20871
CM	5862
CM	63108
FMNH	104021
FMNH	104981
FMNH	127825
FMNH	127826
FMNH	127829
FMNH	135072
FMNH	32933
FMNH	34582
FMNH	34583
FMNH	73034
FMNH	73035
FMNH	98739
FMNH	98952
MSU	37464-BFT
MSU	37465-ECO
MSU	37466-VGS
MSU	36550
MSU	36551
MSU	36552

Table 1.6 (cont'd)

MSU	36558
MSU	36567
MSU	36568
MSU	36569
MSU	36570
MSU	36571
MSU	36581
MSU	12391
MSU	22401
MSU	26055
MSU	2714
MSU	35852
MSU	35853
MSU	35854
MSU	35856
MSU	35857
MSU	35858
MSU	36008
MSU	36011
MSU	36074
MSU	36077
MSU	36078
MSU	36079
MSU	36080
MSU	36083
MSU	36084
MSU	36094
MSU	36160
MSU	36161
MSU	36163
MSU	36165
MSU	36168
MSU	8048
MVZ	165159
MVZ	165160
MVZ	165162
MVZ	165163
MVZ	165165
MVZ	165166
MVZ	165167
MVZ	165169

Table 1.6 (cont'd)

MVZ	165170
MVZ	165175
MVZ	165176
MVZ	165179
MVZ	165180
MVZ	165181
MVZ	165182
MVZ	173733
MVZ	173734
MVZ	173737
MVZ	173743
MVZ	173746
MVZ	173747
MVZ	173748
MVZ	173751
MVZ	173758
MVZ	173759
MVZ	173768
MVZ	173770
MVZ	173771
NMK	175801
NMK	184088
NMK	184089
NMK	2705
NMK	3580
NMK	7189
NMK	7755
NMK	7757
NMK	7761
NMK	7762
NMK	7850
NMNH (USNM)	164506
NMNH (USNM)	164549
NMNH (USNM)	020874
NMNH (USNM)	163099
NMNH (USNM)	163100
NMNH (USNM)	163101
NMNH (USNM)	163102
NMNH (USNM)	163103
NMNH (USNM)	164502
NMNH (USNM)	181516

Table 1.6 (cont'd)

NMNH (USNM)	181518
NMNH (USNM)	181519
NMNH (USNM)	181520
NMNH (USNM)	181521
NMNH (USNM)	181524
NMNH (USNM)	181525
NMNH (USNM)	181526
NMNH (USNM)	181527
NMNH (USNM)	181530
NMNH (USNM)	181533
NMNH (USNM)	181534
NMNH (USNM)	182032
NMNH (USNM)	182085
NMNH (USNM)	182091
NMNH (USNM)	182095
NMNH (USNM)	182103
NMNH (USNM)	182113
NMNH (USNM)	182210
NMNH (USNM)	201010
NMNH (USNM)	239161
NMNH (USNM)	367384
NMNH (USNM)	367385
NMNH (USNM)	368502
NMNH (USNM)	429176
OSU	11969
OSU	11970
OSU	4640
OSU	4650
OSU	4651
OSU	4682
OSU	5711
OSU	5761
PMNHN-OM	MNHNCA1896-450
PMNHN-OM	MNHNCA1894-54
PMNHN-OM	MNHNZ1962-1537
PMNHN-OM	MNHNZ1972-400
PMNHN-OM	MNHNZ1996-2514
PMNHN-OM	MNHNZ1997-415
RBINS	10250
RBINS	10336
RBINS	11799

Table 1.6 (cont'd)

RBINS	11801
RBINS	21278
RBINS	21302
RBINS	21436
RBINS	4612
RBINS	8632
RBINS	8633
RBINS	8634
RBINS	9480
RCSOM	16.5
RCSOM	137.41
RCSOM	137.42
RCSOM	137.43
RMCA	11376
RMCA	11602
RMCA	11701
RMCA	12096
RMCA	12442
RMCA	14367
RMCA	14369
RMCA	14813
RMCA	16719
RMCA	17619
RMCA	18495
RMCA	18627
RMCA	1897
RMCA	2162
RMCA	22802
RMCA	2907
RMCA	36328
RMCA	36543
RMCA	36545
RMCA	3728
RMCA	3788
RMCA	3870
RMCA	5934
RMCA	9292

Table 1.7: *Crocuta crocuta* specimens lateral cranium

Crocuta crocuta specimens lateral cranium	
Museum	Catalog Number
AMNH	114227
AMNH	114256
AMNH	165119
AMNH	187769
AMNH	187771
AMNH	187772
AMNH	187776
AMNH	187777
AMNH	187779
AMNH	187780
AMNH	20809
AMNH	20810
AMNH	216355
AMNH	27765
AMNH	27767
AMNH	52059
AMNH	52060
AMNH	52063
AMNH	52064
AMNH	52065
AMNH	52068
AMNH	52069
AMNH	52097
AMNH	54243
AMNH	54244
AMNH	55467
AMNH	81833
AMNH	83591
AMNH	83592
AMNH	83593
BM	27299
BM	385102
BM	39337
BM	39339
BM	39340
BM	39342
BM	39343
BM	39344

Table 1.7 (cont'd)

BM	39345
BM	39346
BM	39348
BM	39349
BM	39351
BM	39353
BM	39355
BM	39356
BM	39358
BM	39360
BM	39361
BM	39362
BM	39363
BM	39364
BM	39366
BM	39368
BM	39369
BM	39370
BM	39373
BM	39375
BM	39376
BM	39378
BM	39381
BM	39382
BM	39383
BM	39385
BM	39386
BM	39387
BM	39388
BM	39389
BM	39390
BM	39391
BM	39394
BM	39395
BM	39396
BM	39397
BM	39399
BM	39400
BM	39401
BM	39402

Table 1.7 (cont'd)

BM	39407
BM	39403
BM	39404
BM	39408
BM	39409
BM	39410
BM	39411
BM	39412
BM	39413
BM	39414
BM	39416
BM	39417
BM	39419
BM	39420
BM	39421
BM	39422
BM	39423
BM	39424
BM	39425
BM	39427
BM	39428
BM	39429
BM	39430
BM	39431
BM	39432
BM	39433
BM	39435
BM	39437
BM	031822
BM	0862
BM	18927
BM	153690
BM	19613
BM	233414
BM	233415
BM	233416
BM	233419
BM	27738A
BM	27738
BM	281163
BM	291138

Table 1.7 (cont'd)

BM	314113
BM	3012182
BM	311211
BM	3441136
BM	3441137
BM	3441138
BM	3441139
BM	3441140
BM	38101847
BM	385103
BM	58208
BM	62706
Bm	62707
BM	96114
BM	92814
Cambridge	K4062
Cambridge	K4065
Cambridge	K4067
CM	20871
CM	5862
CM	63108
FMNH	104021
FMNH	104981
FMNH	127825
FMNH	127826
FMNH	127829
FMNH	32933
FMNH	34582
FMNH	34583
FMNH	73034
FMNH	73035
FMNH	98739
FMNH	98952
MSU	35852
MSU	35854
MSU	35856
MSU	36008
MSU	36011
MSU	36077
MSU	36079
MSU	36083

Table 1.7 (cont'd)

MSU	36168
MSU	36084
MSU	36163
MSU	36550
MSU	36551
MSU	36552
MSU	36558
MSU	36567
MSU	36568
MSU	36569
MSU	36570
MSU	36571
MSU	37464
MSU	37465
MSU	37466
MSU	36165
MSU	36581
MSU	22401
MSU	24292
MSU	26055
MSU	2714
MSU	35853
MSU	35857
MSU	35858
MSU	36074
MSU	36078
MSU	36080
MSU	36094
MSU	36160
MSU	36161
MSU	8048
MSU	987
MSU	115
MVZ	165159
MVZ	165160
MVZ	165162
MVZ	165163
MVZ	165165
MVZ	165167
MVZ	165169
MVZ	165170

Table 1.7 (cont'd)

MVZ	165179
MVZ	165175
MVZ	165176
MVZ	165180
MVZ	165181
MVZ	165182
MVZ	173733
MVZ	173734
MVZ	173737
MVZ	173741
MVZ	173743
MVZ	173746
MVZ	173747
MVZ	173751
MVZ	173754
MVZ	173758
MVZ	173759
MVZ	173768
MVZ	173771
MVZ	175801
MVZ	184088
MVZ	184089
NMK	2703
NMK	2705
NMK	3580
NMK	7850
NMNH (USNM)	020874
NMNH (USNM)	163099
NMNH (USNM)	163100
NMNH (USNM)	163101
NMNH (USNM)	163102
NMNH (USNM)	163103
NMNH (USNM)	164502
NMNH (USNM)	164506
NMNH (USNM)	164549
NMNH (USNM)	181516
NMNH (USNM)	181518
NMNH (USNM)	181519
NMNH (USNM)	181520
NMNH (USNM)	181521
NMNH (USNM)	181524

Table 1.7 (cont'd)

NMNH (USNM)	181527
NMNH (USNM)	181525
NMNH (USNM)	181526
NMNH (USNM)	181530
NMNH (USNM)	181533
NMNH (USNM)	181534
NMNH (USNM)	182032
NMNH (USNM)	182085
NMNH (USNM)	182091
NMNH (USNM)	182095
NMNH (USNM)	182103
NMNH (USNM)	182105
NMNH (USNM)	182113
NMNH (USNM)	182117
NMNH (USNM)	182210
NMNH (USNM)	201010
NMNH (USNM)	239161
NMNH (USNM)	367384
NMNH (USNM)	367385
NMNH (USNM)	368502
NMNH (USNM)	429176
OSU	11969
OSU	11970
OSU	4640
OSU	4650
OSU	4651
OSU	4682
OSU	5711
OSU	5761
PMNHN-AC	MNHNCA1894-54
PMNHN-AC	MNHNCA1896-450
PMNHN-OM	MNHNZ1962-1537
PMNHN-OM	MNHNZ1972-400
PMNHN-OM	MNHNZ1996-2514
PMNHN-OM	MNHNZ1997-415
RBINS	11801
RBINS	10250
RBINS	10336
RBINS	11799
RBINS	21278
RBINS	21302

Table 1.7 (cont'd)

RBINS	8632
RBINS	21436
RBINS	4612
RBINS	8633
RBINS	8634
RBINS	9480
RCSOM	137.41
RCSOM	137.43
RCSOM	16.5
RCSOM	137.42
RMCA	11376
RMCA	11602
RMCA	12096
RMCA	12442
RMCA	14367
RMCA	14369
RMCA	14813
RMCA	16719
RMCA	16786
RMCA	17619
RMCA	18000
RMCA	18495
RMCA	18627
RMCA	1897
RMCA	2162
RMCA	22802
RMCA	2907
RMCA	36328
RMCA	36543
RMCA	36545
RMCA	3728
RMCA	3788
RMCA	3870
RMCA	5934
RMCA	9292

Table 1.8: *Crocuta crocuta* specimens mandible

Crocuta crocuta specimens mandible	
Museum	Catalog Number
AMNH	114226
AMNH	114227
AMNH	114256
AMNH	165118
AMNH	165119
AMNH	187769
AMNH	187771
AMNH	187772
AMNH	187776
AMNH	187777
AMNH	187782
AMNH	20809
AMNH	20810
AMNH	216355
AMNH	27765
AMNH	27767
AMNH	52059
AMNH	52060
AMNH	52063
AMNH	52064
AMNH	52065
AMNH	52068
AMNH	52069
AMNH	52097
AMNH	54243
AMNH	54244
AMNH	55467
AMNH	83591
AMNH	83592
AMNH	83593
BM	34 4 1 134
BM	0 10 3 1
BM	0 3 18 22
BM	1 8 9 27
BM	15 3 6 90
BM	19 6 1 3
BM	2 8 5 4
BM	21 29 10 30

Table 1.8 (cont'd)

BM	23 3 4 15
BM	23 3 4 11
BM	23 3 4 14
BM	23 3 4 19
BM	24 8 3 4
BM	24 8 3 74
BM	25 12 4 233
BM	27 2 9 9
BM	27 7 3 8A
BM	27 7 3 8
BM	28 11 6 3
BM	29 11 3 8
BM	30 12 182
BM	31 1 2 11
BM	31 4 1 13
BM	34 4 1 136
BM	34 4 1 137
BM	34 4 1 138
BM	34 4 1 139
BM	34 4 1 140
BM	38 10 18 47
BM	38 5 10 2
BM	38 5 10 3
BM	39 337
BM	39 339
BM	39 340
BM	39 342
BM	39 343
BM	39 344
BM	39 345
BM	39 346
BM	39 348
BM	39 349
BM	39 351
BM	39 353
BM	39 356
BM	39 358
BM	39 359
BM	39 360
BM	39 361
BM	39 362

Table 1.8 (cont'd)

BM	39 368
BM	39 363
BM	39 364
BM	39 366
BM	39 369
BM	39 370
BM	39 373
BM	39 375
BM	39 376
BM	39 378
BM	39 381
BM	39 383
BM	39 385
BM	39 386
BM	39 387
BM	39 388
BM	39 389
BM	39 390
BM	39 391
BM	39 394
BM	39 395
BM	39 396
BM	39 397
BM	39 399
BM	39 400
BM	39 401
BM	39 402
BM	39 403
BM	39 404
BM	39 407
BM	39 408
BM	39 409
BM	39 410
BM	39 411
BM	39 412
BM	39 413
BM	39 414
BM	39 416
BM	39 417
BM	39 419
BM	39 420

Table 1.8 (cont'd)

BM	39 425
BM	39 421
BM	39 422
BM	39 423
BM	39 424
BM	39 427
BM	39 428
BM	39 429
BM	39 430
BM	39 431
BM	39 432
BM	39 433
BM	39 435
BM	39 437
BM	58 208
BM	59 272
BM	62 706
BM	62 707
BM	66 792
BM	9 6 1 14
BM	92 8 1 4
Cambridge	K4062
Cambridge	K4065
Cambridge	K4067
CM	20871
CM	5862
CM	63108
CM	6827
FMNH	104021
FMNH	104981
FMNH	127825
FMNH	127826
FMNH	127829
FMNH	32933
FMNH	34582
FMNH	34583
FMNH	73034
FMNH	73035
FMNH	93866
FMNH	98739
FMNH	98952

Table 1.8 (cont'd)

MSU	36011
MSU	225 VGS
MSU	35852
MSU	35854
MSU	35856
MSU	36008
MSU	36077
MSU	36079
MSU	36083
MSU	36084
MSU	36163
MSU	36165
MSU	36168
MSU	36550
MSU	36551
MSU	36552
MSU	36558
MSU	36567
MSU	36568
MSU	36569
MSU	36570
MSU	36571
MSU	36581
MSU	486 ECO
MSU	897 BFT
MSU	12391
MSU	22401
MSU	24292
MSU	26055
MSU	2714
MSU	35853
MSU	35857
MSU	35858
MSU	36074
MSU	36078
MSU	36080
MSU	36094
MSU	36160
MSU	36161
MSU	8048
MSU	NHM115

Table 1.8 (cont'd)

MVZ	165170
MVZ	165160
MVZ	165162
MVZ	165163
MVZ	165165
MVZ	165167
MVZ	165169
MVZ	165175
MVZ	165176
MVZ	165179
MVZ	165180
MVZ	165181
MVZ	165182
MVZ	173733
MVZ	173734
MVZ	173737
MVZ	173741
MVZ	173743
MVZ	173745
MVZ	173746
MVZ	173751
MVZ	173768
MVZ	173770
MVZ	173771
MVZ	175801
MVZ	184088
MVZ	184089
NMK	2703
NMK	2705
NMK	7189
NMK	7755
NMK	7757
NMK	7761
NMK	7762
NMK	7850
NMNH (USNM)	020874
NMNH (USNM)	122544
NMNH (USNM)	163099
NMNH (USNM)	163100
NMNH (USNM)	163101
NMNH (USNM)	163102

Table 1.8 (cont'd)

NMNH (USNM)	181520
NMNH (USNM)	163103
NMNH (USNM)	164502
NMNH (USNM)	164506
NMNH (USNM)	164549
NMNH (USNM)	181516
NMNH (USNM)	181518
NMNH (USNM)	181519
NMNH (USNM)	181521
NMNH (USNM)	181524
NMNH (USNM)	181525
NMNH (USNM)	181526
NMNH (USNM)	181527
NMNH (USNM)	181530
NMNH (USNM)	181533
NMNH (USNM)	181534
NMNH (USNM)	182032
NMNH (USNM)	182085
NMNH (USNM)	182091
NMNH (USNM)	182095
NMNH (USNM)	182103
NMNH (USNM)	182105
NMNH (USNM)	182113
NMNH (USNM)	182117
NMNH (USNM)	182210
NMNH (USNM)	201010
NMNH (USNM)	239161
NMNH (USNM)	367384
NMNH (USNM)	367385
NMNH (USNM)	368502
NMNH (USNM)	429176
PMNHN-AC	MNHNCA1894-54
PMNHN-OM	MNHNZ1962-1537
PMNHN-OM	MNHNZ1972-400
PMNHN-OM	MNHNZ1996-2514
RBINS	10250
RBINS	10336
RBINS	11799
RBINS	11801
RBINS	11804
RBINS	21278

Table 1.8 (cont'd)

RBINS	9480
RBINS	21302
RBINS	21436
RBINS	4612
RBINS	7705
RBINS	8632
RBINS	8633
RBINS	8634
RBINS	9967
RCSOM	137.41
RCSOM	137.42
RCSOM	137.43
RCSOM	16.5
RMCA	11376
RMCA	11602
RMCA	11701
RMCA	12096
RMCA	12442
RMCA	14367
RMCA	14369
RMCA	16719
RMCA	17619
RMCA	17740
RMCA	18000
RMCA	18495
RMCA	18627
RMCA	1897
RMCA	19272
RMCA	19273
RMCA	2162
RMCA	22802
RMCA	2907
RMCA	36328
RMCA	36543
RMCA	3728
RMCA	3788
RMCA	384
RMCA	3870
RMCA	5934
RMCA	9292
RMCA	9579

Table 1.8 (cont'd)

OSU	4650
OSU	11969
OSU	4640
OSU	4651
OSU	4682
OSU	5711
OSU	5761

APPENDIX C

LANDMARK DEFINITIONS

Table 1.9: Ventral landmarks definitions

Landmark	Definition
1	Juncture between the incisors on the premaxilla
2	Premaxilla-maxilla suture intersection with the medial edge of the left canine
3	Most posterior point of the left incisive foramen
4	Most posterior point of the right incisive foramen
5	Premaxilla-maxilla suture intersection with the medial edge of the right canine
6	Posterior edge of premaxilla-maxilla suture on the palate
7	Center of Maxilla-palatine midline suture
8	Center of left fourth premolar
9	Center of right fourth premolar
10	Posterior edge of the midline suture between the left and right palatine.
11	Most posterior edge of the left maxilla-jugal suture
12	Most posterior edge of the right maxilla-jugal suture
13	Most posterior edge of the left jugal-squamosal suture
14	Most posterior edge of the right jugal-squamosal suture
15	Most anterior point of the foramen magnum
16	Posterior end of the left maxilla-palatine suture
17	Posterior end of the right maxilla-palatine suture
18	Center of left, jugular canal
19	Center of right, jugular canal
20	Most anterior point of left retroarticular process
21	Most anterior point of right retroarticular process
22	Posterior edge of left second premolar
23	Posterior edge of right second premolar
24	Most distal point of the left external auditory meatus
25	Most distal point of the right external auditory meatus

Table 1.10 Lateral Landmarks definations

Landmark	Definition
1	Anterior edge of the third incisor
2	Anterior edge of canine
3	Posterior edge of canine
4	The most posterior part of the infraorbital foramen
5	The intersection of the maxilla, lacrimal and jugal
6	The most lateral projection of post-orbital process
7	Most dorsal anterior part of the squamosal
8	Most ventral posterior part of the jugal
9	The most ventral-posterior point of the jugal-maxilla suture
10	The most posterior edge of the suture of palatine and pterygoid process
11	Suture of the squamosal and occipital inside the auditory meatus
12	Anterior upper edge of the occipital condyle
13	Posterior most edge of the sagittal crest
14	Anterior edge of the nasal-premaxilla suture

32 Semi-landmarks along curve of dorsal cranium, 14 to 13

Table 1.11 Mandible landmarks definitions

Landmark	Definition
1	Anterior edge of third incisor
2	Anterior edge of canine
3	Posterior edge of canine
4	Dorsal apex of the coronoid process
5	Most posterior projection of the coronoid process
6	Anterior edge of the mandibular condyle, distal to the vertical plane of the coronoid
7	Posterior most edge of the mandibular condyle
8	Posterior most point of the articular process
9	Intersection of the mandibular body and ramus
10	Intersection of anterior margin of first incisor with the dentary

32 Semi-landmarks along ventral curve of the mandible, 10 to 8

11 Semi-landmarks along posterior curve between articular process and mandibular condyle, 8 to 7

16 Semi-landmarks along posterior curve between mandibular condyle and coronoid process, 6 to 5

17 Semi-landmarks along anterior curve of ramus, 4 to 9

WORKS CITED

WORKS CITED

Adams, D. C., Collyer, M. L., & Sherratt, E. (2015). Geomorph: Software for geometric morphometric analyses. R package version 2.1.

Adams, D. C., & Otárola-Castillo, E. (2013). geomorph: an R package for the collection and analysis of geometric morphometric shape data. *Methods in Ecology and Evolution, 4*(4), 393-399.

Alexander, R. M. (2005). Models and the scaling of energy costs for locomotion. *J Exp Biol, 208*(Pt 9), 1645-1652.

Allen, J. A. (1877). The influence of physical conditions in the genesis of species. *Radical Review, 1*.

Allen, J. A., Lang, H., & Chapin, J. P. (1924). Carnivora collected by the American Museum Congo Expedition. Bulletin of the AMNH; v. 47, article 3.

Arsznov, B. M., Lundrigan, B. L., Holekamp, K. E., & Sakai, S. T. (2010). Sex and the frontal cortex: A developmental CT study in the spotted hyena. *Brain Behav Evol, 76*(3-4), 185-197.

Ashton, K. G., Tracy, M. C., & Queiroz, A. d. (2000). Is Bergmann's rule valid for mammals? *The American Naturalist, 156*(4), 390-415.

Bergmann, C. (1847). About the relationships between heat conservation and body size of animals. *Goett Stud, 1*, 595-708.

Bidau, C. J., & Martinez, P. A. (2016). Sexual size dimorphism and Rensch's rule in Canidae. *Biological Journal of the Linnean Society, 119*(4), 816-830.

Bonner, J. T. (2004). Perspective: the size-complexity rule. *Evolution, 58*(9), 1883-1890.

Bookstein, F. L. (1997). Landmark methods for forms without landmarks: morphometrics of group differences in outline shape. *Medical image analysis, 1*(3), 225-243.

Botes, A., McGeoch, M. A., Robertson, H. G., van Niekerk, A., Davids, H. P., & Chown, S. L. (2006). Ants, altitude and change in the northern Cape Floristic Region. *33*(1), 71-90.

Brown, J. H., & West, G. B. (2000). *Scaling in biology*: Oxford University Press.

Buckland-Wright, J. (1969). Craniological observations on Hyaena and Crocuta (Mammalia). *Journal of Zoology, 159*(1), 17-29.

Calder, W. A. (1996). *Size, function, and life history*: Courier Corporation.

Carbone, C., & Gittleman, J. L. (2002). A common rule for the scaling of carnivore density. *Science, 295*(5563), 2273-2276.

Cardini, A., Jansson, A.-U., & Elton, S. (2007). A geometric morphometric approach to the study of ecogeographical and clinal variation in vervet monkeys. *Journal of Biogeography, 34*(10), 1663-1678.

Caro, T., & Stoner, C. (2003). The potential for interspecific competition among African carnivores. *Biological Conservation, 110*(1), 67-75.

Cavallini, P. (1995). *Variation in the body size of the red fox.* Paper presented at the Annales Zoologici Fennici.

Chapman, A. D., & Wieczorek, J. (2006). Guide to best practices for georeferencing. *Copenhagen: Global Biodiversity Information Facility*, 1-77.

Christiansen, P., & Adolfssen, J. S. (2005). Bite forces, canine strength and skull allometry in carnivores (Mammalia, Carnivora). *Journal of Zoology, 266*(2), 133-151.

Clutton-Brock, T. H., & Harvey, P. H. (1977). Primate ecology and social organization. *Journal of Zoology, 183*(1), 1-39.

Cressie, N. (1993). *Statistics for Spatial Data*. New York, United States: John Wiley & Sons, Incorporated.

Damuth, J. (1981). Population-density and body size in mammals. *Nature, 290*(5808), 699-700.

Dobson, F. S., & Kjelgaard, J. D. (1985). The influence of food resources on life history in Columbian ground squirrels. *Canadian Journal of Zoology, 63*(9), 2105-2109.

Ebinger, C. J. (1989). Tectonic development of the western branch of the East African rift system. *Geological Society of America Bulletin, 101*(7), 885-903.

Esri. (2018). ArcMap: Release 10.6. 1.

Ferger, S. W., Schleuning, M., Hemp, A., Howell, K. M., & Böhning-Gaese, K. (2014). Food resources and vegetation structure mediate climatic effects on species richness of birds. *Global Ecology and Biogeography, 23*(5), 541-549.

Ferrer-Castán, D., Morales-Barbero, J., & Vetaas, O. R. (2016). Water-energy dynamics, habitat heterogeneity, history, and broad-scale patterns of mammal diversity. *Acta Oecologica, 77*, 176-186.

Fick, S. E., & Hijmans, R. J. (2017). WorldClim 2: new 1-km spatial resolution climate surfaces for global land areas. *International journal of climatology*, *37*(12), 4302-4315.

Foster, J. B. (1964). Evolution of Mammals on Islands. *Nature, 202*, 234.

Fox, J.-P., & Wyrick, C. (2008). A mixed effects randomized item response model. *Journal of Educational and Behavioral Statistics, 33*(4), 389-415.

Frank, L. G. (1986). Social organization of the spotted hyaena (*Crocuta crocuta*). I. Demography. *Animal Behaviour, 34*(5), 1500-1509.

Gittleman, J. L., & Valkenburgh, B. V. (1997). Sexual dimorphism in the canines and skulls of carnivores: effects of size, phylogency, and behavioural ecology. *Journal of Zoology, 242*(1), 97-117.

Green, D., Johnson-Ulrich, L., Couraud, H., & Holekamp, K. (2018). Anthropogenic disturbance induces opposing population trends in spotted hyenas and African lions. *Biodiversity and Conservation, 27*(4), 871-889.

Green, W. (1996). *The thin-plate spline and images with curving features.* Paper presented at the Proceedings in image fusion and shape variability techniques.

Hayward, M. W., & Slotow, R. (2009). Temporal partitioning of activity in large African carnivores: tests of multiple hypotheses. *African Journal of Wildlife Research, 39*(2), 109-125.

Heim, N. A., Payne, J. L., Finnegan, S., Knope, M. L., Kowalewski, M., Lyons, S. K., McShea D.W., Novack-Gottshall P. M., Smith F. A., Wang, S. C. (2017). Hierarchical complexity and the size limits of life. *Proceedings of the Royal Society B: Biological Sciences, 284*(1857), 20171039.

Heller, E. (1914). Four new subspecies of large mammals from equatorial Africa.

Hill, R. W., Wyse, G. A., Anderson, M., & Anderson, M. (2004). *Animal physiology* (Vol. 2): Sinauer Associates Massachusetts.

Hillebrand, H. (2004). On the Generality of the Latitudinal Diversity Gradient. *The American Naturalist, 163*(2), 192-211.

Holekamp, K. E., & Dloniak, S. M. (2010). Chapter 6 - Intraspecific Variation in the Behavioral Ecology of a Tropical Carnivore, the Spotted Hyena. In R. Macedo (Ed.), *Advances in the Study of Behavior* (Vol. 42, pp. 189-229): Academic Press.

Holekamp, K. E., Smith, J. E., Trelioff, C. C., Van horn, R. C., & Watts, H. E. (2012). Society, demography and genetic structure in the spotted hyena. *Molecular Ecology, 21*(3), 613-632.

Honěk, A. (1993). Intraspecific Variation in Body Size and Fecundity in Insects: A General Relationship. *Oikos, 66*(3), 483-492.

Höner, O. P., Wachter, B., East, M. L., & Hofer, H. (2002). The response of spotted hyaenas to long-term changes in prey populations: functional response and interspecific kleptoparasitism. *Journal of Animal Ecology, 71*(2), 236-246.

Hudson, R. J. (2018). *Bioenergetics of wild herbivores*: CRC press.

IUCN. (2021). The IUCN Red List of Threatened Species. Version 2021-2. . Retrieved from http://www.iucnredlist.org/

Jenks, G. F. (1963). Generalization in statistical mapping. *Annals of the Association of American Geographers, 53*(1), 15-26.

Jones, S., Waldschmidt, S., & Potvin, M. (1987). An experimental manipulation of food and water: growth and time-space utilization of hatchling lizards (*Sceloporus undulatus*). *Oecologia, 73*(1), 53-59.

Klein, R. G., & Scott, K. (1989). Glacial/interglacial size variation in fossil spotted hyenas (Crocuta crocuta) from Britain. *Quaternary Research, 32*(1), 88-95.

Kruuk, H. 1972. The spotted hyena; a study of predation and social behavior. Chicago: University of Chicago Press.

Kurten, B. (1957). The bears and hyenas of the interglacials. *Quaternaria, 4*, 69-81.

Legendre, P., & Legendre, L. (1998). Numerical ecology: developments in environmental modelling. *Developments in Environmental Modelling, 20*.

Li, G., Yin, B., Wan, X., Wei, W., Wang, G., Krebs, C. J., & Zhang, Z. (2016). Successive sheep grazing reduces population density of Brandt's voles in steppe grassland by altering food resources: a large manipulative experiment. *Oecologia, 180*(1), 149-159.

Loeuille, N., & Loreau, M. (2006). Evolution of body size in food webs: does the energetic equivalence rule hold? *Ecol Lett, 9*(2), 171-178.

Mann, M. D., Frank, L. G., Glickman, S. E., & Towe, A. L. (2018). Brain and Body Size Relations among Spotted Hyenas (*Crocuta crocuta*). *Brain, Behavior and Evolution*.

Martin, A. P., & Palumbi, S. R. (1993). Body size, metabolic rate, generation time, and the molecular clock. *Proceedings of the National Academy of Sciences, 90*(9), 4087.

Massey, A. L., King, A. A., & Foufopoulos, J. (2014). Fencing protected areas: A long-term assessment of the effects of reserve establishment and fencing on African mammalian diversity. *Biological Conservation, 176*, 162-171.

Matthews, L. H. (1939). The bionomics of the Spotted Hyaena, Crocuta crocuta Erxl. *Proceedings of the Zoological Society of London Series a-General and Experimental, 109*, 43-56.

Mavropoulos, A., Bresin, A., & Kiliaridis, S. (2004). Morphometric analysis of the mandible in growing rats with different masticatory functional demands: adaptation to an upper posterior bite block. *European Journal of Oral Sciences, 112*(3), 259-266.

Mayaux, P., Bartholomé, E., Fritz, S., & Belward, A. (2004). A new land-cover map of Africa for the year 2000. *Journal of Biogeography, 31*(6), 861-877.

Mayr, E. (1956). Geographical character gradients and climatic adaptation. *Evolution, 10*(1), 105-108.

McElhinny, T. L. (2009). *Morphological Variation in a Durophagous Carnivore, the Spotted Hyena, Crocuta Crocuta*: Michigan State University. East Lansing, Michigan.

McNab, B. K. (2010). Geographic and temporal correlations of mammalian size reconsidered: a resource rule. *Oecologia, 164*(1), 13-23.

Meester, J. (1986). *Classification of southern African mammals*: Transvaal Museum.

Meiri, S., Dayan, T., & Simberloff, D. (2004). Carnivores, biases and Bergmann's rule. *Biological Journal of the Linnean Society, 81*(4), 579-588.

Meiri, S., Dayan, T., & Simberloff, D. (2005). Variability and sexual size dimorphism in carnivores: testing the niche variation hypothesis. *Ecology, 86*(6), 1432-1440.

Meiri, S., & Thomas, G. H. (2007). The geography of body size–challenges of the interspecific approach. *Global Ecology and Biogeography, 16*(6), 689-693.

Meyer, A. (1987). Phenotypic plasticity and heterochrony in Cichlasoma managuense (Pisces, Cichlidae) and their implications for speciation in cichlid fishes. *Evolution, 41*(6), 1357-1369.

Mills, M. (1990). Kalahari hyaenas: the behavioural ecology of two species. 1990 London. *UK: Unwin Hyman*.

Mills, M., & Hofer, H. (1998). Status survey and conservation action plan. Hyaenas. *IUCN/SSC Hyaena Specialist Group, IUCN, Switzerland*.

O'Donnell, M. S., & Ignizio, D. A. (2012). Bioclimatic predictors for supporting ecological applications in the conterminous United States. *US Geological Survey Data Series, 691*(10).

Olalla-Tárraga, M., xc, Rodr, xed, guez, M., xc, & Hawkins, B. A. (2006). Broad-Scale Patterns of Body Size in Squamate Reptiles of Europe and North America. *Journal of Biogeography, 33*(5), 781-793.

Peters, D. P. C., Pielke, R. A., Bestelmeyer, B. T., Allen, C. D., Munson-McGee, S., & Havstad, K. M. (2007). Spatial Nonlinearities: Cascading Effects in the Earth System. In J. G. Canadell, D. E. Pataki, & L. F. Pitelka (Eds.), *Terrestrial Ecosystems in a Changing World* (pp. 165-174). Berlin, Heidelberg: Springer Berlin Heidelberg.

Peters, R. H., & Karen, W. (1983). The Effect of Body Size on Animal Abundance. *Oecologia, 60*(1), 89-96.

R Core Team. (2017). R: A language and environment for statistical computing. R version 3.4. 1 edn. R Foundation for Statistical Computing, Vienna, Austria.

Ralls, K. (1976). Mammals in Which Females are Larger Than Males. *The Quarterly Review of Biology, 51*(2), 245-276.

Renaud, S., Auffray, J.-C., & De la Porte, S. (2010). Epigenetic effects on the mouse mandible: common features and discrepancies in remodeling due to muscular dystrophy and response to food consistency. *BMC evolutionary biology, 10*(1), 28.

Rensch, B. (1950). Die Abhängigkeit der relativen Sexualdifferenz von der Körpergrösse. *J Bonner Zoologische Beiträge, 1*, 58-69.

Riggio, J., Jacobson, A., Dollar, L., Bauer, H., Becker, M., Dickman, A., . . . Pimm, S. (2013). The size of savannah Africa: a lion's (Panthera leo) view. *Biodiversity and Conservation, 22*(1), 17-35.

Rios, N. (2019). GEOLocate - Software for Georeferencing Natural History Data. [Web application software]. Retrieved from http://www.geo-locate.org

Rohlf, F. J. (2015). The tps series of software. *Hystrix, 26*(1), 9-12.

Royston, P. (1995). Remark AS R94: A remark on algorithm AS 181: The W-test for normality. *Journal of the Royal Statistical Society. Series C, 44*(4), 547-551.

Sakamoto, Y., Ishiguro, M., & Kitagawa, G. J. D., The Netherlands: D. Reidel. (1986). Akaike information criterion statistics. *81*.

Sand, H., Cederlund, G., & Danell, K. (1995). Geographical and Latitudinal Variation in Growth Patterns and Adult Body Size of Swedish Moose (*Alces alces*). *Oecologia, 102*(4), 433-442. Retrieved from

Schwenk, K. (2000). *Feeding: form, function and evolution in tetrapod vertebrates*: Elsevier.

Scott, J. E., McAbee, K. R., Eastman, M. M., & Ravosa, M. J. (2014). Teaching an old jaw new tricks: diet-induced plasticity in a model organism from weaning to adulthood. *Journal of Experimental Biology, 217*(22), 4099-4107.

Shine, R. (1988). The evolution of large body size in females: a critique of Darwin's" fecundity advantage" model. *The American Naturalist, 131*(1), 124-131.

Sillero-Zubiri, C., & Gottelli, D. (1992). Population ecology of spotted hyaena in an equatorial mountain forest. *African Journal of Ecology, 30*, 292-300.

Silva, M., Brimacombe, M., Downing, J. A. J. G. E., & Biogeography. (2001). Effects of body mass, climate, geography, and census area on population density of terrestrial mammals. *10*(5), 469-485.

Simard, A. M., Côté, S. D., Weladji, R. B., & Huot, J. (2008). Feedback effects of chronic browsing on life-history traits of a large herbivore. *Journal of Animal Ecology, 77*(4), 678-686.

Sinclair, A. R. E., & Arcese, P. (1995). *Serengeti II: dynamics, management, and conservation of an ecosystem* (Vol. 2): University of Chicago Press.

Sinclair, A. R. E., & Norton-Griffiths, M. (1984). *Serengeti: dynamics of an ecosystem*: University of Chicago Press.

Sinclair, A. R. E., Packer, C., Mduma, S. A. R., & Fryxell, J. M. (2008). *Serengeti III: Human impacts on ecosystem dynamics*. Chicago: Chicago Univ. Press.

Skinner, J. (1976). Ecology of the brown hyaena Hyaena brunnea in the Transvaal with a distribution map for southern Africa. *South African Journal of Science, 72*(9), 262.

Skogland, T. (1983). The Effects of Density Dependent Resource Limitation on Size of Wild Reindeer. *Oecologia, 60*(2), 156-168.

Smale, L., Frank, L. G., & Holekamp, K. E. (1993). Ontogeny of dominance in free-living spotted hyaenas: juvenile rank relations with adult females and immigrant males. *Animal Behaviour, 46*(3), 467-477.

Smith, F. A., & Lyons, S. K. (2013). *Animal body size: linking pattern and process across space, time, and taxonomic group*: University of Chicago Press.

Speakman, J. R. (2005). Body size, energy metabolism and lifespan. *J Exp Biol, 208*(Pt 9), 1717-1730.

Swanson, E. M., McElhinny, T. L., Dworkin, I., Weldele, M. L., Glickman, S. E., & Holekamp, K. E. (2013). Ontogeny of sexual size dimorphism in the spotted hyena (*Crocuta crocuta*). *Journal of Mammalogy, 94*(6), 1298-1310.

Tanner, J. B., Dumont, E. R., Sakai, S. T., Lundrigan, B. L., & Holekamp, K. E. (2008). Of arcs and vaults: the biomechanics of bone-cracking in spotted hyenas (Crocuta crocuta). *Biological Journal of the Linnean Society, 95*(2), 246-255.

Tanner, J. B., Zelditch, M. L., Lundrigan, B. L., & Holekamp, K. E. (2010). Ontogenetic change in skull morphology and mechanical advantage in the spotted hyena (*Crocuta crocuta*). *J Morphol, 271*(3), 353-365.

van Gelder, H. A., Poorter, L., & Sterck, F. J. (2006). Wood mechanics, allometry, and life-history variation in a tropical rain forest tree community. *New Phytol, 171*(2), 367-378.

Venables, W.N., & Ripely, B. D. (2002). Modern applied statistics with S., New York: Spronger science+ business media. 7.3-23.

Watt, C., Mitchell, S., & Salewski, V. (2010). Bergmann's rule; a concept cluster? *Oikos, 119*(1), 89-100.

Watts, H. E., & Holekamp, K. E. (2008). Interspecific competition influences reproduction in spotted hyenas. *Journal of Zoology, 276*(4), 402-410.

Watts, H. E., Tanner, J. B., Lundrigan, B. L., & Holekamp, K. E. (2009). Post-weaning maternal effects and the evolution of female dominance in the spotted hyena. *Proc Biol Sci, 276*(1665), 2291-2298.

Wilson, D. E., & Reeder, D. M. (2005). *Mammal species of the world: a taxonomic and geographic reference* (Vol. 1): JHU Press.

Yom-Tov, Y., & Geffen, E. (2006). Geographic variation in body size: the effects of ambient temperature and precipitation. *Oecologia, 148*(2), 213-218.

Yu, X., Zhong, M. J., Li, D. Y., Jin, L., Liao, W. B., & Kotrschal, A. (2018). Large-brained frogs mature later and live longer. *Evolution, 72*(5), 1174-1183.

Zedrosser, A., Dahle, B., & Swenson, J. E. (2006). Population Density and Food Conditions Determine Adult Female Body Size in Brown Bears. *Journal of Mammalogy, 87*(3), 510-518.

Zelditch, M. L., Swiderski, D. L., & Sheets, H. D. (2012). Geometric morphometrics for biologists: a primer. academic press.

Zhao, M., Christie, M., Coleman, J., Hassell, C., Gosbell, K., Lisovski, S., Minton, C., Klaassen, M. (2017). Time versus energy minimization migration strategy varies with body size and season in long-distance migratory shorebirds. *Mov Ecol, 5*, 23.

Zuur, A. F., Ieno, E. N., & Elphick, C. S. (2010). A protocol for data exploration to avoid common statistical problems. *1*(1), 3-14.

Chapter 2: Geographic variation in striped hyena skull size supports Bergmann's rule and the seasonality hypothesis

ABSTRACT

Body size determines most aspects of a species biology. Identifying factors that influence body size variation is central to understanding the evolution of size. Striped hyenas are an excellent model for investigating factors influencing geographic variation because their range spans three continents including areas both north and south of the equator. In this study we used 2D landmark-based geometric morphometrics of the skull to assess sexual size dimorphism and described size variation in striped hyenas across their geographic range. We investigated the influence of climatic variables, food resources and human impact on observed geographic patterns of skull size. We modeled intraspecific variation in skull size of striped hyenas against proposed drivers of geographic variation in size using general linear models. We found slight male biased sexual size dimorphism. We did not find evidence to support our prediction that striped hyenas would be larger in areas with higher net primary productivity or increased access to human-provided foods. Striped hyenas follow Bergmann's rule; larger individuals are found at higher latitudes. Our results support the argument that geographic variation in body size is primarily driven by seasonal climatic variables, which is consistent with the seasonality hypothesis. Future studies of geographic variation in striped hyenas should use a larger sample of specimens so that spatial correlation structures can be included in the model to account for the high correlation between covariates.

1 | INTRODUCTION

Body size differences are among the most notable aspects of variation among organisms. Body size dictates diet (Barnes, Maxwell, Reuman, & Jennings, 2010; Smith et al., 2010), behavior (Dial, Greene, & Irschick, 2008), and fitness (Darwin, 1872; Sibly & Brown, 2007). Because of its importance, hundreds of studies have focused on identifying factors that influence body size variation within and among species.

In mammals, the Order Carnivora is a common focus for investigations of size variation, as this group includes many charismatic species that are well studied, widespread geographically, and well-represented in the fossil record. In a review of the carnivoran literature, Meiri et al. (2004) found that body size increased with latitude (in accord with Bergmann's rule) in 22 of 44 (50% of) extant species. Meiri et al. (2007) suggested that temperature is not a particularly strong predictor of intraspecific size variation in this clade (Meiri, Yom-Tov, & Geffen, 2007). Huston and Wolverton (2011) argued that intraspecific size variation is the result of food availability rather than thermoregulation, and that net primary productivity during the growing season is a better predictor of this pattern than temperature. Studies examining intraspecific size variation in several carnivore species show patterns consistent with food availability being a better size indicator than temperature (Damuth, 1981; Gortázar, Travaini, & Delibes, 2000; Hilderbrand et al., 1999; Kolb, 1978; McNab, 2010; Meiri et al., 2007; Rosenzweig, 1968; Y. Yom-Tov, 2003; Yoram Yom-Tov, Heggberget, Wiig, & Yom-Tov, 2006; Zedrosser, Dahle, & Swenson, 2006).

Boyce (1979) suggested that larger body size would be favored in areas with greater seasonality. The reasoning for this seasonality hypothesis is twofold: there is reduced density-

dependent competition because of seasonal high mortality and a resistance to starvation for larger individuals (Ashmole, 1963; Calder, 1984; Damuth, 1981; Lindsey, 1966; Lindstedt & Boyce, 1985). A lower population density means more food per capita, and thus more available energy to be put forth for growth (Damuth, 1981; Geist, 1987). Larger individuals have more body mass to dedicate to fat stores and a lower mass specific rate of metabolism than smaller individuals (Lindstedt & Boyce, 1985; Pitts & Bullard, 1968). An increase in size to improve survival during periods of resource shortages has been suggested to be the driving force behind the latitudinal size increase known as Bergmann's rule, as seasonality increases with increasing absolute latitude (Lindstedt & Boyce, 1985). The relationship among climatic variables, food availability, and body size is complicated by annual fluctuations and population density (Boyce, 1979; Damuth, 1981; Lindstedt & Boyce, 1985). Seasonal changes can lead to severe temporary resource shortages that favor larger individuals, presumably because they metabolize somatic stores at a lower weight-specific rate (Lindstedt & Boyce, 1985). Seasonality increases with distance from the tropics, especially in areas of low humidity such as deserts (O'Donnell & Ignizio, 2012).

Humans can also influence body size directly by providing food (Bateman, Fleming, & Le Comber, 2012; Manlick & Pauli, 2020). Yom-Tov (2003), reported an increase in body length in striped hyenas from the 1940s to the early 2000s in Israel, attributed to a substantial increase in the amount of garbage and agricultural crops available (Y. Yom-Tov, 2003).

In a previous study (Chapter 1), we examined skull size variation across the geographic range of the spotted hyena, *Crocuta crocuta*, a large-bodied carnivore that is broadly distributed in Sub-Saharan Africa (Bohm & Höner, 2015). This species has received

considerable attention from researchers as it is a dominant predator with a broad geographic range and an extensive fossil record (Werdelin, Solounias, & strata, 1991; Werdelin & Turner, 2019) Spotted hyenas are also of special interest because females are dominant to males, in contrast to the typical pattern found in social carnivores (Ralls, 1976; Smale, Frank, & Holekamp, 1993). Among the goals of the spotted hyena study was to test the hypothesis that intraspecific size variation increases with latitude (i.e., follows Bergmann's rule) in accord with previous analyses based on tooth size of fossil and extant forms (Klein & Scott, 1989; Kurten, 1957).

In spotted hyenas we found a strong geographic pattern in skull size, but size did not increase consistently with increasing latitude as predicted by Bergmann's rule. Rather the smallest individuals were clustered in East Africa, with larger individuals elsewhere. This pattern of size variation in spotted hyenas corresponded to population densities: smaller individuals were found at higher population densities. An inverse relationship between population density and body size at the intraspecific level has been observed in a number of other carnivores (Carbone & Gittleman, 2002; Cavallini, 1995; Zedrosser et al., 2006). We also found that female spotted hyenas are slightly larger than males (Swanson et al., 2013), in contrast to the typical condition found in social mammals.

Here, we examine the pattern of geographic size variation and sexual dimorphism in the closely related striped hyena (*Hyaena hyaena*), a species that has received much less attention from researchers. Spotted, striped, and brown hyenas comprise the clade of extant bone-crushing hyaenids, descendants of a bone crushing ancestor that dates to ~ 6 Mya (Westbury et al., 2021). Although striped hyenas are, on average, somewhat smaller than spotted hyenas,

they have a similar body form and skull morphology, including a vaulted cranium and exceptionally robust premolars, both adaptations for durophagy (Hartstone-Rose & Steynder, 2013; Tanner, Dumont, Sakai, Lundrigan, & Holekamp, 2008).

As is the case for spotted hyenas, striped hyenas have an extremely flexible diet that can include insects, small mammals, birds, fish, tortoises, crocodiles, dogs, wild ungulates, primates, livestock, human remains, seeds, leaves, and fruits (Bhandari, Morley, Aryal, & Shrestha, 2020; Kruuk, 1976; Leakey et al., 1999; Wagner, 2006). However, in contrast to spotted hyenas, which often hunt cooperatively (Green, Johnson-Ulrich, Couraud, & Holekamp, 2018; Holekamp, Smith, Trelioff, Van horn, & Watts, 2012), striped hyenas usually forage alone, scavenging carrion or opportunistically taking small prey (Mills & Hofer, 1998). This less carnivorous diet may couple striped hyenas more closely to their habitat than is the case for spotted hyenas; thus, we expect striped hyena size to better reflect differences in temperature and resources than population density.

Striped hyena population densities vary with geography (Shamoon & Shapira, 2019), but do not reach the high levels seen in East African spotted hyenas (Chapter 1). Striped hyenas (*Hyaena hyaena*) are often considered to be solitary (AbiSaid & Dloniak, 2015), although recent research in Kenya suggests a more complex and variable social structure (Califf et al 2020: Wagner et al 2008). Two populations in Kenya approximately 300 km apart exhibit markedly different space-use patterns. The Laikipia population formed stable polyandrous social groups composed of multiple males and a single female, with male home ranges overlapping considerably with those of other males, whereas the Shompole population exhibited less male home range overlap and a high degree of female home range overlap (Califf et al., 2019;

Wagner, Frank, & Creel, 2008). Female striped hyenas have been reported to be dominant to males in captive populations (Rieger, 1979). Wagner (2006) found that females are not dominant to males in wild populations, also reporting that studies in Africa and Israel found no significant sexual dimorphism in linear body measurements or weight. However, Rieger (1979) found a slight, although not statistically significant, male bias in skull size in a broader geographic examination of skull sizes with data pooled from several studies (n=65).

Striped hyenas are exceptional for investigating factors influencing geographic variation because their range spans three continents, extending from the Atlantic coast of western Africa, to far eastern India and Nepal, north along the foothills of the Himalayas and the Caspian Sea to Turkey, and south to Tanzania (Figure 2.1) (AbiSaid & Dloniak, 2015). Species inhabiting the tropics are often excluded from studies of Bergmann's rule (Meiri et al., 2004). Examining Bergmann's rule in striped hyenas north and south of the equator provides us with an excellent opportunity to compare a wide-ranging species to a more tropically distributed relative, spotted hyenas.

Although striped hyenas are currently considered monotypic (Wilson & Reeder, 2005), morphological variation across the species' huge range has been noted by a number of researchers. Indeed, prior to the 1930s, as many as 28 subspecies were recognized, based mainly on pelage density, color, and pattern (Pocock, 1934; Rieger, 1979). Pocock's (1934) revision recognized five subspecies based on variation in several morphological features, including size. Both Pocock and Rieger noted that individuals from northeast Africa and the Arabian Peninsula (*H. h. dubbah* and *H. h. sultana*) were smaller than individuals from

northwest Africa, the eastern Mediterranean, and Asia (*H. h. barbara*, *H. h syriaca* and *H. h indica*).

In this study, we describe skull size variation in striped hyenas across their geographic range, investigate the influence of climatic variables and food resources on observed geographic patterns, and assess sexual size dimorphism. Among climatic variables, we include both annualized values (e.g., annual mean temp) and seasonal measures (e.g., isothermality). The latter can capture yearly fluctuations in the environment that can be especially impactful on individual survival. Food resources are assessed indirectly using net primary production, defined as the amount of atmospheric carbon fixed by plants and accumulated as biomass (after Huston & Wolverton, 2009). We also assess the effect of human pressure on body size variation using Human Footprint, a globally standardized measure of infrastructure, land cover, and human access (Venter et al., 2016).

2 | MATERIALS AND METHODS

2.1 | Specimens

The sample comprised 126 adult striped hyena skulls (48 females, 50 males, 28 sex unknown) obtained from 14 natural history collections (APPENDIX B). Adult maturity was defined by full eruption of permanent teeth, and complete, or nearly complete, closure of the lambdoid and basilar sutures. Specimens were collected from the field between 1902 and 2008. The sample includes individuals from 20 countries, stretching from Nepal to Tanzania and from Algeria to India (Figure 2.1A). The distribution of collecting localities encompasses much of the current geographical range of *H. hyaena*, including areas where it appears to have been recently extirpated, and contains a variety of climatic regions (IUCN, 2021). However, west Africa, where populations are patchy and numbers low (Hofer & Mills, 1998), is represented by only a single specimen. Collecting data for each specimen, including date of collection, locality, and sex (determined at the time of collection), were obtained from museum records. Specimens without associated geographic coordinates were georeferenced from specimen locality data, using established guidelines from Chapman and Wieczorek (2006), and the georeferencing software GEOLocate Web Application (Rios, 2019).

2.2 | Morphological Data

Ventral measurements of the cranium have been shown to correlate strongly with overall body size in carnivorans, including in the closely related spotted hyena (McElhinny, 2009; Turner & O'Regan, 2002; Valkenburgh, 1990). Therefore, we use ventral skull size as a proxy for overall body size in this study. Skulls were photographed using a digital camera, orienting specimens with the palate parallel to the photographic plane (Figure 2.2). A 10-mm

scale was included in all photographs. To quantify differences in skull size, we used 2D landmark-based geometric morphometrics. Landmarks (Figure 2.2, APPENDIX C) selected to capture size (Zelditch et al., 2012) were digitized by the same observer (CNC), using tpsDig2.32 (Rohlf, 2015). Landmark configurations were superimposed to remove variation in scale, position, and orientation by a generalized least-squares Procrustes superimposition using the 'geomorph' package (Adams, Collyer, & Sherratt, 2015; Adams & Otárola-Castillo, 2013) in R version 3.4.1(R Core Team, 2017). Centroid size is the square root of the summed squared distances of each landmark from the centroid of the landmark configuration (Zelditch et al., 2012); with landmarks strategically placed, it can capture differences between individuals in the overall size of the ventral skull more effectively than standard linear measurements such as basal length. We used ventral-view centroid size as the size metric for all analyses.

2.3 | Climatic Variables

Climatic variables are often highly correlated with latitude, complicating statistical analyses aimed at identifying the factors underlying observed patterns of geographical variation. To simplify our analyses, we chose a relatively small number of climate covariates, focusing on what we believed might be important to striped hyenas. These include two annual climatic variables (Annual Mean Temperature and Annual Mean Precipitation) and seven variables reflecting seasonality (Mean Temperature of Warmest Quarter, Mean Temperature of Coldest Quarter, Temperature Seasonality, Isothermality, Precipitation Seasonality, Precipitation of Wettest Quarter, and Precipitation of Driest Quarter). Temperature Seasonality is the standard deviation of the 12 mean monthly temperature values; a larger standard deviation indicates greater variability in temperature (O'Donnell & Ignizio, 2012). Precipitation

Seasonality is the ratio of the standard deviation of the monthly total precipitation to the mean monthly total precipitation, expressed as a percentage. The larger the percentage, the greater the variability in precipitation (O'Donnell & Ignizio, 2012). Isothermality measures how large the day to night temperature oscillation is relative to the summer to winter (annual) temperature oscillation (O'Donnell & Ignizio, 2012). It is calculated using the ratio of the mean diurnal temperature range to the annual temperature range and then multiplying by 100 to get a percent (O'Donnell & Ignizio, 2012). An isothermal value of 100% indicates that diurnal temperature range is equal to the annual temperature range. An isothermal value of less than 100% specifies a smaller level of temperature variability within an average month relative to the year. All climactic variables were extracted at a spatial resolution of 10 minutes (~340 km2) from WorldClim global climate database for each specimen's collection locality (Fick & Hijmans, 2017).

2.4 | Resource Variables

Terrestrial Net Primary Production (NPP) and Human Footprint were used to evaluate the relationship between striped hyena skull size and available resources. NPP is the amount of atmospheric carbon fixed by plants and accumulated as biomass (Huston & Wolverton, 2009). As our metric of NPP, we used average annual terrestrial NPP estimated using a monthly normalized difference vegetation index (NDVI) from the Advanced Very High Resolution Radiometer (AVHRR), the Carnegie-Ames-Stanford Approach (CASA) model, and climate drivers for 1982-1998, with a spatial resolution of approximately 28 x 28 km at the equator (Imhoff & Bounoua, 2006). We chose this approach because it provides a robust and comprehensive

analysis of global terrestrial NPP during the time when many of our samples were collected and reduces the impact of short-term variations in surface conditions.

Human pressures on the environment can have profound implications for other species. To assess direct and indirect human pressures on the environment, we used Human Footprint, a globally standardized measure of infrastructure, land cover, and human access into natural areas at 1 km2 resolution for 2009 (Venter et al., 2016). We chose this metric because it is comprehensive, including weighted estimates for the extent of built-up environments, crop land, pasture land, human population density, night-time lights, railways, roads, and navigable waterways (Venter et al., 2016).

2.5 | Statistical Analysis

To assess the magnitude of sexual size dimorphism, we calculated the mean female to male skull centroid size ratio (Ralls, 1976). Because sexual size dimorphism was extremely small relative to size difference related to geography, the sexes were pooled in analyses of climatic variables, and an additional 28 individuals of unknown sex were added to the dataset.

To evaluate the strength of association between climatic parameters, a covariance matrix was constructed, using Pearson's coefficient (r) from the Cor function in the R package 'stats v3.6.2'. Several covariates had coefficient (r) values above 0.7 or below -0.7 , which was considered highly correlated (Zuur, Leno, & Smith, 2007). This was not unexpected given that these climatic parameters are driven by the interaction of atmospheric processes and the physical and chemical features of the Earth (Wallace & Hobbs, 2006), which vary geographically (Tobler, 1979). High correlation between covariates is an obstacle for correctly fitting models (Zuur,

Leno, & Elphick, 2010). If the sample size is large enough, this problem can be addressed by adding spatial correlation structures to the model (Zuur et al., 2010). Because we had a relatively small sample of skulls, and there were temporal mismatches between response and predictor variables, we chose to fit simple general linear models and compare model performance, rather than attempt to fit more complex multiple regression or spatiotemporal models (Zuur & Leno, 2016; Zuur, Leno, & Elphick, 2010).

Model performance was assessed using adjusted R2 squared, root mean squared error (RMSE), and accuracy. Accuracy as used here is the correlation coefficient between the actual and the predicted value of the outcome. It was calculated using the 'performance_accuracy' function from the R package 'performance' with 5000 bootstrap-samples. The benefit of this approach is that we were able to compare predictors of interest and inhibit data violations of model assumptions as well as avoid estimating overparameterized models with little biological significance, spatiotemporal concordance, and/or statistical power (Bell & Schlaepfer, 2016; Mac Nally, 2000; Zuur et al., 2010). To check that assumptions of general linear models were met, we used the check_collinearity, check_normality, check_heteroscedasticity, and check_autocorrelation functions from the R package 'performance' and regression diagnostic plots from the R package 'base'.

To account for autocorrelated residuals due to the spatial structure of the data, we included latitude as a control predictor. Due to nonlinear patterns detected in model residuals, we included both linear, and if necessary, higher order polynomials of latitude (Blackburn & Hawkins, 2004). This helped account for some spatial structure in the residual (error) variance and thereby increased parameter certainty (e.g., by shrinking standard errors of the coefficient

estimates) and generated more precise model results. Ecological responses to spatial change often exhibit nonlinear behavior (Peters et al., 2007), such that a small change in the driving variable (geography) can have a large but discontinuous influence on the response variable.

All model analyses were performed in R VERSION 4.0.2 (2020-06-22) (R CORE TEAM, 2020). To visualize size patterns across geography, centroid size was divided into 3 categories (small, medium, large) using Jenks natural breaks and mapped using specimen locality data. Maps were created using ArcMap 10.6 (Esri, 2018).

3 | RESULTS

3.1| Model performance

All models except Precipitation of Driest Quarter had an adjusted R2 greater than 0.50 and a RMSE of less than 14 (Table 2.1), indicating data concentrated around the line of best fit. Model accuracy was greater than 70 % for all models except Precipitation of Driest Quarter, which had a model accuracy of only 44.3%.

3. 2| Sexual dimorphism

Male skulls were significantly larger than female skulls after taking into account the effects of latitude (P= 0.001, Table 2.1). However, the magnitude of the difference between males and females was very small (Figure 2.3), with a male to female ventral view size ratio of only 1.037 (N = 50 males and 48 females).

3.3| Geographic variables

We observed a considerable range in skull ventral centroid size across geography (Figure 2.1), with adults from the smallest of the three size classes as much as 25% smaller than those from the largest size class (Figure 1B). Absolute Latitude was a significant predictor of striped hyena skull size (P< 0.001, Table 2.1 and Figure 2.4). For every decimal degree increase in latitude, skull centroid size increases 1.265. All large individuals (centroid size greater than 349) were from above 20° North, while small and medium sized individuals were more evenly distributed throughout the species' range (Figure 2.1A).

3.4| Climatic variables

Isothermality and Precipitation of Driest Quarter were important predictors of skull size for striped hyenas (Table 2.1; $P< 0.001$ and $P< 0.001$, respectively). Skull size decreases markedly with increasing Isothermality, such that for every one percent increase in Isothermality, centroid size decreases by 0.89 (Figure 2.5). The isothermality model has high explanatory power with an adjusted R^2 of 0.504. Striped hyena skull size also decreases with increasing Precipitation of Driest Quarter, although this relationship is not linear, since most skull samples are from regions with either low or high values for Precipitation of Driest Quarter, resulting in two distinct clusters. The adjusted R^2 is 0.196 for the Precipitation of Driest Quarter model, indicating significant but low explanatory power. Neither Isothermality nor Precipitation of Driest Quarter models included absolute latitude as a covariate, hence the explanatory power of the models relies solely on the covariates and not latitude. No other climatic variables tested were significant predictors of striped hyena skull size (Table 2.1). The significant relationship between striped hyena skull size and these two variables suggests that these seasonal climatic variables are important factors influencing size in striped hyenas.

3.5| Resource variables

Neither annual terrestrial net primary productivity (NPP) nor Human Footprint were significant predictors of striped hyena skull size (Table 2.1). These two variables were intended as measures of food availability but may not be adequate indicators given the eclectic diet of striped hyenas.

4| DISCUSSION

4.1| Geographic pattern

Striped hyenas exhibit a strong latitudinal cline in skull size, with the largest individuals restricted to northern parts of the range, above 20° North. This roughly marks the demarcation between stable tropical environments and the more variable temperate environments. This pattern of geographic variation in size is remarkably consistent with Bergmann's rule, which predicts an increase in body size with latitude (Bergmann, 1847). It is also consistent with previous taxonomic work that described northern subspecies, found above approximately 28°N, as larger than southern subspecies (Pocock, 1934; Rieger, 1979).

These findings contrast with a similar analysis of skull size variation in the closely related spotted hyena (Cavalieri Chapter 1; n=332). In that species, there is a strong tendency for the smallest individuals to occur in East Africa, between -5.00^{o} and 10.00^{o} latitude and east of 28.50^{o} longitude, with larger individuals found elsewhere in the range. Striped and spotted hyenas are both members of the bone cracking lineage of hyenas and co-occur through much of north central and east Africa. Thus, we might expect them to experience similar selective pressures at the same latitude and exhibit a similar pattern of size variation across geography. The different pattern of latitudinal variation in skull size between striped and spotted hyena could reflect their markedly different behavior and ecology.

Spotted hyenas are highly social and hunt cooperatively, and thus experience intense intraspecific competition for food among clan members (Green et al., 2018; Holekamp et al., 2012). In East Africa where the largest ungulate migration in the world is found, spotted hyena reach very high population densities (e.g., 0.83 individuals per km2 in Mara), which is

associated with small body size (Green et al., 2018; Sinclair & Norton-Griffiths, 1979; Walpole, 2003) (Cavalieri Chapter 1). In contrast, striped hyenas are usually found alone or in small groups (Hofer & Mills, 1998; Kruuk, 1976), generally not thought to actively hunt prey larger than themselves and occur at low population densities (0.03-0.011/km^2) (AbiSaid & Dloniak, 2015). Thus density-dependent competition for food would not be a driving factor in intraspecific size variation in striped hyenas.

4.2| Sexual Dimorphism

Striped hyena skulls exhibit slight male-biased sexual size dimorphism, with a female to male size ratio of 0.963 (Figure 2.3). This is consistent with the findings for total skull length and zygomatic breath from pooled data reported by Rieger (1979). It is also consistent with males having slightly greater body mass as reported by Mills and Hofer (1998). Our findings are in agreement with data reported by Kruuk (1976) of slightly heavier males than females in Israel (n=5), but contrast with his reports of no difference in the body weight of striped hyena males and females from the Serengeti (n=2).

Male biased sexual size dimorphism is common in the Order Carnivora, is generally related to breeding system, and is strongest in polygynous species with intense competition between males for access to females (Gittleman, 1983). Spatial and social structure of striped hyenas is not well-known. The better-studied spotted hyena exhibits slight female biased size dimorphism (female to male size ratio of 1.011; Cavalieri Chapter 1) and has a social system composed of a linear dominance hierarchy in which females and their offspring are known to be dominant to breeding males (Frank, 1986; Smale et al., 1993). This social structure is assumed to facilitate access to resources for the offspring of high-ranking females, as

competition for food is intense in large spotted hyena clans. Spatial and social structure of striped hyenas may be flexible and appears to vary across geography. Two populations in Kenya approximately 300 km apart, exhibit markedly different space-use patterns. The Laikipia population formed small stable polyandrous social groups composed of multiple males and a single female, with male home ranges overlapping considerably with those of other males, whereas the Shompole population had less male home range overlap and a high degree of female home range overlap (Califf et al., 2019; Wagner et al., 2008). These contrasting striped hyena social structures create opposing selection pressures on size, making it difficult to detect patterns when examined across the entire geographic range. Detecting patterns is further complicated if social structures are variable across time as well as space. As our samples did not allow us to investigate sexual size dimorphism within populations it is not surprising that we only found slight male-biased sexual size dimorphism in striped hyenas across their entire geographic range. In both known types of striped hyena society competition between individuals is less intense than in spotted hyena clans, making intraspecific size differences evolutionarily advantageous.

4.3| Climatic variables

Temperature and precipitation covary with latitude and are often proposed as driving forces behind latitudinal size clines (Bonan, 2015; James, 1970). Because we found a strong relationship between latitude and striped hyena skull size, we expected our temperature variables to also be significant predictors of skull size. However, none of the annual temperature variables included in our analysis were statistically significant. The long-accepted explanation for latitudinal increase in size is the heat conservation hypothesis, i.e., species at

higher latitudes are selected for large size because a larger body loses less heat to the environment (Bergmann, 1847). Our results do not indicate that annual mean temperature is an important correlate of the increase in size seen with increasing absolute latitude in striped hyenas.

Annual mean precipitation was also not a significant predictor of striped hyena skull size. This was unexpected, as size is positively correlated with annual precipitation for many other mammals (Blois, Feranec, & Hadly, 2008; Gay & Best, 1996). Yom-Tov (2006) found that mean annual rainfall across a 30-year period was positively correlated with body size of adults striped hyenas (represented by PCA of body weight, body length, and greatest skull length) for a sample of 31 striped hyenas from Israel. While statistically significant, the adjusted R2 for this model of precipitation was only 0.101, indicating a small amount of the variation in size was explained by annual rainfall. The difference between our results and Yom-Tov et al. (2006) could be that at a larger geographic scale other factors are more powerful drivers of skull size or that we looked at precipitation from a given year and not precipitation accumulated over 30 years at a finer scale. Perhaps this temporal mismatch is why none of our annual climate variables were significant predictors of striped hyena skull size. Our results do not support the heat conservation hypothesis proposed by Bergmann (1847), and fail to suggest that annual measures of climate are important factors driving skull size in striped hyenas.

We did find a high correlation between skull size and two seasonal climatic variables, isothermality and precipitation of driest quarter. Isothermality is an indicator of degree of seasonal temperature change - high isothermality is associated with stable environments often found in the tropics, and low isothermality with large seasonal fluctuations that are frequently

associated with periods of resource shortage. Striped hyena skulls are significantly larger in areas with lower isothermality (Figure 2.5 and 2.8). Other authors have reported a positive correlation between body size and measures of seasonality (Boyce, 1978; Gordon, Johnson, & Louis, 2016; Lindstedt & Boyce, 1985; Ritke & Kennedy, 1988). We did not find a significant relationship between striped hyena skull size and any of the other seasonal temperature variables. This was surprising as they strongly correlated with one another and with isothermality. Thus, our results provide stronger support for the seasonality hypothesis proposed by Lindstedt and Boyce (1985) than for the heat conservation hypothesis proposed by Bergmann (1847).

Distinguishing the influences of temperature, precipitation, and resource availability is inherently difficult because temperature and precipitation influence plant productivity and therefore the amount of nutrients available to consumers. Thus, we expected precipitation to be an important factor influencing size in striped hyenas. While we did not find a relationship between annual mean precipitation, precipitation seasonality, or precipitation of the wettest quarter, we did find a negative significant relationship between skull size and precipitation in the driest quarter. However, the explanatory power of the model was low (Table 2.1) suggesting that precipitation in the driest quarter is not a very important driver of striped hyena skull size.

Indeed, the range of centroid sizes found at high precipitation in the driest quarter falls within the range of centroid sizes found at low precipitation in the driest quarter (Figure 2.6). Fewer skulls occur in areas with high precipitation in the driest quarter and there is an absence

of striped hyenas collected in areas between 115 and 291 mm of precipitation in the driest quarter.

4.4| Resource availability

Primary productivity is largely determined by precipitation (Knapp, Carroll, & Fahey, 2014) and in arid environments such as those areas where striped hyenas often occur, small changes in precipitation can greatly affect primary productivity (Knapp et al., 2014; Yoram Yom-Tov & Geffen, 2006). While we predicted that net primary production would be a strong predictor of striped hyena skull size, we found no significant relationship between these two variables. This could reflect the fact that striped hyenas are omnivores with an extremely diverse diet and can consume foods from multiple trophic levels. Since they can access energy from more than one trophic level they are not limited by net primary productivity and so do not exhibit the same pattern seen in other mammals restricted to one trophic level (Geist, 1987; Rosenzweig, 1968). Increased access to resources should result in a larger body size because there is more energy available to devote to growth (Damuth, 1981; Geist, 1987). Striped hyenas in Israel had increased access to human garbage and crops from the 1940s to the early 2000s; this was associated with an increase in body length (Y. Yom-Tov, 2003). Therefore, we expected to find a strong positive correlation between human footprint and striped hyena skull size in our larger geographic sample. We did not find a significant relationship between skull size and human footprint. This could be because our measure of human footprint encompasses a broader range of human impact on the environment than just refuse and crops or because our sample includes striped hyenas collected over a much broader temporal range than this measure of human impact on the environment.

Striped hyenas are sexually dimorphic with males being slightly larger than females. There is a strong geographic pattern of size variation, with larger individuals found at higher latitudes (Figure 2.1A), as predicted by Bergmann's rule (Bergmann, 1847; Watt, Mitchell, & Salewski, 2010). In this study, we modeled intraspecific variation in skull size of striped hyenas against proposed drivers of geographic variation in size. We found evidence that seasonal climatic variables are better predictors of hyena skull size than annual climatic variables. We did not find evidence to support our prediction that striped hyenas would be larger in areas with higher net primary productivity or increased access to human-provided foods. Our findings support the notion that geographic variation in body size is primarily driven by seasonal climatic variables, which is consistent with the seasonality hypothesis (Lindstedt & Boyce, 1985).

APPENDICES

APPENDIX A

FIGURES AND TABLES

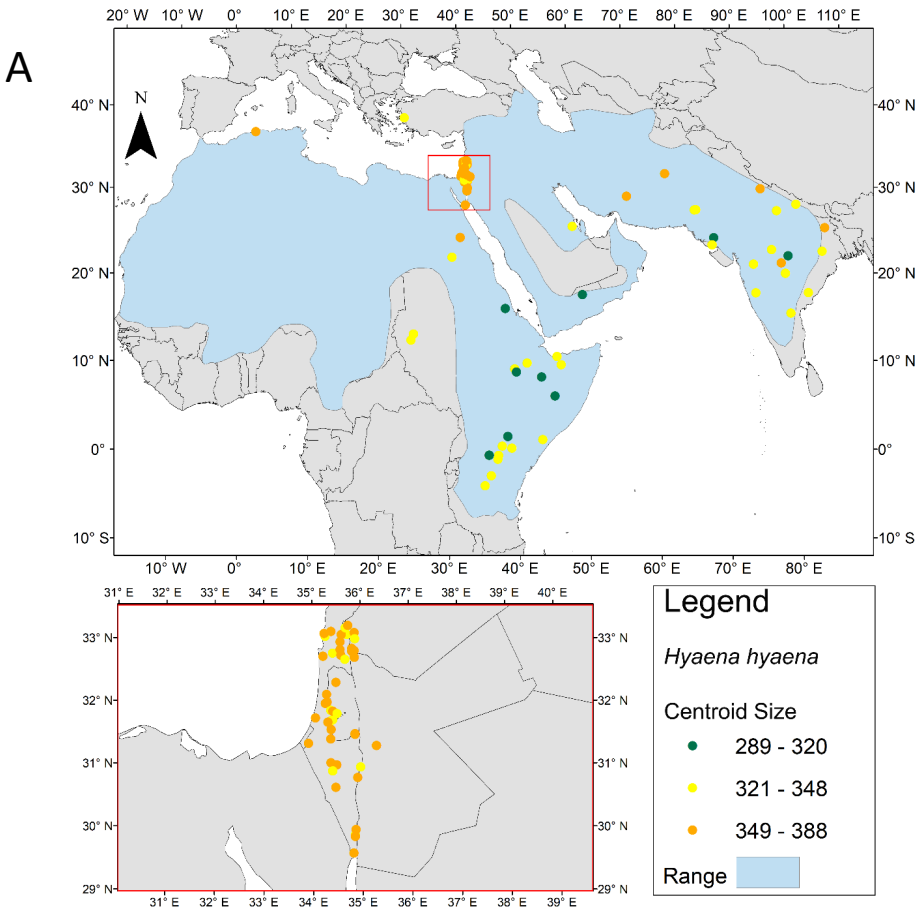

Figure 2.4: A: Specimen localities for *Hyaena hyaena* skulls used in this study. Point color indicates ventral view centroid size class delineated using Jenks natural breaks: small (green), medium (yellow), large (orange). The current geographical range for the species is highlighted in blue. Latitude and longitude in decimal degrees are labeled on the axes. The red square indicates the area magnified in the lower map. B: Diagram comparing median centroid sizes for representatives from each of the three size classes, drawn to scale. Green (CS = 305, USNM 182047), Yellow (CS = 337, NMK 3474), and Orange (CS = 357, TAU 7238). The blue bar represents the species' range.

Figure 2.1 (cont'd)

B

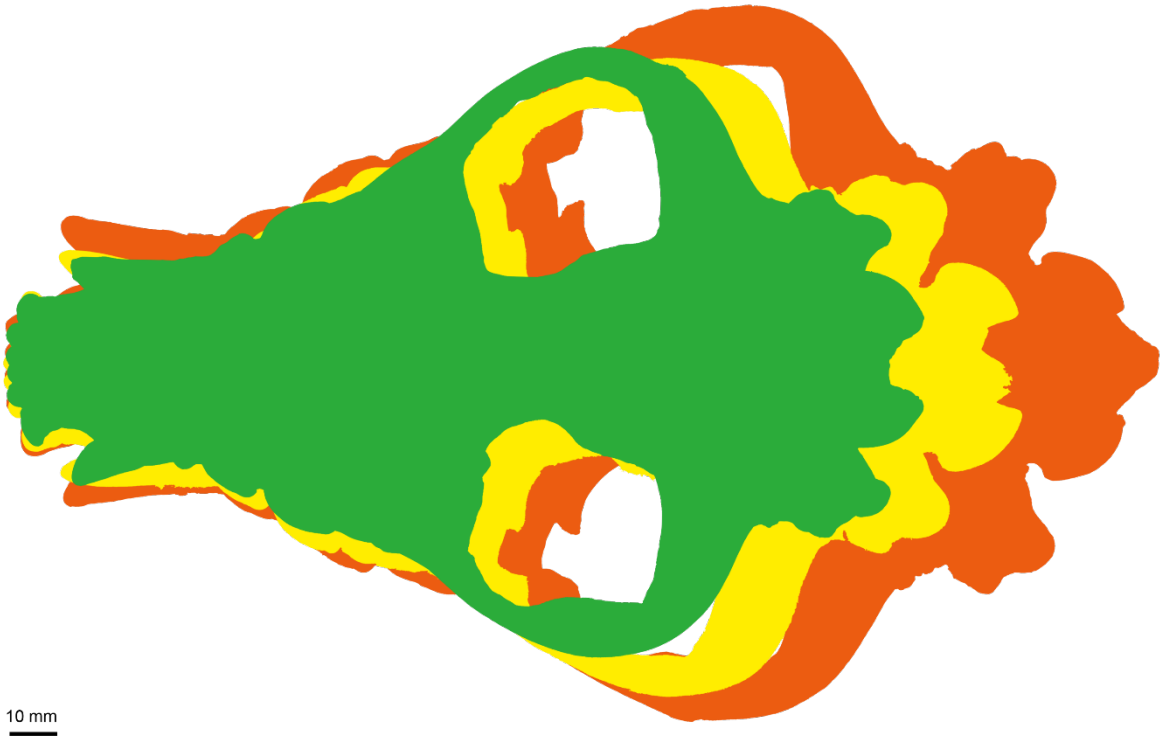

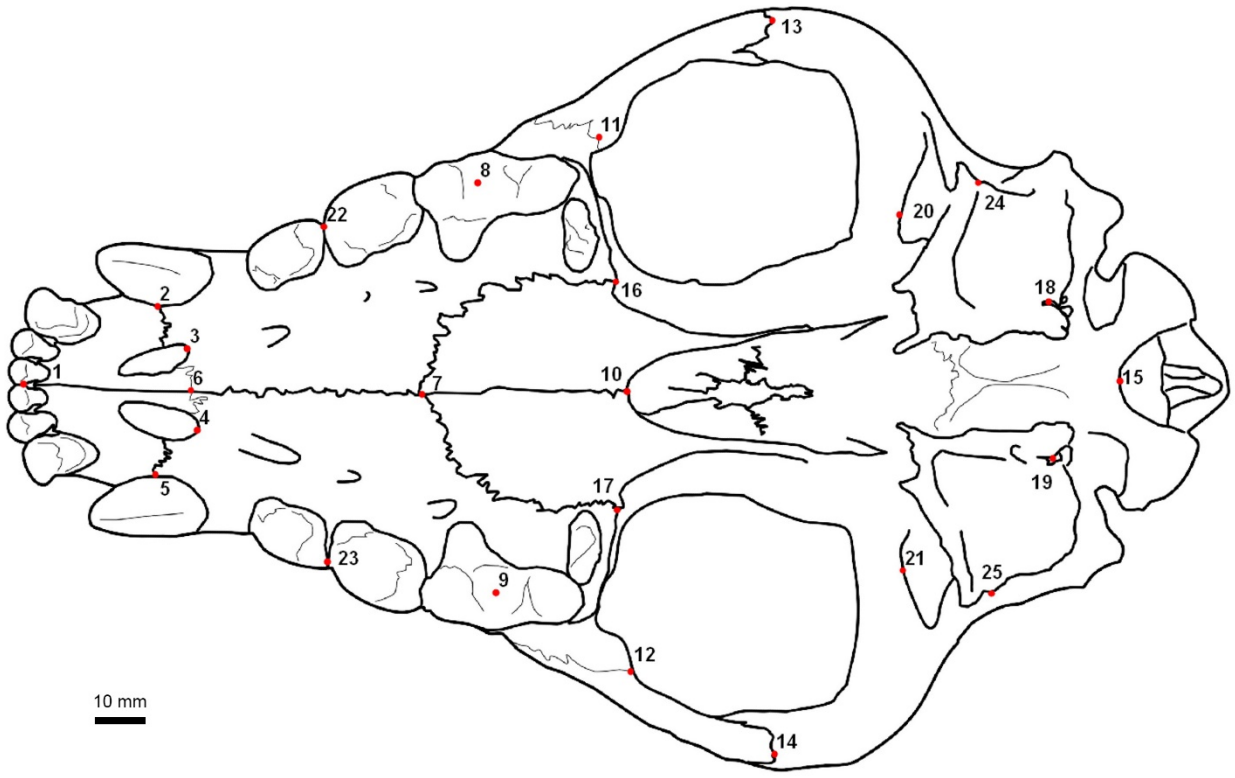

Figure 2.5: Position of landmarks on a skull of striped hyena (*Hyaena hyaena*) for the ventral cranium.

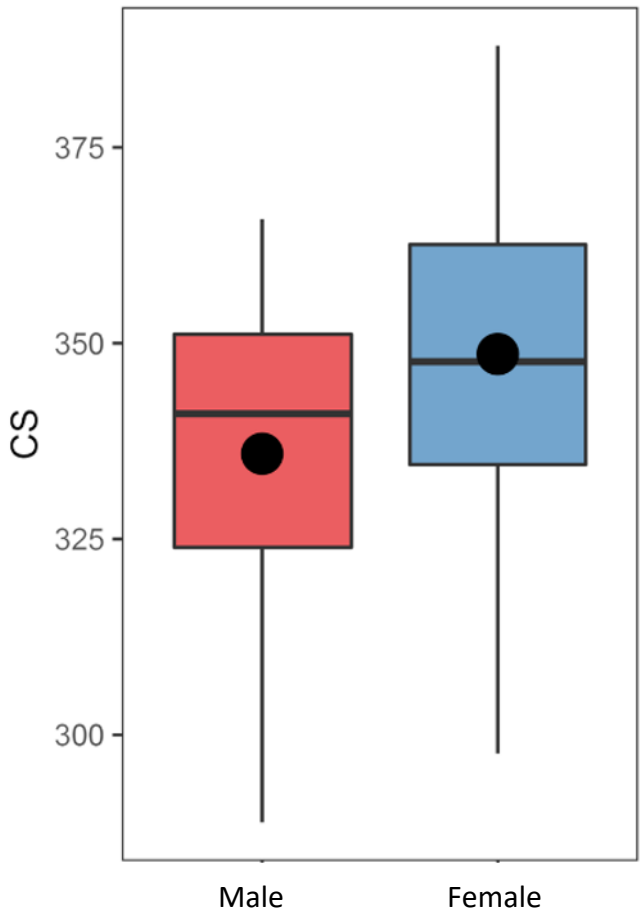

Figure 2.6: Boxplots of *Hyaena hyaena* centroid size for female (red) and male (blue) ventral view of skull (N = 48 females and 50 males). Boxplots illustrate the means (black dots) and medians (horizontal lines) for each sex. The lower and upper hinges correspond to the 25th and 75th percentiles, respectively. The upper and lower whiskers extends from the hinge to the largest value no further than 1.5 * interquartile range from the hinge.

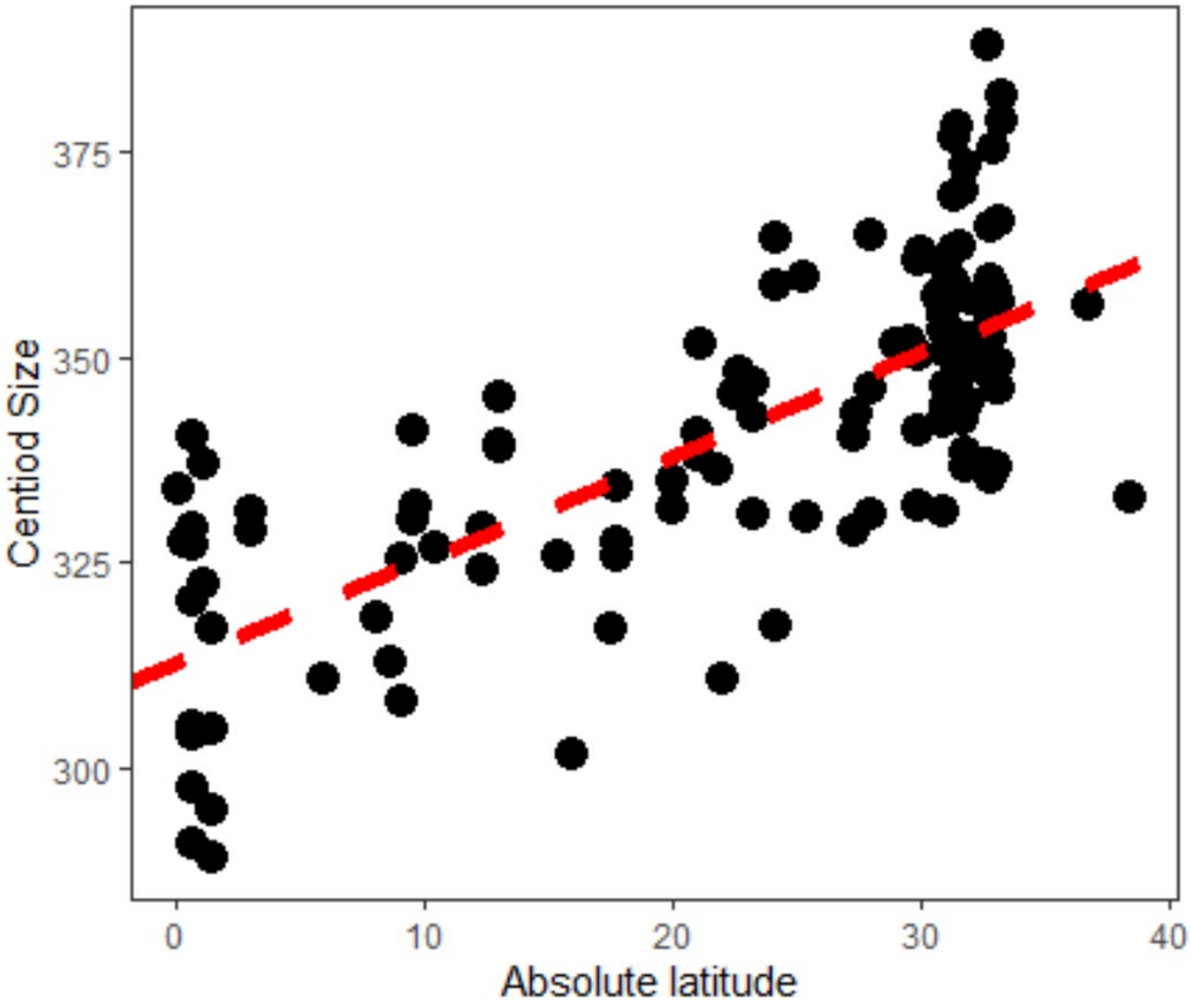

Figure 2.7: Regression of ventral centroid size of the skull of *Hyaena hyaena* on absolute latitude. The red dashed line shows the regression of model lm(CS~Abslat,data=Data).

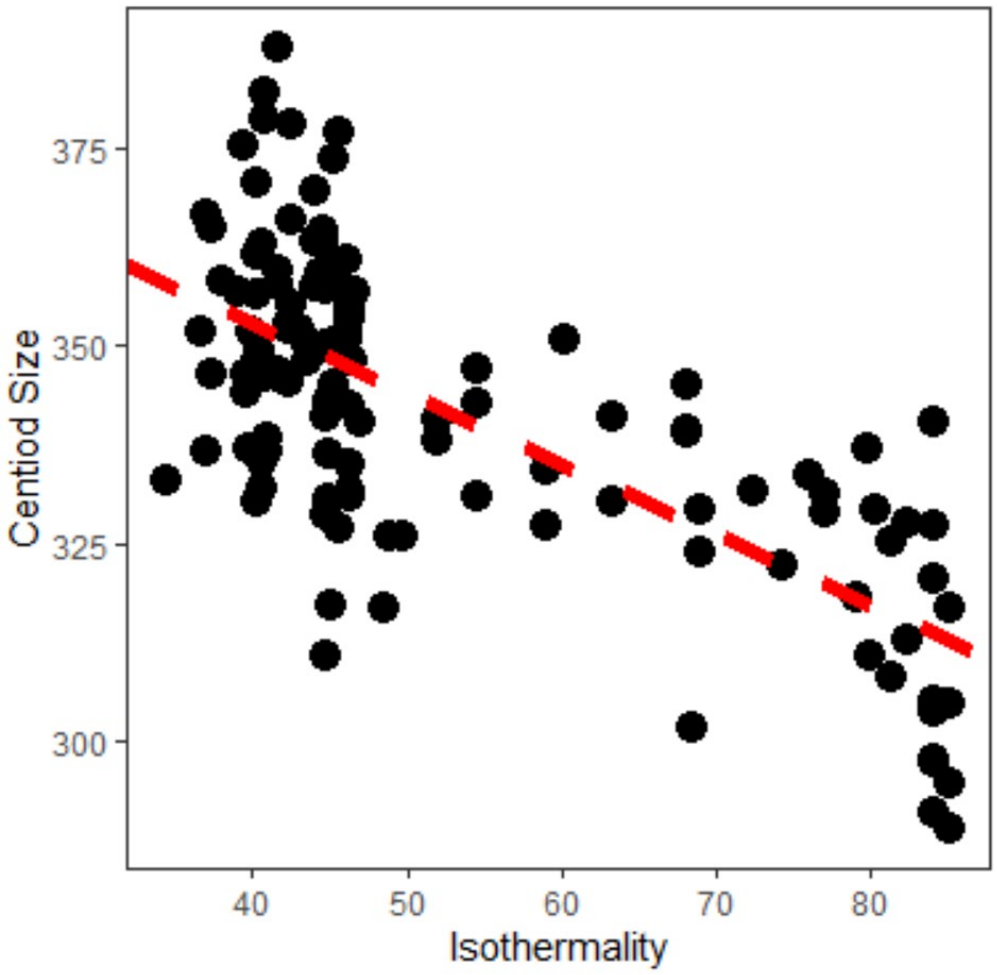

Figure 2.8: Regressions of centroid size and Isothermality for ventral view of the skull for *Hyaena hyaena*. The red dashed line shows the regression of model lm(CS ~ 1 + BIO10M_03_, data = Data).

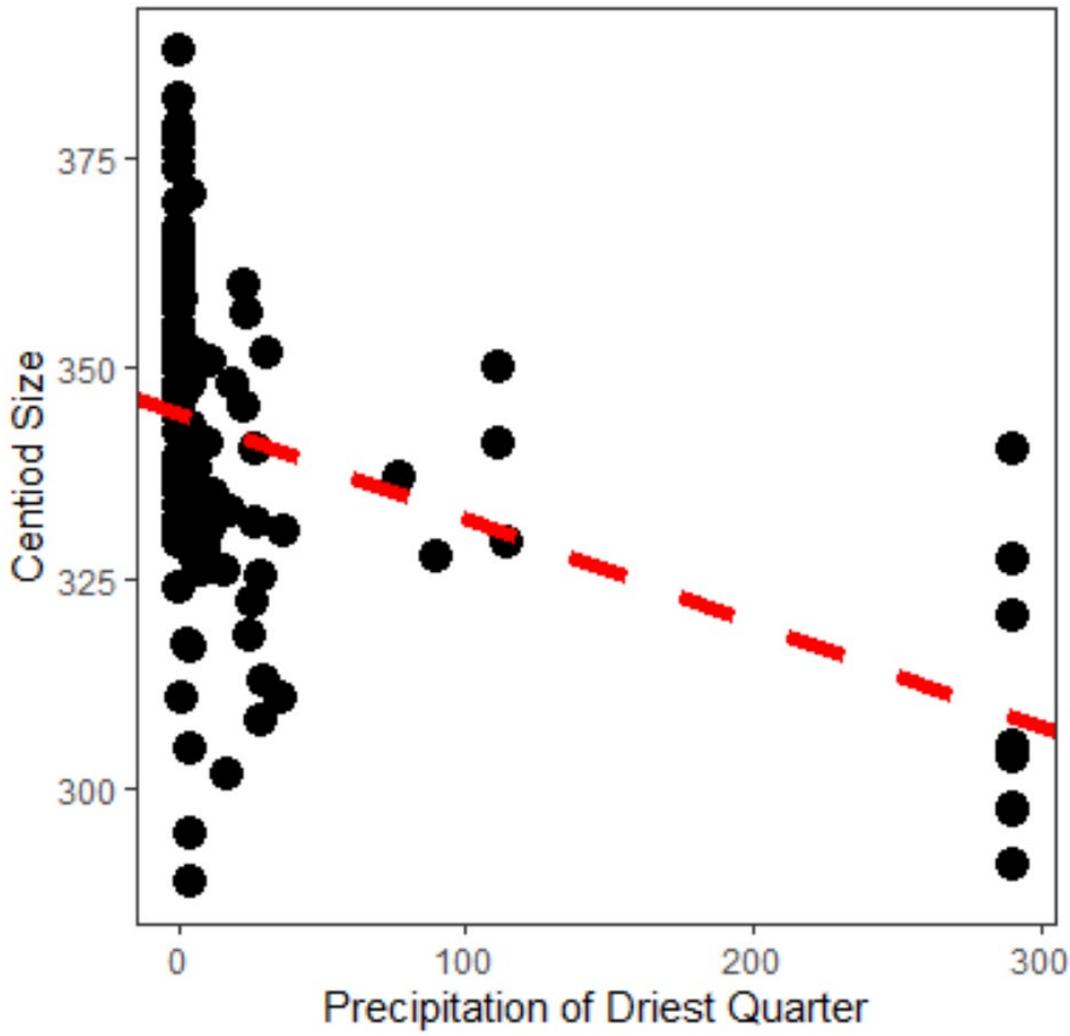

Figure 2.9: Regressions of centroid size and Precipitation of Driest Quarter for ventral view of the skull for *Hyaena hyaena*. The red dashed line shows the regression of model lm(CS~1+BIO10M_17_, data=Data).

Table 2.12: Comparison of general linear model performance assessing effects of geographic and environmental variables on ventral cranium size in *Hyaena hyaena*: Estimate, Standard Error, t value, p-values, adjusted R squared, root mean square error and accuracy. For factor variables, reference levels were set as female for sex and barren or sparsely vegetated for landcover. Significant values are noted with an asterisk and significant main covariates are noted in bold.

		Variables	Estimate	Standard Error	t	p	Significance	Adjusted R squared	Root mean square error	Accuracy
Demographic variables	Sex	(Intercept)	306.026	3.149	97.196	0.000		0.624	12.794	0.795
		Sex	**9.075**	**2.644**	**3.432**	**0.001**	*			
		Absolute Latitude	1.368	0.116	11.811	0.000	*			
Geographic variables	Latitude	(Intercept)	312.699	2.623	119.194	0.000		0.546	13.334	0.741
		Absolute Latitude	**1.265**	**0.103**	**12.291**	**0.000**	*			
Annual climatic variables	Annual Mean Temperature	(Intercept)	315.679	9.569	32.989	0.000		0.540	13.300	0.749
		Annual Mean Temperature	-0.075	0.464	-0.163	0.871				
		Absolute Latitude	0.983	0.600	1.639	0.104				
		Absolute Latitude ^{2}	0.008	0.017	0.447	0.656				
	Annual Mean Precipitation	(Intercept)	322.007	8.750	36.802	0.000		0.546	13.267	0.746
		Annual Mean Precipitation	-0.415	0.372	-1.115	0.267				
		Absolute Latitude	1.140	0.152	7.476	0.000	*			
Seasonal climatic variables	Isothermality	(Intercept)	388.751	4.372	88.910	0.000		0.504	13.937	0.710
		Isothermality	**-0.894**	**0.079**	**-11.305**	**0.000**	*			
	Temperature Seasonality	(Intercept)	312.013	2.759	113.078	0.000		0.544	13.298	0.745
		Temperature Seasonality	0.010	0.012	0.814	0.417				

Table 2.1 (cont'd)

	Variables	Estimate	Standard Error	t	p	Significance	Adjusted R squared	Root mean square error	Accuracy
	Absolute Latitude	1.095	0.233	4.700	0.000	*			
Precipitation Seasonality	(Intercept)	317.261	4.083	77.709	0.000		0.550	13.221	0.749
	Precipitation Seasonality	-0.057	0.039	-1.454	0.149				
	Absolute Latitude	1.314	0.108	12.180	0.000	*			
Mean Temperature of Warmest Quarter	(Intercept)	315.678	7.386	42.740	0.000		0.543	13.324	0.744
	Mean Temperature of Warmest Quarter	-0.123	0.285	-0.432	0.667				
	Absolute Latitude	1.279	0.108	11.830	0.000	*			
Mean Temperature of Coldest Quarter	(Intercept)	317.397	11.248	28.217	0.000		0.551	12.978	0.768
	Mean Temperature of Coldest Quarter	-0.029	0.522	-0.056	0.956				
	Absolute Latitude	-2.374	4.783	-0.496	0.621				
	Absolute Latitude ^{2}	0.726	0.835	0.870	0.386				
	Absolute Latitude ^{3}	-0.057	0.055	-1.032	0.304				
	Absolute Latitude ^{4}	0.002	0.002	1.198	0.233				
	Absolute Latitude ^{5}	0.000	0.000	-1.356	0.178				
Precipitation of Wettest Quarter	(Intercept)	315.526	3.134	100.676	0.000		0.552	13.193	0.750
	Precipitation of Wettest Quarter	-0.007	0.004	-1.624	0.107				

Table 2.2 (cont'd)

		Variables	Estimate	Standard Error	t	p	Significance	Adjusted R squared	Root mean square error	Accuracy
		Absolute Latitude	1.245	0.103	12.082	0.000	*			
	Precipitation of Driest Quarter	(Intercept)	344.789	1.704	202.335	0.000		0.196	17.736	0.443
		Precipitation of Driest Quarter	**-0.125**	**0.022**	**-5.610**	**0.000**	*			
Resource variables	Net primary production	(Intercept)	314.657	2.706	115.179	0.000		0.544	13.304	0.745
		Net primary production	-0.000	0.270	-1.438	0.153				
		Absolute Latitude	1.223	0.106	12.272	0.000	*			
	Human Footprint	(Intercept)	312.605	3.062	102.080	0.000		0.542	13.334	0.744
		Human Footprint	0.007	0.123	0.060	0.952				
		Absolute Latitude	1.262	0.115	11.003	0.000	*			

APPENDIX B

SPECIMENS LIST

Table 2.13: *Hyaena hyaena* specimens ventral cranium

Hyaena hyaena specimens ventral cranium	
Museum	Catalog Number
OSU	5261
OSU	5585
OSU	5586
OSU	5712
OSU	5758
USNM	163110
USNM	172923
USNM	182034
USNM	182040
USNM	182045
USNM	182047
USNM	182079
USNM	182080
USNM	182086
USNM	182100
USNM	182134
USNM	182135
USNM	182136
USNM	318112
USNM	329351
USNM	523000
TAU	9930
TAU	11821
TAU	11945
TAU	276
TAU	9418
TAU	6640
TAU	594
TAU	7644
TAU	7216
TAU	7238
TAU	7256
TAU	7455
TAU	8666
TAU	9010
TAU	7480
TAU	8294
TAU	7898

Table 2.2 (cont'd)

TAU	7645
TAU	7672
TAU	7217
BMNH	34112814
TAU	9811
TAU	7737
TAU	6140
TAU	7119
TAU	5127
TAU	6510
TAU	10616
TAU	7962
TAU	10617
TAU	11249
TAU	11515
TAU	11130
BMNH	34112813
TAU	11248
NMK	4628
NMK	8297
TAU	10236
TAU	10683
TAU	11533
TAU	11099
TAU	6804
FMNH	140216
FMNH	140218
TAU	11687
BMNH	34112812
BMNH	311210
NMK	3474
TAU	6895
BMNH	39439
BMNH	58624125
TAU	7
TAU	9743
BMNH	3411288
TAU	3316
BMNH	3831388
BMNH	3411283
BMNH	55282

Table 2.2 (cont'd)

BMNH	58209
BMNH	34112810
TAU	2814
BMNH	3411284
BMNH	518251
BMNH	39440
BMNH	3411285
TAU	3597
BMNH	3411286
TAU	12128
TAU	7839
BMNH	23349
BMNH	05121
BMNH	34112811
BMNH	2610873
TAU	9160
MSU	13003
MSU	11143
BMNH	92282
BMNH	2721427
BMNH	521483
BMNH	34847
BMNH	34112818
BMNH	565650
BMNH	34112816
TAU	9739
TAU	6202
TAU	4746
BMNH	2610872
RCSOM	13731
TAU	7813
BMNH [not on tag]	241055
TAU	4376
BMNH	1938101848
BMNH	872412
TAU	8295
FMNH	103991
FMNH	103992
BMNH	2010271
BMNH	231178
TAU	4035

Table 2.2 (cont'd)

BMNH	231179
BMNH	6543
TAU	7618
BMNH	231180
BMNH	2010272
TAU	22
TAU	11846

APPENDIX C

LANDMARK DEFINITIONS

Table 2.14: Ventral landmarks definitions

Landmark	Definition
1	Juncture between the incisors on the premaxilla
2	Premaxilla-maxilla suture intersection with the medial edge of the left canine
3	Most posterior point of the left incisive foramen
4	Most posterior point of the right incisive foramen
5	Premaxilla-maxilla suture intersection with the medial edge of the right canine
6	Posterior edge of premaxilla-maxilla suture on the palate
7	Center of Maxilla-palatine midline suture
8	Center of left fourth premolar
9	Center of right fourth premolar
10	Posterior edge of the midline suture between the left and right palatine.
11	Most posterior edge of the left maxilla-jugal suture
12	Most posterior edge of the right maxilla-jugal suture
13	Most posterior edge of the left jugal-squamosal suture
14	Most posterior edge of the right jugal-squamosal suture
15	Most anterior point of the foramen magnum
16	Posterior end of the left maxilla-palatine suture
17	Posterior end of the right maxilla-palatine suture
18	Center of left, jugular canal
19	Center of right, jugular canal
20	Most anterior point of left retroarticular process
21	Most anterior point of right retroarticular process
22	Posterior edge of left second premolar
23	Posterior edge of right second premolar
24	Most distal point of the left external auditory meatus
25	Most distal point of the right external auditory meatus

Table 2.15: Lateral Landmarks definations

Landmark	Definition
1	Anterior edge of the third incisor
2	Anterior edge of canine
3	Posterior edge of canine
4	The most posterior part of the infraorbital foramen
5	The intersection of the maxilla, lacrimal and jugal
6	The most lateral projection of post-orbital process
7	Most dorsal anterior part of the squamosal
8	Most ventral posterior part of the jugal
9	The most ventral-posterior point of the jugal-maxilla suture
10	The most posterior edge of the suture of palatine and pterygoid process
11	Suture of the squamosal and occipital inside the auditory meatus
12	Anterior upper edge of the occipital condyle
13	Posterior most edge of the sagittal crest
14	Anterior edge of the nasal-premaxilla suture

32 Semi-landmarks along curve of dorsal cranium, 14 to 13

Table 2.16: Mandible landmarks definitions

Landmark	Definition
1	Anterior edge of third incisor
2	Anterior edge of canine
3	Posterior edge of canine
4	Dorsal apex of the coronoid process
5	Most posterior projection of the coronoid process
6	Anterior edge of the mandibular condyle, distal to the vertical plane of the coronoid
7	Posterior most edge of the mandibular condyle
8	Posterior most point of the articular process
9	Intersection of the mandibular body and ramus
10	Intersection of anterior margin of first incisor with the dentary

32 Semi-landmarks along ventral curve of the mandible, 10 to 8

11 Semi-landmarks along posterior curve between articular process and mandibular condyle, 8 to 7

16 Semi-landmarks along posterior curve between mandibular condyle and coronoid process, 6 to 5

17 Semi-landmarks along anterior curve of ramus, 4 to 9

WORKS CITED

WORKS CITED

AbiSaid, M., & Dloniak, S. (2015). *Hyaena hyaena*. *The IUCN Red List of Threatened Species*, 2015-2012.

Adams, D. C., Collyer, M. L., & Sherratt, E. (2015). Geomorph: Software for geometric morphometric analyses. R package version 2.1.

Adams, D. C., & Otárola-Castillo, E. (2013). geomorph: an R package for the collection and analysis of geometric morphometric shape data. *Methods in Ecology and Evolution, 4*(4), 393-399.

Ashmole, N. P. (1963). The regulation of numbers of tropical oceanic birds. *Ibis, 103*(3), 458-473.

Barnes, C., Maxwell, D., Reuman, D. C., & Jennings, S. (2010). Global patterns in predator–prey size relationships reveal size dependency of trophic transfer efficiency. *Ecology, 91*(1), 222-232.

Bateman, P. W., Fleming, P. A., & Le Comber, S. (2012). Big city life: carnivores in urban environments. *Journal of Zoology, 287*(1), 1-23.

Bell, D. M., & Schlaepfer, D. R. (2016). On the dangers of model complexity without ecological justification in species distribution modeling. *Ecological Modelling, 330*, 50-59.

Bergmann, C. (1847). About the relationships between heat conservation and body size of animals. *Goett Stud, 1*, 595-708.

Bhandari, S., Morley, C., Aryal, A., & Shrestha, U. B. (2020). The diet of the striped hyena in Nepal's lowland regions. *Ecology and Evolution, 10*(15), 7953-7962.

Blackburn, T. M., & Hawkins, B. A. (2004). Bergmann's rule and the mammal fauna of northern North America. *Ecography, 27*(6), 715-724.

Blois, J. L., Feranec, R. S., & Hadly, E. A. (2008). Environmental influences on spatial and temporal patterns of body-size variation in California ground squirrels (*Spermophilus beecheyi*). *Journal of Biogeography, 35*(4), 602-613.

Bohm, T., & Höner, O. (2015). *Crocuta crocuta*. *The IUCN Red List of Threatened Species, 9*, 2015-2013.

Bonan, G. (2015). *Ecological climatology: concepts and applications*: Cambridge University Press.

Boyce, M. S. (1978). Climatic Variability and Body Size Variation in the Muskrats (*Ondatra zibethicus*) of North America. *Oecologia, 36*(1), 1-19.

Boyce, M. S. (1979). Seasonality and Patterns of Natural Selection for Life Histories. *The American Naturalist, 114*(4), 569-583.

Calder, W. (1984). *Size, Function, and Life History*. Cambridge, Massachusetts: Harvard University Press.

Califf, K. J., Green, D. S., Wagner, A. P., Scribner, K. T., Beatty, K., Wagner, M. E., & Holekamp, K. E. (2019). Genetic relatedness and space use in two populations of striped hyenas (*Hyaena hyaena*). *Journal of Mammalogy*.

Carbone, C., & Gittleman, J. L. (2002). A common rule for the scaling of carnivore density. *Science, 295*(5563), 2273-2276.

Cavallini, P. (1995). *Variation in the body size of the red fox.* Paper presented at the Annales Zoologici Fennici.

Chapman, A. D., & Wieczorek, J. (2006). Guide to best practices for georeferencing. *Copenhagen: Global Biodiversity Information Facility*, 1-77.

Damuth, J. (1981). Population-density and body size in mammals. *Nature, 290*(5808), 699-700.

Darwin, C. (1872). The descent of man, and selection in relation to sex (Vol. 2). D. Appleton.

Dial, K. P., Greene, E., & Irschick, D. J. (2008). Allometry of behavior. *Trends in Ecology & Evolution, 23*(7), 394-401.

Esri. (2018). ArcMap: Release 10.6. 1.

Fick, S. E., & Hijmans, R. J. (2017). WorldClim 2: new 1-km spatial resolution climate surfaces for global land areas. *International journal of climatology*, *37*(12), 4302-4315.

Frank, L. G. (1986). Social organization of the spotted hyaena (*Crocuta crocuta*). I. Demography. *Animal Behaviour, 34*(5), 1500-1509.

Gay, S. W., & Best, T. L. (1996). Relationships between abiotic variables and geographic variation in skulls of pumas (*Puma concolor*: Mammalia, Felidae) in North and South America. *Zoological Journal of the Linnean Society, 117*(3), 259-282.

Geist, V. (1987). Bergmann's rule is invalid. *Canadian Journal of Zoology, 65*(4), 1035-1038.

Gittleman, J. L. (1983). The behavioural ecology of carnivores. University of Sussex, Falmer, East Sussex, England.

Gordon, A. D., Johnson, S. E., & Louis, E. E. (2016). Environmental correlates of body mass in true lemurs (*Eulemur* spp.). *International Journal of Primatology, 37*(1), 89-108.

Gortázar, C., Travaini, A., & Delibes, M. (2000). Habitat-related microgeographic body size variation in two Mediterranean populations of red fox (*Vulpes vulpes*). *Journal of Zoology, 250*(3), 335-338.

Green, D., Johnson-Ulrich, L., Couraud, H., & Holekamp, K. (2018). Anthropogenic disturbance induces opposing population trends in spotted hyenas and African lions. *Biodiversity and Conservation, 27*(4), 871-889.

Hartstone-Rose, A., & Steynder, D. D. (2013). Hypercarnivory, durophagy or generalised carnivory in the Mio-Pliocene hyaenids of South Africa? *South African Journal of Science, 109*(5), 1-10.

Hilderbrand, G. V., Schwartz, C., Robbins, C., Jacoby, M., Hanley, T., Arthur, S., & Servheen, C. (1999). The importance of meat, particularly salmon, to body size, population productivity, and conservation of North American brown bears. *Canadian Journal of Zoology, 77*(1), 132-138.

Hofer, H., & Mills, G. (1998). Species accounts: striped hyena Hyaena (Hyaena hyaena Linnaeus, 1758). *Mills, G. & H. Hofer (Comp.) Status Survey and Conservation Action Plan. IUCN/SSC Hyaena Specialist Group, IUCN, Gland, Switzerland, and Cambridge, UK*, 21-26.

Holekamp, K. E., Smith, J. E., Trelioff, C. C., Van horn, R. C., & Watts, H. E. (2012). Society, demography and genetic structure in the spotted hyena. *Molecular Ecology, 21*(3), 613-632.

Huston, M. A., & Wolverton, S. (2009). The global distribution of net primary production: resolving the paradox. *Ecological Monographs, 79*(3), 343-377.

Huston, M. A., & Wolverton, S. (2011). Regulation of animal size by eNPP, Bergmann's rule, and related phenomena. *Ecological Monographs, 81*(3), 349-405.

Imhoff, M. L., & Bounoua, L. (2006). Exploring global patterns of net primary production carbon supply and demand using satellite observations and statistical data. *Journal of Geophysical Research: Atmospheres, 111*(D22).

IUCN. (2021). The IUCN Red List of Threatened Species. Version 2021-2. . Retrieved from http://www.iucnredlist.org/

James, F. C. (1970). Geographic Size Variation in Birds and Its Relationship to Climate. *Ecology, 51*(3), 365-390.

Klein, R. G., & Scott, K. (1989). Glacial/interglacial size variation in fossil spotted hyenas (Crocuta crocuta) from Britain. *Quaternary Research, 32*(1), 88-95.

Knapp, A. K., Carroll, C. J. W., & Fahey, T. J. (2014). Patterns and Controls of Terrestrial Primary Production in a Changing World. In R. K. Monson (Ed.), *Ecology and the Environment* (pp. 205-246). New York, NY: Springer New York.

Kolb, H. (1978). Variation in the size of foxes in Scotland. *Biological Journal of the Linnean Society, 10*(3), 291-304.

Kruuk, H. (1976). Feeding and social behaviour of the striped hyaena (*Hyaena vulgaris* Desmarest). *African Journal of Ecology 14*, 91-111.

Kurten, B. (1957). The bears and hyenas of the interglacials. *Quaternaria, 4*, 69-81.

Leakey, L., Milledge, S., Leakey, S., Edung, J., Haynes, P., Kiptoo, D., & McGeorge, A. (1999). Diet of striped hyaena in northern Kenya. *African Journal of Ecology, 37*(3), 314-326.

Lindsey, C. C. (1966). Body Sizes of Poikilotherm Vertebrates at Different Latitudes. *Evolution, 20*, 456-465.

Lindstedt, S. L., & Boyce, M. S. (1985). Seasonality, fasting endurance, and body size in mammals. *The American Naturalist, 125*(6), 873-878.

Mac Nally, R. (2000). Regression and model-building in conservation biology, biogeography and ecology: The distinction between – and reconciliation of – 'predictive' and 'explanatory' models. *Biodiversity & Conservation, 9*(5), 655-671.

Manlick, P. J., & Pauli, J. N. (2020). Human disturbance increases trophic niche overlap in terrestrial carnivore communities. *Proceedings of the National Academy of Sciences, 117*(43), 26842-26848.

McElhinny, T. L. (2009). *Morphological Variation in a Durophagous Carnivore, the Spotted Hyena, Crocuta Crocuta*: Michigan State University. East Lansing, Michigan.

McNab, B. K. (2010). Geographic and temporal correlations of mammalian size reconsidered: a resource rule. *Oecologia, 164*(1), 13-23.

Meiri, S., Dayan, T., & Simberloff, D. (2004). Carnivores, biases and Bergmann's rule. *Biological Journal of the Linnean Society, 81*(4), 579-588.

Meiri, S., & Thomas, G. H. (2007). The geography of body size – challenges of the interspecific approach. *Global Ecology and Biogeography, 16*(6), 689-693.

Meiri, S., Yom-Tov, Y., & Geffen, E. (2007). What determines conformity to Bergmann's rule? *Global Ecology and Biogeography, 16*(6), 788-794.

Mills, M., & Hofer, H. (1998). Status survey and conservation action plan. Hyaenas. *IUCN/SSC Hyaena Specialist Group, IUCN, Switzerland*.

O'Donnell, M. S., & Ignizio, D. A. (2012). Bioclimatic predictors for supporting ecological applications in the conterminous United States. *US Geological Survey Data Series, 691*(10).

Peters, D. P. C., Pielke, R. A., Bestelmeyer, B. T., Allen, C. D., Munson-McGee, S., & Havstad, K. M. (2007). Spatial Nonlinearities: Cascading Effects in the Earth System. In J. G. Canadell, D. E. Pataki, & L. F. Pitelka (Eds.), *Terrestrial Ecosystems in a Changing World* (pp. 165-174). Berlin, Heidelberg: Springer Berlin Heidelberg.

Pitts, G., & Bullard, T. (1968). Some interspecific aspects of body composition in mammals. *Body composition in animals and man. Washington, DC: National Academy of Sciences*, 45-70.

Pocock, R. I. (1934). The Races of the Striped and Brown Hyænas. *Proceedings of the Zoological Society of London, 104*(4), 799-825.

R Core Team. (2017). R: A language and environment for statistical computing. R version 3.4. 1 edn. R Foundation for Statistical Computing, Vienna, Austria.

Ralls, K. (1976). Mammals in Which Females are Larger Than Males. *The Quarterly Review of Biology, 51*(2), 245-276.

Rieger, I. (1979). A review of the biology of striped hyaenas, Hyaena hyaena (Linne, 1758). *Sugetierkundliche Mitteilungen, 27*, 81-95.

Rios, N. (2019). GEOLocate - Software for Georeferencing Natural History Data. [Web application software]. Retrieved from http://www.geo-locate.org

Ritke, M. E., & Kennedy, M. L. (1988). Intraspecific Morphologic Variation in the Raccoon (*Procyon lotor*) and Its Relationship to Selected Environmental Variables. *The Southwestern Naturalist, 33*(3), 295-314.

Rohlf, F. J. (2015). The tps series of software. *Hystrix, 26*(1), 9-12.

Rosenzweig, M. L. (1968). The Strategy of Body Size in Mammalian Carnivores. *The American Midland Naturalist, 80*(2), 299-315.

Shamoon, H., & Shapira, I. (2019). Limiting factors of Striped Hyaena, Hyaena hyaena, distribution and densities across climatic and geographical gradients (Mammalia: Carnivora). *Zoology in the Middle East, 65*(3), 189-200.

Sibly, R. M., & Brown, J. H. (2007). Effects of body size and lifestyle on evolution of mammal life histories. *Proceedings of the National Academy of Sciences, 104*(45), 17707-17712.

Sinclair, A. R. E., & Norton-Griffiths, M. (1979). *Serengeti: Dynamics of an ecosystem* (2 ed.). Chicago: Chicago Univ. Press.

Smale, L., Frank, L. G., & Holekamp, K. E. (1993). Ontogeny of dominance in free-living spotted hyaenas: juvenile rank relations with adult females and immigrant males. *Animal Behaviour, 46*(3), 467-477.

Smith, F. A., Boyer, A. G., Brown, J. H., Costa, D. P., Dayan, T., Ernest, Evans, A. R., Fortelius, M., Gittleman, J. L., Hamilton, M. J., Harding, L. E., Lintulaakso, K., Lyons, S. K., McCain, C., Okie, J. G., Saarinen, J.J., Sibly, R. M., Stephens, P. R., Theodor, J., & Uhen, M. D. (2010). The Evolution of Maximum Body Size of Terrestrial Mammals. *Science, 330*(6008), 1216-1219.

Swanson, E. M., McElhinny, T. L., Dworkin, I., Weldele, M. L., Glickman, S. E., & Holekamp, K. E. (2013). Ontogeny of sexual size dimorphism in the spotted hyena (*Crocuta crocuta*). *Journal of Mammalogy, 94*(6), 1298-1310.

Tanner, J. B., Dumont, E. R., Sakai, S. T., Lundrigan, B. L., & Holekamp, K. E. (2008). Of arcs and vaults: the biomechanics of bone-cracking in spotted hyenas (*Crocuta crocuta*). *Biological Journal of the Linnean Society, 95*(2), 246-255.

Tobler, W. R. (1979). Cellular geography. In *Philosophy in geography* (pp. 379-386): Springer.

Turner, A., & O'Regan, H. (2002). The assessment of size in fossil Felidae. *Estudios Geológicos, 58*(1-2), 45-54.

Valkenburgh, B. (1990). Skeletal and dental predictors of body mass in carnivores. In *Body size in Mammalian Paleobiology Estimation and biological implications.* (pp. 181-205).

Venter, O., Sanderson, E. W., Magrach, A., Allan, J. R., Beher, J., Jones, K. R., Possingham, H., Laurance, W.F., Wood, P., & Fekete, B. M. (2016). Sixteen years of change in the global terrestrial human footprint and implications for biodiversity conservation. *Nature communications, 7*(1), 1-11.

Venter, O., Sanderson, E. W., Magrach, A., Allan, J. R., Beher, J., Jones, K. R., Possingham, H.P., Laurance, W.F., Fekete, B.M.,Levy, M.A., Watson, J. E. (2016). Global Terrestrial Human Footprint Maps for 1993 and 2009. *Scientific Data*, 160067.

Wagner, A. P. (2006). Behavioral ecology of the striped hyena (*Hyaena hyaena*). Montana State University Bozeman, Montana.

Wagner, A. P., Frank, L. G., & Creel, S. (2008). Spatial grouping in behaviourally solitary striped hyaenas, Hyaena hyaena. *Animal Behaviour, 75*(3), 1131-1142.

Wallace, J. M., & Hobbs, P. V. (2006). 2 - The Earth System. In J. M. Wallace & P. V. Hobbs (Eds.), *Atmospheric Science (Second Edition)* (pp. 25-61). San Diego: Academic Press.

Walpole, M. J. (2003). *Wildlife and People: Conflict and Conversation in Masai Mara, Kenya: Proceedings of a Workshop Series. 13-16 August 2001*: IIED.

Watt, C., Mitchell, S., & Salewski, V. (2010). Bergmann's rule; a concept cluster? *Oikos, 119*(1), 89-100.

Werdelin, L., Solounias, N. J. F., & strata. (1991). The Hyaenidae: taxonomy, systematics and evolution. *Fossils and strata, 30*, 1-104.

Werdelin, L., & Turner, A. (2019). The fossil and living Hyaenidae of Africa: present status. In *Palaeoecology and palaeoenvironments of Late Cenozoic mammals* (pp. 637-659): University of Toronto Press.

Westbury, M. V., Le Duc, D., Duchêne, D. A., Krishnan, A., Prost, S., Rutschmann, S., Grau, J. H., Dalén, L., Weyrich, A., Norén, K., Werdelin, L., Dalerum, F., Schöneberg, T., & Hofreiter, M. (2021). Ecological Specialization and Evolutionary Reticulation in Extant Hyaenidae. *Molecular Biology and Evolution, 38*(9), 3884-3897.

Wilson, D. E., & Reeder, D. M. (2005). *Mammal species of the world: a taxonomic and geographic reference* (Vol. 1): JHU Press.

Yom-Tov, Y. (2003). Body sizes of carnivores commensal with humans have increased over the past 50 years. *Functional Ecology*.

Yom-Tov, Y., & Geffen, E. (2006). Geographic variation in body size: the effects of ambient temperature and precipitation. *Oecologia, 148*(2), 213-218.

Yom-Tov, Y., Heggberget, T. M., Wiig, Ø., & Yom-Tov, S. (2006). Body size changes among otters, *Lutra lutra*, in Norway: the possible effects of food availability and global warming. *Oecologia, 150*(1), 155-160.

Zedrosser, A., Dahle, B., & Swenson, J. E. (2006). Population Density and Food Conditions Determine Adult Female Body Size in Brown Bears. *Journal of Mammalogy, 87*(3), 510-518.

Zelditch, M. L., Swiderski, D. L., & Sheets, H. D. (2012). Geometric morphometrics for biologists: a primer. academic press.

Zuur, A., Leno, E. N., & Smith, G. M. (2007). *Analyzing ecological data*: Springer.

Zuur, A. F., Leno, E. N., & Elphick, C. S. (2010). A protocol for data exploration to avoid common statistical problems. *Methods in Ecology and Evolution, 1*(1), 3-14.

Chapter 3: Cranial shape variation among proposed subspecies of the striped hyena, *Hyaena hyaena*

ABSTRACT

Previous research found that skulls of striped hyenas follow Bergmann's rule, and that they also exhibit slight male-biased sexual size dimorphism. This prompted an investigation into how skull shape may vary with sex and geographic location. Geographically distinct subspecies designations can serve as initial categorizations for inferring the influence of ecological and evolutionary processes across geography. In this study, we investigate whether the geographic pattern of skull shape variation in striped hyenas supports the historic delineation of subspecies proposed by Pocock (1934), and whether skull shape is sexually dimorphic in striped hyenas using 2D landmark-based geometric morphometrics. The influence of sex, size, and subspecies on shape was assessed using Procrustes ANOVAs. We found no evidence for sexual shape dimorphism in the skull of striped hyenas. Striped hyenas vary in skull morphology across their range, but historic subspecies do not effectively capture this variation. We found a more robust morphology with adaptations that would facilitate subduing large struggling prey in northern subspecies of striped hyena; this pattern is consistent with morphological expectations based on anecdotal information on dietary differences across the species range. Future studies should examine morphological and genetic data from across the geographic range of the striped hyena to assess population structure and inform conservation decisions in regard to this declining species.

1| INTRODUCTION

Populations of a species that exhibit marked variation in form are often classified into subspecies (Haig et al., 2006; Mayr, 1942; Wilson & Brown Jr, 1953). Since subspecies share a similar phylogenetic history, the differences between them are usually interpreted as results of adaptation to local conditions. Indeed, comparative studies of subspecies have illuminated how local conditions and selection pressures influence the evolution of morphology (Caumul & Polly, 2005), sexual dimorphism (Frey & Riede, 2013), behavior (Fujii et al., 2015), diet (Mitchell et al., 2020) and phenotypic plasticity (Cheviron et al., 2013). Subspecies designations provide a foundation for inferring the influence of ecological and evolutionary processes across vast spatial scales, which is especially valuable for making predictions about variation in species with extensive geographic ranges or that include populations occupying inaccessible areas.

In this study, we examine variation in skull morphology among populations of the striped hyena (*Hyaena hyaena*), one of four extant species in family Hyaenidae. Striped hyaenas have an extensive geographical range spanning three continents, from India to the Atlantic coast of Africa, and from Tanzania to Nepal (Figure 3.1) (AbiSaid & Dloniak, 2015a). Across this range, striped hyenas experience a temperature gradient of from -3.4°C to 43.5 °C, and precipitation ranging from 0 mm to 504 mm (Fick & Hijmans, 2017; O'Donnell & Ignizio, 2012). These varying conditions are associated with 11 unique vegetation types and extreme diversity in the ecological communities in which striped hyenas occur (Mayaux et al., 2004).

Although striped hyenas are currently considered monotypic (Wilson and Reeder, 2005), researchers have noted sufficient morphological and behavioral variations among populations to propose subspecific classifications (Pocock, 1934; Rieger, 1979). In the most rigorous

taxonomic analysis to date, Pocock (1934) evaluated all proposed striped hyena subspecies using data collected from every striped hyena specimen then in the British Museum as well as measurements and descriptions from the literature (n=63). Using linear skull and tooth measurements, and pelage characteristics, he condensed the large number of previously named subspecies into just five: *H. h. barbara, H. h. dubbah, H. h. syriaca, H. h. indica, and H. h. sultana*.

Rieger (1979) reexamined striped hyaena taxonomy using information gleaned from the literature, including data from Pocock (1934). He focused on skull dimensions (i.e., total skull length and zygomatic width, n=64), as well as behavioral and ecological data, and concluded that Pocock's (1934) five subspecies should be collapsed into two: a 'northern' form (including *H. h. barbara, H. h. syriaca, and H. h. indica*) and a 'southern' form (including *H. h. dubbah and H. h. sultana*). Rieger (1979) did not formally change the existing subspecies or provide explicit geographical ranges for his proposed northern and southern forms, describing them only as larger in the north and smaller in the south. The most recent formal taxonomy for Class Mammalia, Wilson and Reeder (2005), did not recognize any striped hyena subspecies, arguing simply that 'previous morphological (Pocock, 1934) and molecular studies (Jenks & Werdelin, 1998) are not sufficient' for their recognition. It is worth reexamining the extent to which historic subspecies delineations, especially those proposed by Pocock (1934), align with morphology as this could inform future studies of the species and impact future conservation decisions.

We focus on variation in skull morphology among adult striped hyenas. The mammalian skull is a complex multipurpose structure; it serves as a feeding apparatus and houses the brain and sensory organs. This places it under strong selective pressure, which makes it useful for exploring species' ecology and evolution (Cheverud, 1982; Machado et al., 2018). Striped hyenas, along with their closest living relatives (spotted hyenas, *Crocuta crocuta*, and brown hyenas, *Hyaena brunnea*), are of special interest because they are durophagous, able to break open large bones to access the marrow within. Features associated with durophagy include robust and reduced dentition with specialized enamel (Ungar, 2010), a vaulted forehead, a pronounced sagittal crest, wide zygomatic arch breadth, increased cortical thickness of the dentary bone, and large jaw adductor muscles (Tanner, Zelditch, Lundrigan, & Holekamp, 2010; Van Valkenburgh, 2007).

Striped hyenas are opportunistic omnivores reported to feed on insects, small mammals, birds, fish, tortoises, crocodiles, dogs, wild ungulates, primates, livestock, human remains, bones, seeds, leaves, and fruits (Bhandari et al., 2020; Kruuk, 1976; Leakey et al., 1999; Wagner, 2006). Striped hyenas usually forage alone, scavenging carrion or opportunistically taking small prey (Mills & Hofer, 1998). Anecdotal evidence reported in Reiger (1979) suggests that 'northern' striped hyenas are active hunters, regularly killing livestock larger than themselves. If this hunting hypothesis were true, the 'northern' form would contrast with the 'southern' form in East African striped hyenas (*H. h. dubbah*) which occasionally hunt livestock smaller than themselves (young goats and sheep) (Leakey et al 1999), but feed largely on scavenged carcasses, insects, fruit, and small vertebrate prey (Kruuk, 1976). While dietary data are available for only a small fraction of the current range of striped hyenas, there is some

material evidence that diet varies geographically, as feces of individuals from the Indian subcontinent (*H. h. indica)* are very white, indicating high amounts of ingested bone (Prater, 1965), while feces of *H. h. dubbah* in the Serengeti are not as white, and based on chemical analysis, contain significantly less calcium than feces of spotted hyenas inhabiting the same area (Kruuk, 1976).

Mechanical demands of different diets are reflected in masticatory morphology. If Reiger (1979) is correct that striped hyenas in 'northern' populations (in contrast to 'southern' ones) regularly capture and kill prey larger than themselves, we expect enhancement of the temporalis muscles (to increase bite strength) and neck muscles (for large prey manipulation) in those individuals. These changes in musculature would manifest on the skull as a more pronounced sagittal crest, providing increased surface area for temporalis muscle attachment, and a more prominent nuchal crest, to accommodate enlarged neck muscles (Brassard et al., 2020; Curth et al., 2017; Figueirido et al., 2011; Hoshi, 1971). In addition, the jaw joint would need to be exceptionally stable in the 'northern' form, manifest by an occlusal plane situated at the level of the condyloid process, restricting lateral movement of the mandible.

In this study, we assess whether the five subspecies proposed by Pocock (1934) are supported by skull morphology. A previous examination of skull size variation in striped hyenas concluded that striped hyenas follow Bergmann's rule, i.e. larger individuals are found at higher latitudes, and exhibit slight male-biased sexual size dimorphism (Cavalieri Chapter 2). Here we examine skull shape variation using the same specimens, a large sample of adult striped hyena skulls from museum collections. We use geometric morphometrics to investigate the influence of sex on skull shape, evaluate skull shape allometry, and determine to what extent subspecies

delineations proposed by Pocock (1934) explain the observed patterns of variation. Finally, we ask whether patterns of shape variation among historic subspecies correspond to morphological predictions based on diet.

2 | MATERIALS AND METHODS

2.1 | Specimens

The sample comprised 126 adult striped hyena skulls (48 females, 51 males, 27 sex unknown), obtained from 14 natural history collections (APPENDIX B). Adult maturity was defined by complete, or nearly complete, closure of the lambdoid and basilar sutures and full eruption of permanent teeth. Specimens were collected from the field between 1902 and 2008. The sample includes individuals from 20 countries, stretching north to south from the Himalayas to Tanzania, and west to east from Algeria to India (Figure 3.1). The distribution of collection localities covers much of the current geographic range of *H. hyaena*, including areas where it appears to have been recently extirpated (IUCN Red List, 2017). However, samples sizes are small from west Africa, Europe and the Arabian Peninsula. Associated data for each specimen, including date of collection, locality, and sex (determined at the time of collection), were obtained from museum records. Specimens without associated geographic coordinates were georeferenced from specimen locality data using established guidelines from Chapman and Wieczorek (2006) and the georeferencing software GEOLocate Web Application (Rios, 2019).

2.2 | Morphological Data

Skulls were photographed using a digital camera in three views: ventral cranium, lateral cranium, and lateral mandible (Figure 3.2). Images of the cranium in ventral view were obtained by orienting specimens with the palate parallel to the photographic plane, in lateral view by orienting the mid-sagittal plane parallel to the photographic plane, and in lateral view of the mandible by orienting the long axis of the dentary parallel to the photographic plane. A 10-mm scale was included in all photographs.

To quantify skull shape, we used 2D landmark-based geometric morphometrics. Landmarks and semilandmarks were selected to capture the complex curvature and overall shape and size of the cranium and mandible (Zelditch et al., 2012). Landmarks and semilandmarks (Figure 3.2 APPENDIX C) were digitized by the same observer (CNC) using tpsDig2.32 (Rohlf, 2015; Zelditch, Swiderski, & Sheets, 2012). Landmarks were digitized on both sides, but to avoid inflating degrees of freedom the coordinates for bilaterally homologous landmarks were reflected and averaged by performing an analysis for bilaterally symmetric objects using the function bilat.symmetry in the R package 'geomorph' (Klingenberg, Barluenga, & Meyer, 2002; Zelditch et al., 2012). Landmarks were superimposed by generalized procrustes analysis (GPA) and by sliding semilandmarks to minimize bending energy using the 'geomorph' package in R version 3.3.2 (R Core Team, 2017) (Adams, Collyer, & Sherratt, 2015; Adams & Otárola-Castillo, 2013; Bookstein, 1997; Green, 1996; Zelditch et al., 2012). We used centroid size to quantify skull size as it better captures the overall size of an object than linear measurements. Centroid size is the square root of the summed squared distances of each landmark from the centroid of the landmark configuration (Zelditch et al., 2012).

2.3 | Subspecies Designation

Skulls were assigned to one of five subspecies following the detailed geographic information provided by Pocock (1934). In this study, we strictly followed Pocock's (1934, p. 819-820) geographic descriptions when labeling subspecies. This proved challenging due to changing country borders and antiquated geographical regions, such as Asia Minor and Persian Mesopotamia, whose geographic boundaries are vastly different depending on when and which scholar drew the map (Bausani, 1971; Kia, 2016). There were two skulls from modern-day Egypt

that fell just outside of Pocock's range maps; those were assigned to the subspecies *H. h. dubbah*, as it is the closest subspecies geographically.

As Rieger's (1979) coalescence of striped hyenas into 'northern' (*H. h. barbara, H. h. syriaca, and H. h. indica*) and 'southern' (*H. h. dubbah and H. h. sultana*) subspecies does not represent a novel geographic delineation it was not included in the Procrustes ANOVA. Shape variation of subspecies designated by (Rieger, 1979) can be interpreted visually by looking at figures labeled with Pocock's (1934) subspecies designations.

2.4 | Statistical Analysis

The magnitude of sexual shape dimorphism was assessed first to determine if sexes should be treated separately or could be pooled to increase statistical power. For each view, and all known-sex individuals, we performed a Procrustes ANOVA with residual randomization using procD.lm in the 'geomorph' package, where Procrustes shape variables were treated as the response variable and sex was treated as the independent variable. Sex was not a significant predictor of striped hyena skull shape (Table 3.1), thus males, females, and individuals of unknown sex, were pooled in all subsequent analyses.

The influence of size and subspecies on shape was assessed by performing a Procrustes ANOVA using the procD.lm function in the 'geomorph' package with residual randomization, a Type I sums of squares, and 999 iterations for significance testing (Adams, Collyer, Kaliontzopoulou, & Sherratt, 2021). Procrustes shape variables were treated as the response variables, and log centroid size, subspecies (as described by Pocock 1934), and the interaction of log centroid size and subspecies, were treated as the independent variables. Log centroid

size (to control for the effect of size on shape) was the first parameter in the model, as Type I sums of squares is sensitive to the order in which parameters are entered (Zelditch et al., 2012). To check that assumptions of models were met, we used diagnostic plots from the R package 'base.' Model performance was evaluated using R^2. All model analyses were performed in R version 4.0.2 (2020-06-22) (R CORE TEAM, 2020).

To investigate allometry, a regression of shape onto size was plotted using standardized shape scores from the regression as a function of log centroid size for each view of the skull using the plotAllometry function in the 'geomorph' package. Principal Components Analyses was used to explore patterns of shape variation among the subspecies described by Pocock (1934). For each view of the skull, a between-group principal component analysis (bgPCA) with 10,000 permutations was performed using Procrustes shape coordinates with subspecies as a grouping variable (Cardini & Polly, 2020; Mitteroecker & Bookstein, 2011). To assess the reliability of the between group principal component analysis cross-validation scores and percent overall classification accuracy were calculated for subspecies designated by Pocock (1934) (Mitteroecker & Bookstein, 2011). To visualize morphospace occupation by subspecies, the first two principal components of the PCA were plotted with minimum convex hulls of subspecies groupings. All maps were created in ArcMap 10.6 (Esri, 2018) using a Mollweide projection.

3 | RESULTS

3.1 | Sexual Dimorphism

Sex was not a significant predictor of shape for any view of the striped hyena skull (Table 3.1). Male, female, and individuals of unknown sex were pooled in subsequent analyses as there is no evidence to suggest that striped hyenas exhibit sexual shape dimorphism of the skull.

3.2 | Procrustes ANOVA

Procrustes ANOVA showed that striped hyenas have significant skull shape variation associated with size and that shape varies significantly among the 5 subspecies described by Pocock (Table 3.2). Log centroid size was a significant predictor of skull shape for all three views ($p = 0.001$, Table 3.2). The largest percentage of shape variation ($R^2 = 21.9\%$) was explained by log centroid size for the lateral cranial view. Log centroid size explained less of the shape variation for the ventral cranium ($R^2 = 11.5\%$) and mandible view ($R^2 = 5.2\%$) of the skull.

Subspecies described by Pocock was also a significant predictor of skull shape for all three views ($P=0.001$, Table 3.2), explaining almost 19% of shape variation in the lateral view of the skull, and lower percentages for ventral ($R^2 = 11.9\%$) and mandible ($R^2 = 16.9\%$) views. The interaction between log centroid size and the subspecies described by Pocock was marginally significant for both the ventral cranium ($p = 0.041$) and mandible ($p = 0.029$) views, but not significant for lateral cranium ($p = 0.687$). The very low R^2 values for the interaction between the log centroid size and subspecies for the ventral cranium ($R^2 = 2.9\%$) and the mandible ($R^2 = 4.3\%$) indicate that the interaction of these factors is not an important predictor of skull shape.

3.3 | Allometry

There is a strong linear pattern of size-shape covariation (allometry) for the ventral view of the cranium (Figure 3.3). The most notable size-related shape change is in skull breadth: larger individuals in this view tend to have relatively wider zygomatic arches and a broader palate (Figure 3.2 and 3.3). The regression of ventral shape onto size (Figure 3.3) indicates that *H. h. dubbah* tends toward smaller individuals for this view, while *H. h. syriaica* is represented mostly by larger individuals. The other subspecies are interspersed between *H. h. dubbah* and *H. h. syriaica*.

The lateral cranium also shows a strong linear pattern of size-shape variation, although none of the subspecies described by Pocock are well differentiated in this view (Figure 3.5). The most striking allometric shape change coincides with the site of origin on the cranium of the largest masticatory muscle, the temporalis. Smaller individuals have a dome-shaped forehead and a relatively small sagittal crest, while in larger individuals the forehead slopes more gradually and the sagittal crest is more pronounced, with parietal and interparietal bones extending well posterior to the occipital condyle. Additionally, the squamosal portion of the zygomatic arch is more strongly vaulted in smaller individuals than in larger conspecifics. Of the five subspecies described by Pocock *H. h. indica* is the only one showing any tendency to cluster (Figure 3.5). This lack of a clear allometric pattern among subspecies described by Pocock is not unexpected as the interaction of log centroid size and subspecies described by Pocock was not a significant predictor of shape variation in the Procrustes ANOVA for this view of the skull.

Although log centroid size was a significant covariate of shape variation for the mandible view ($p = 0.001$), there is not a clear linear pattern of size-shape covariation (Figure 3.7). This is

not surprising given the low explanatory power of log centroid size (R^2 = 5.2%) for this view. The subspecies described by Pocock form loose clusters that are almost entirely overlapping. The body of the mandible tends to be deeper and more robust in smaller individuals. In larger individuals the ventral margin of the body of the mandible is strongly curved and the angular process of larger individuals is relatively longer and often strongly curved (Figure 3.7).

3.4 | Principal Components Analysis

The principal components analysis for ventral view shows *H. h. dubbah* and *H. h. syriaica* occupying opposite ends of shape space but overlapping with each other and all other subspecies to a considerable degree (Figure 3.4). Higher scores for PC1 and PC2 indicate individuals with a relatively wider palate and broader zygomatic arches, the same morphological features that characterized larger (versus smaller) individuals for ventral view in the analysis of allometry (Figure 3.3). The intersection in shape space of *H. h. dubbah* and *H. h. syriaica* in the ventral crania is not the result of individuals collected from areas of integration between the subpopulations, as *H. h. dubbah* individuals positioned within the *H. h. syriaica* convex hull were collected in Kenya (Figure 3.4).

Subspecies overlap in shape space is also high for the lateral cranium view (Figure 3.6). However, in this view PC1 explains more than 44% of the variance and separates 11 hyenas from the Indian subcontinent (i.e., *H. h. indica*) from all others. These hyenas are characterized by a forehead that slopes gradually (i.e., not dome-shaped) and parietal and interparietal bones extending well posterior to the occipital condyle, the same characteristics are evident in individuals with a large centroid size for this view (Figure 3.5). The deep projections of two *H. h. dubbah* individuals into lateral crania shape space occupied by *H. h. syriaica* are not

subspecies classification errors but appears to be the result of similarities in shape of individuals near the shared boundary of these two subspecies (Figure 3.6). Pocock (1934) identifies Syria, Asia Minor, Transcaucasia and Persian Mesopotamia as geographic boundaries for *H. h. syriaica*; even the most generous maps of Asia Minor and the Persian Empire do not show them extending to the southern portion of the Sinai Peninsula (Bausani, 1971; Düring, 2010; Kia, 2016). Reassigning their subspecies would not effectively reduce the amount of shape space overlap between *H. h. dubbah* and *H. h. syriaica*, as individuals from Israel also project deeply into *H. h. dubba*h shape space.

The principal components analysis for mandible view is similar to the one for ventral view in that *H. h. dubbah* and *H. h. syriaica* occupy opposite ends of shape space but overlap extensively with each other and with all other subspecies (Figure 4). The highest values on PC1 (25% of variance) are held by a small number of H. h. dubbah with a short straight angular process and more posteriorly curved coronoid and condyloid process. Individuals representing *H. h. syriaca* have relatively high values for PC2, reflecting the anteriorly positioned coronoid process, and longer angular process. The intersection of *H. h. dubbah* and *H. h. syriaica* in mandible shape space is similar to that found in the ventral crania with *H. h. dubbah* individuals collected in Kenya and Tanzania positioned within the *H. h. syriaica* convex hull (Figure 3.4 and 3.8).

3.5 | Cross validation and overall classification accuracy

The overall classification accuracy for subspecies described by Pocock was moderately accurate (Table 3.3). The ventral crania had the highest classification accuracy (84.13%), while the mandible had the lowest classification accuracy (69.92%). Subspecies with small sample

sizes, *H. h. barbara* and *H. h.* sultana, were misclassified more often than subspecies with larger sample sizes.

4 | DISCUSSION

This study is the first to quantify and evaluate the geographical pattern of skull shape in striped hyenas. This is the largest sample of striped hyena skulls ever assembled and the only study of variation in striped hyena skulls that does not rely on measurements from the literature. Two historic subspecies classifications based on skull size have been proposed for striped hyenas. Neither Pocock's (1934) nor Reiger's (1979) subspecies classification is strongly supported by the data. However, our results demonstrate the existence of a geographic pattern in striped hyena skull shape. This pattern should be further investigated with additional samples from North-West Africa and the Arabian Peninsula and genetic data from across the species range.

4.1 | Sexual Dimorphism

This is the first study of sexual shape dimorphism in striped hyenas. We found no evidence of sexual shape dimorphism in the skull of striped hyenas. Sexual shape dimorphism has been documented in many carnivorans, but is not as well studied as size dimorphism because most studies rely on linear measurements (Christiansen & Harris, 2012; Law & Mehta, 2018; MacLeod & Horwitz, 2020; Jeremy S Morris & Brandt, 2014; J. S. Morris & Carrier, 2016; Rezić et al., 2017). The lack of sexual shape dimorphism in this study is not surprising. Previous studies found very limited male-biased sexual size dimorphism (Cavalieri Chapter 2) and there are no reports of feeding differences between males and females, thus there is no reason to expect differences in skull shape based on niche differentiation (Shine, 1989).

4.2 | Allometry and Subspecies designation

Shape change associated with change in size (allometry) has been well documented in mammals (Cardini & Polly, 2013; Klingenberg, 2016; Mitteroecker, Gunz, Windhager, & Schaefer, 2013). The presence of allometry can account for a large proportion of morphological variation (Cardini, 2019), which is why we included it as the first term in the Procrustes ANOVA. We found a significant allometric signal for all views of the striped hyena skull, and size explained more of the shape variation than subspecies in lateral cranium view. In that view, individuals with small centroid size have a dome-shaped forehead and a relatively small sagittal crest, while in larger individuals the forehead slopes more gradually and the sagittal crest is more pronounced, with parietal and interparietal bones extending posteriorly (Figure 3.5). Hyenas representing the Indian subcontinent (i.e., *H. h. indica*) fall most clearly into the latter group, although there is overlap with other subspecies. A similar cranial allometric shape difference was found between subspecies of another durophagous carnivoran, the sea otter (*Enhydra lutris*). The southern sea otter, *E. l. nereis*, is larger in lateral view centroid size, with a taller braincase at the midpoint, larger sagittal and lambdoidal crests, and deeper, more robust zygomatic arches than the northern sea otter, *E. l. kenyoni* (Campbell & Santana, 2017). Campbell and Santana (2017), suggest that this robust morphology allows southern sea otters to procure a greater diversity of food, thus increasing their access to food resources. We may be seeing a similar pattern in striped hyenas in which individuals with a more robust morphology may be more capable of subduing large-bodied prey, thus increasing resource access. These shape-size changes appear to be especially associated with a durophagous skull

morphology, as they have not been observed in other intraspecific allometric comparisons within Carnivora (Machado & Teta, 2020; Suzuki, Abe, & Motokawa, 2012).

Variation in ventral view mirrors that of lateral view in that larger centroid size is associated with a more robust morphology, in this case characterized by greater breadth of the palate and zygomatic arches. However, in this view the largest individuals are represented by *H. h. syriaica* and the smallest by *H. h. dubbah* (Figure 3.3). Rieger (1979) based his subspecies designations mainly on differences in total skull length and zygomatic width, which are best captured by our ventral view analyses. His classification is consistent with our data in that *H. h. syriaca* and *H. h. dubbah* fall into 'northern' (larger size) and 'southern' (smaller size) groups, respectively. However, these overlap extensively, and the other 'northern' and 'southern' taxa have intermediate scores for both size (Figure 3.3) and shape (Figures 3.4).

Hollister (1918), noted differences in alignment of the upper premolars in striped hyenas from Kenya (n=11) compared to those from Eritrea and Northwestern Somalia (n=2). The Kenyan hyenas had upper premolars arranged in a nearly straight line, in association with a gradual broadening of the maxilla, whereas in individuals from Eritrea and northwestern Somalia, the second premolar turned diagonally, tracking an abrupt widening of the maxilla at that location. Pocock (1934) investigated this phenomenon in his own sample and found the characteristic abrupt widening of the palatal margin to be highly variable, sometimes differing between the left and right side of the same individual. In our larger sample, we did not observe a diagonal placement of the second premolar and did not find a geographic pattern in the abrupt widening of the palatal margin. It may be that the observed differences between the right and left sides of striped hyena skulls are the result of plastic shape change due to chewing

side preference.

Pocock (1934) reported that Satunin (a Russian zoologist in the late 1800s) used the width of the muzzle at the fourth premolar to distinguish striped hyenas from Transcaucasian (Armenia, Georgia, and Azerbaijan), which have a relatively broader muzzle, from individuals from Persian Mesopotamia. While we did not have samples from Transcaucasia, we did find a similar pattern with *H. h. syriaca* individuals from Israel having a broader palate than *H. h. indica* from Iran.

Of the three views, mandible was the least informative with respect to correctly distinguishing subspecies as it had the lowest classification accuracy. Log centroid size was a significant predictor of mandible shape indicating an allometric relationship, however it explained very little of shape variation (R^2=0.052). We observed a tendency for smaller striped hyenas from the southern part of range to have a deeper ramus and a higher occlusal plane relative to the condyloid process. The latter may facilitate lateral movements of the mandible and aid in grinding vegetal matter (Hoshi, 1971; L. Radinsky, 1985). The mammalian mandible has been shown to be very plastic (Larsson et al., 2005; Tsolakis, Verikokos, Perrea, Bitsanis, & Tsolakis, 2019), capable of change in shape multiple times within the life of an animal (Mavropoulos, Ödman, Ammann, & Kiliaridis, 2010), and dietary hardness has been shown to have multigenerational effects on the shape of mammalian mandibles (Hassan et al., 2020). Shape variation in striped hyena mandibles may be due to plastic remodeling of the mandible based on dietary experience rather than inheritance of a shape adapted to local conditions.

4.3 | Reiger's hunting hypothesis

Rieger (1979), argued that striped hyenas in the northern part of their range (in contrast

to southern populations) are active hunters of prey larger than themselves. In this study, we found morphological evidence consistent with that hypothesis, i.e. northern individuals of *H. h. barbara, H. h. syriaca, and H. h. indica* had more robust crania than *H. h. dubbah and H. h. sultana* from the south, characterized by wider palate and zygomatic arches, well-developed sagittal crest, and posteriorly extended parietal and interparietal bones. The expanded zygomatic arches and sagittal crest increase surface area for attachment of the masseter and temporalis muscles, resulting in increased bite force and the ability to keep the jaw closed on struggling prey (Radinsky, 1981; Van Valkenburgh, 2007). The extended parietal and interparietal bones increase area for attachment of the splenius, sternocephalicus muscles and trapezius ligament of the neck, permitting larger, stronger muscles in the neck and forelimbs which aid in taking down large struggling prey (Radinsky, 1981; Van Valkenburgh, 1996). Reiger's behavioral data were based on anecdotal observations from the literature, but reveal potential value of examining the relationship between diet and morphology across the range of widely distributed species.

In this study, we investigated whether striped hyena skull shape is sexually dimorphic and whether the geographic pattern of skull shape variation supports the historic delineation of subspecies proposed by Pocock (1934). We found no evidence for sexual shape dimorphism in the skull of striped hyenas. While we found considerable morphological overlap between historic subspecies, some parts of morphological shape space were occupied by a single subspecies, suggesting that striped hyenas vary in morphology across geography, but that historic subspecies are not effectively capturing this variation. We found striped hyena subspecies from the northern part of their range to have a morphology that is robust with

adaptations that would facilitate subduing large struggling prey. This is consistent with morphological expectations based on anecdotal information on dietary differences across their range. We suggest future studies that examine morphological and genetic data from across the geographic range to assess population structure and inform conservation decisions in this declining species.

APPENDICES

APPENDIX A

FIGURES AND TABLES

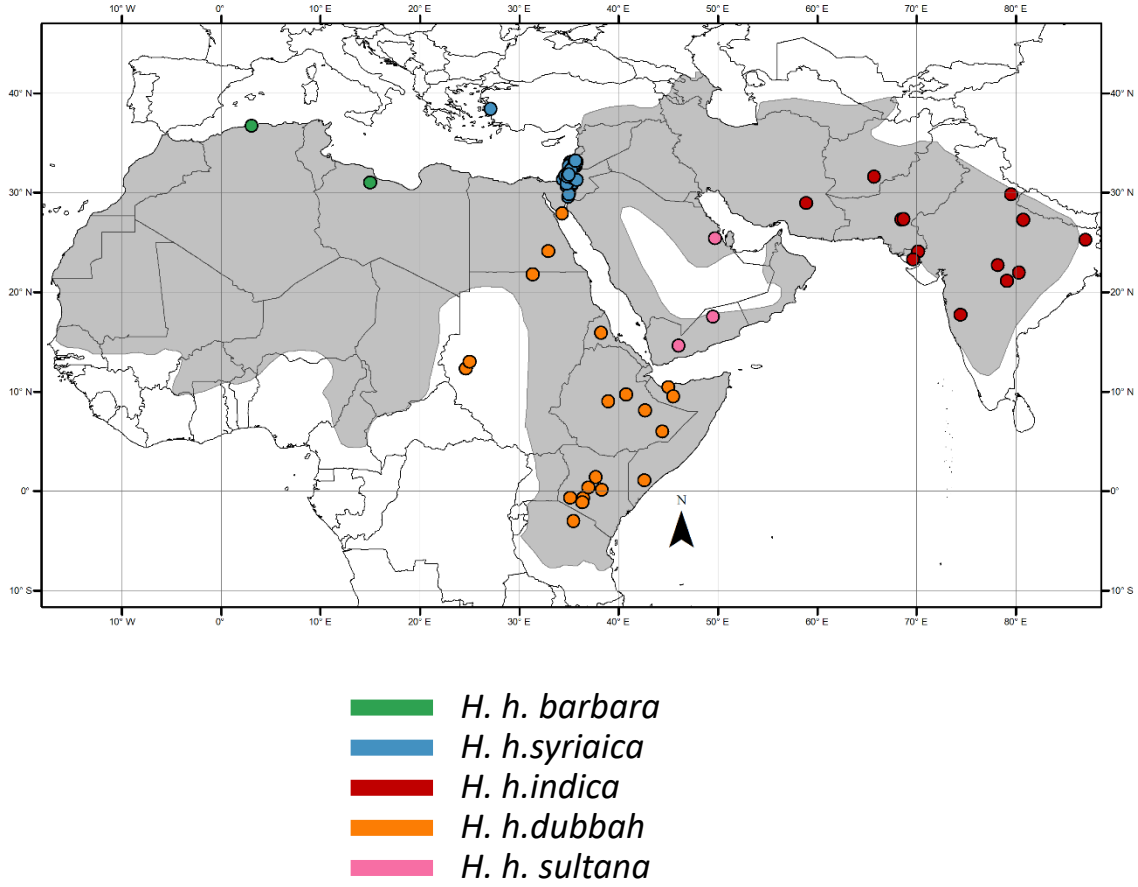

Figure 3.10: Specimen localities for *Hyaena hyaena* skulls used in this study. Point color indicates subspecies designations by Pocock (1932) (*H. h. barbara*,- green, *H. h. syriaca* - blue , *H. h. hyaena* - red , *H. h. dubbah* - orange, and *H. h. sultana* - pink). The current geographical range for the species is highlighted in gray. Decimal latitude and longitude are labeled on the axes.

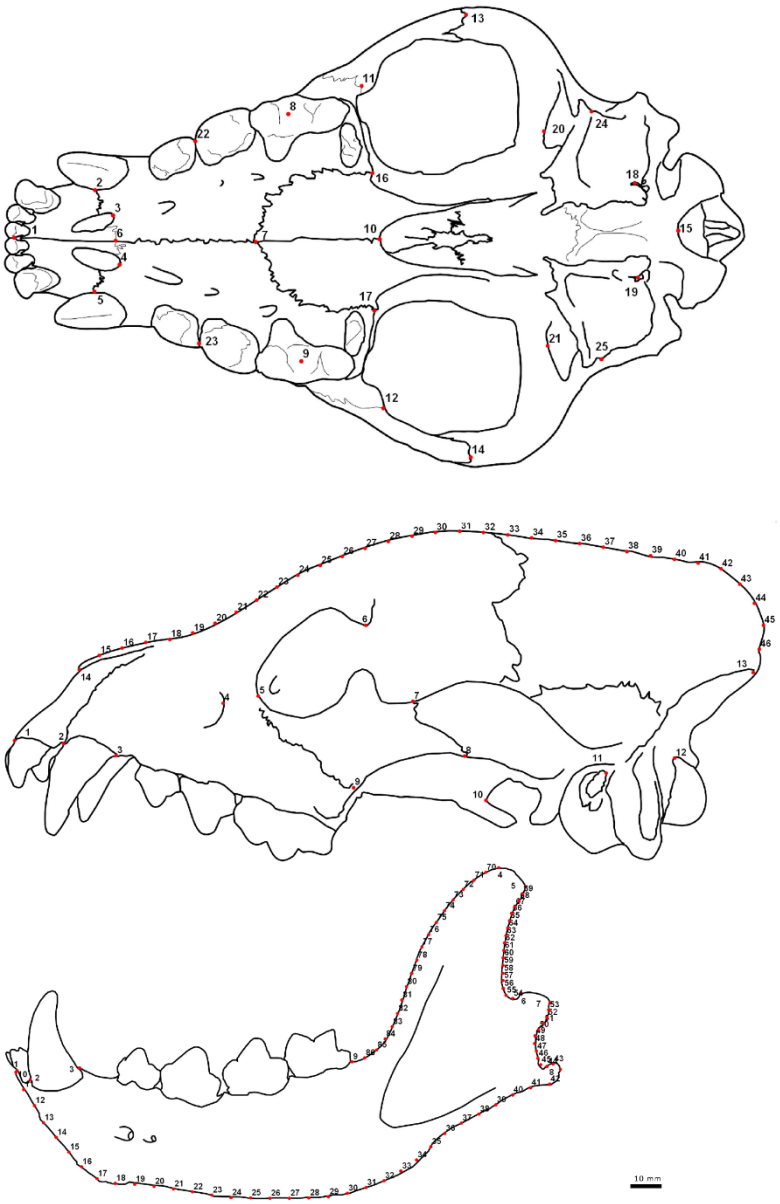

Figure 3.11: Position of landmarks and semilandmarks on a skull of striped hyena (*Hyaena hyaena*) for the ventral cranium, lateral cranium, and mandible.

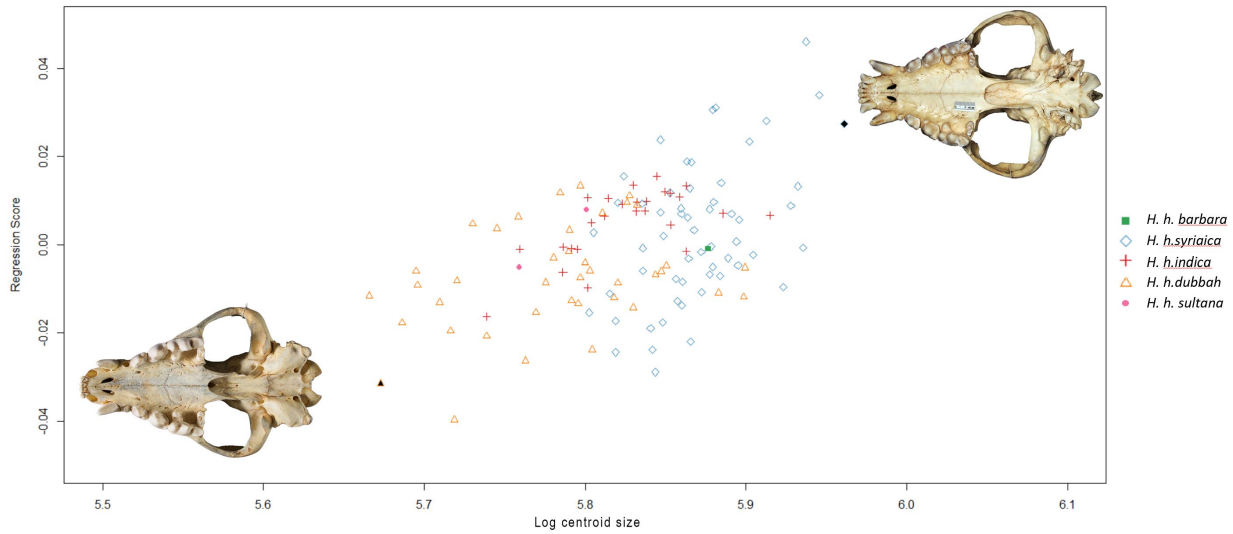

Figure 3.12: Regression of shape onto size. Standardized shape scores from the regression as a function of log centroid size illustrating allometric growth of striped hyena (*Hyaena hyaena*) for the ventral cranium view. Point color and shape indicates subspecies designations by Pocock (1932) (*H. h. barbara*,- green filled square, *H. h. syriaca* – blue open diamond, *H. h. hyaena* – red cross, *H. h. dubbah* – orange open triangle, and *H. h. sultana* – pink filled circle). Photographs of skulls represent shapes at the opposite extremes of the range of allometric variation. Symbols filled with black indicate individual from photograph

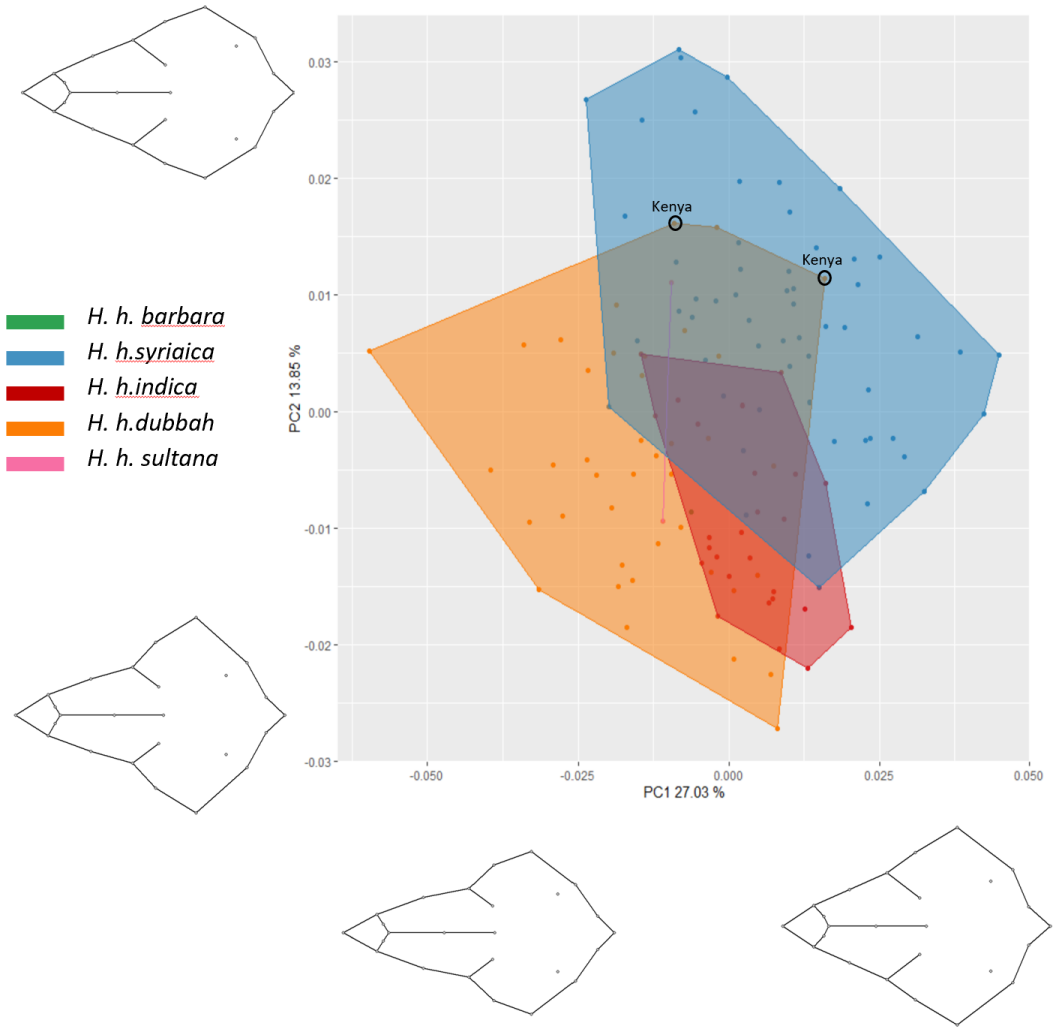

Figure 3.13: Plot of the first two principal components of the PCA based on Procrustes shape coordinates for the ventral cranium of striped hyena (*Hyaena hyaena*). Point color indicates subspecies designations by Pocock (1932) (*H. h. barbara*,- green, *H. h. syriaca* - blue , *H. h. hyaena* - red , *H. h. dubbah* - orange, and *H. h. sultana* - pink). The areas are the convex hulls of the subspecies. The wireframe figures illustrate shape at the minimum and maximum PC scores.

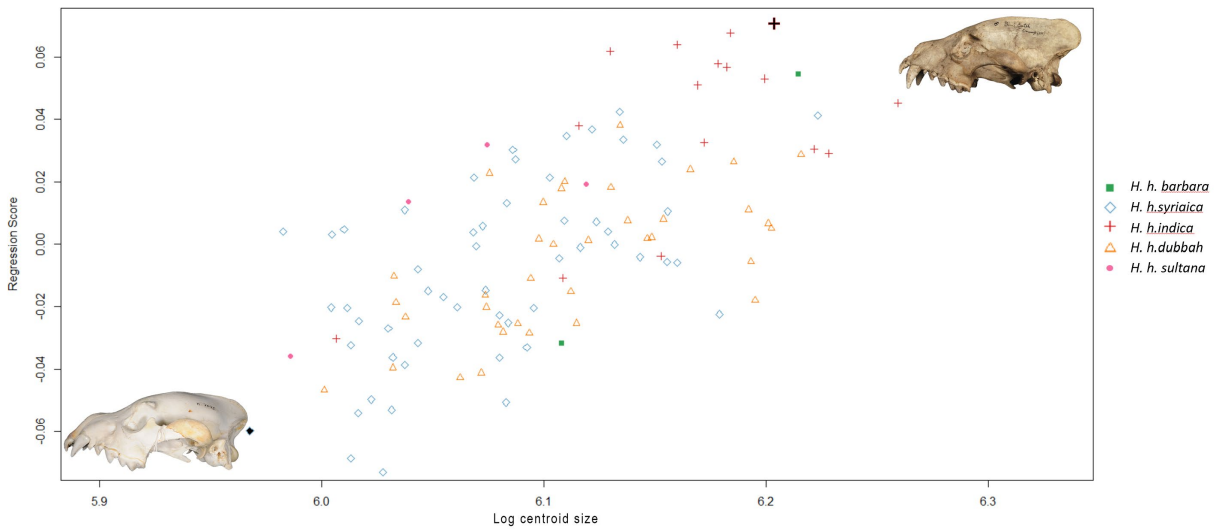

Figure 3.14: Regression of shape onto size. Standardized shape scores from the regression as a function of log centroid size illustrating allometric growth of striped hyena (*Hyaena hyaena*) for the lateral cranium view. Point color and shape indicates subspecies designations by Pocock (1932) (*H. h. barbara*,- green filled square, *H. h. syriaca* – blue open diamond, *H. h. hyaena* – red cross, *H. h. dubbah* – orange open triangle, and *H. h. sultana* – pink filled circle). Photographs of skulls represent shapes at the opposite extremes of the range of allometric variation. Symbols filled with black indicate individual from photograph.

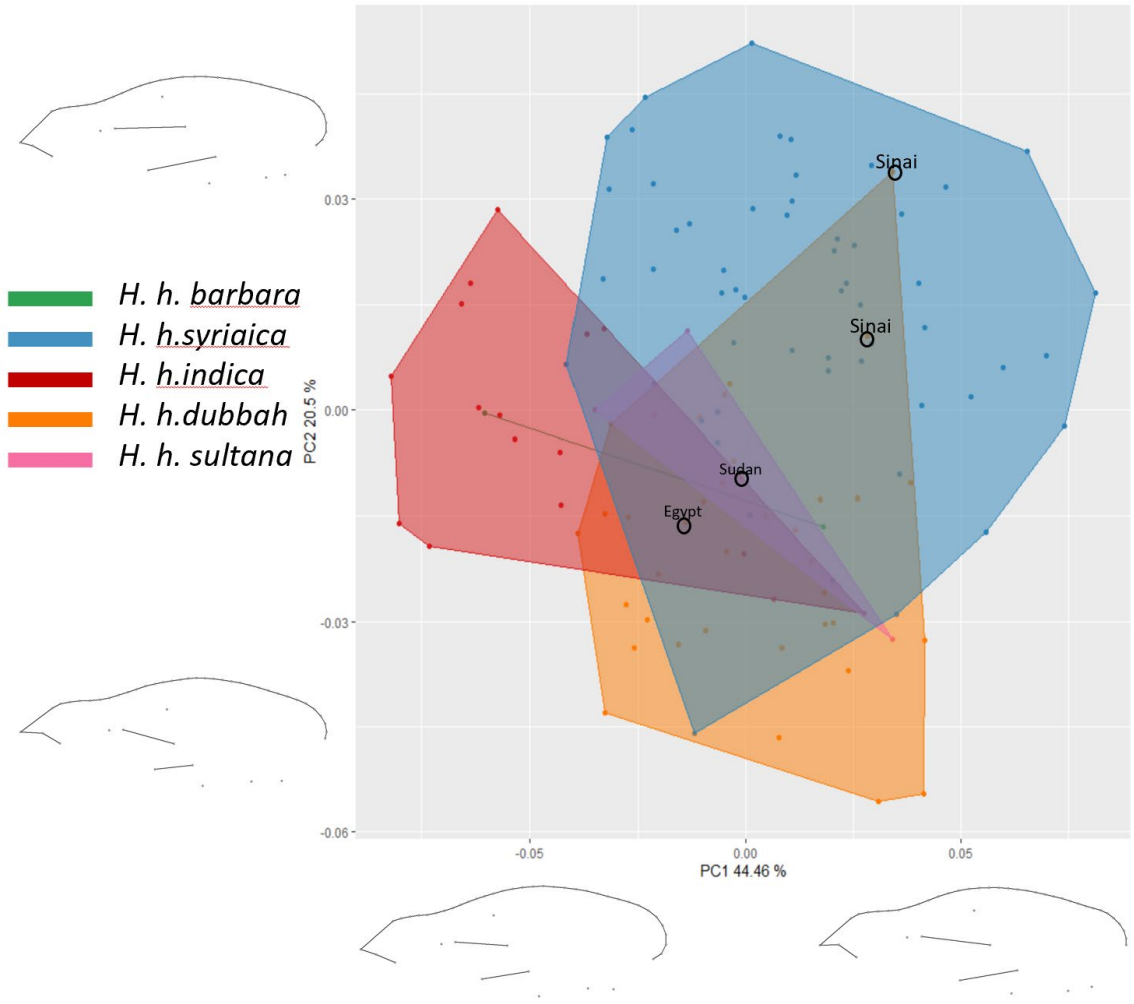

Figure 3.15: Plot of the first two principal components of the PCA based on Procrustes shape coordinates for the lateral cranium of striped hyena (*Hyaena hyaena*). Point color indicates subspecies designations by Pocock (1932) (*H. h. barbara*,- green, *H. h. syriaca* - blue, *H. h. hyaena* - red , *H. h. dubbah* - orange, and *H. h. sultana* - pink). The areas are the convex hulls of the subspecies. The wireframe figures illustrate shape at the minimum and maximum PC scores.

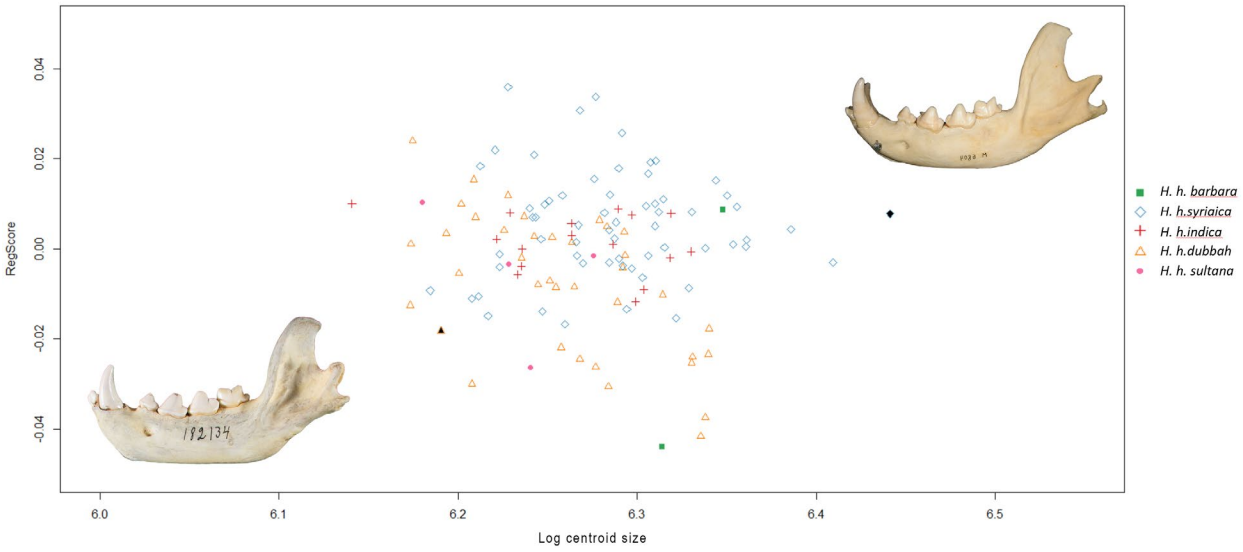

Figure 3.16: Regression of shape onto size. Standardized shape scores from the regression as a function of log centroid size illustrating allometric growth of striped hyena (Hyaena hyaena) for the mandible view. Point color and shape indicates subspecies designations by Pocock (1932) (*H. h. barbara*,- green filled square, *H. h. syriaca* – blue open diamond, *H. h. hyaena* – red cross, *H. h. dubbah* – orange open triangle, and *H. h. sultana* – pink filled circle). Photographs of skulls represent shapes at the opposite extremes of the range of allometric variation. Symbols filled with black indicate individual from photograph.

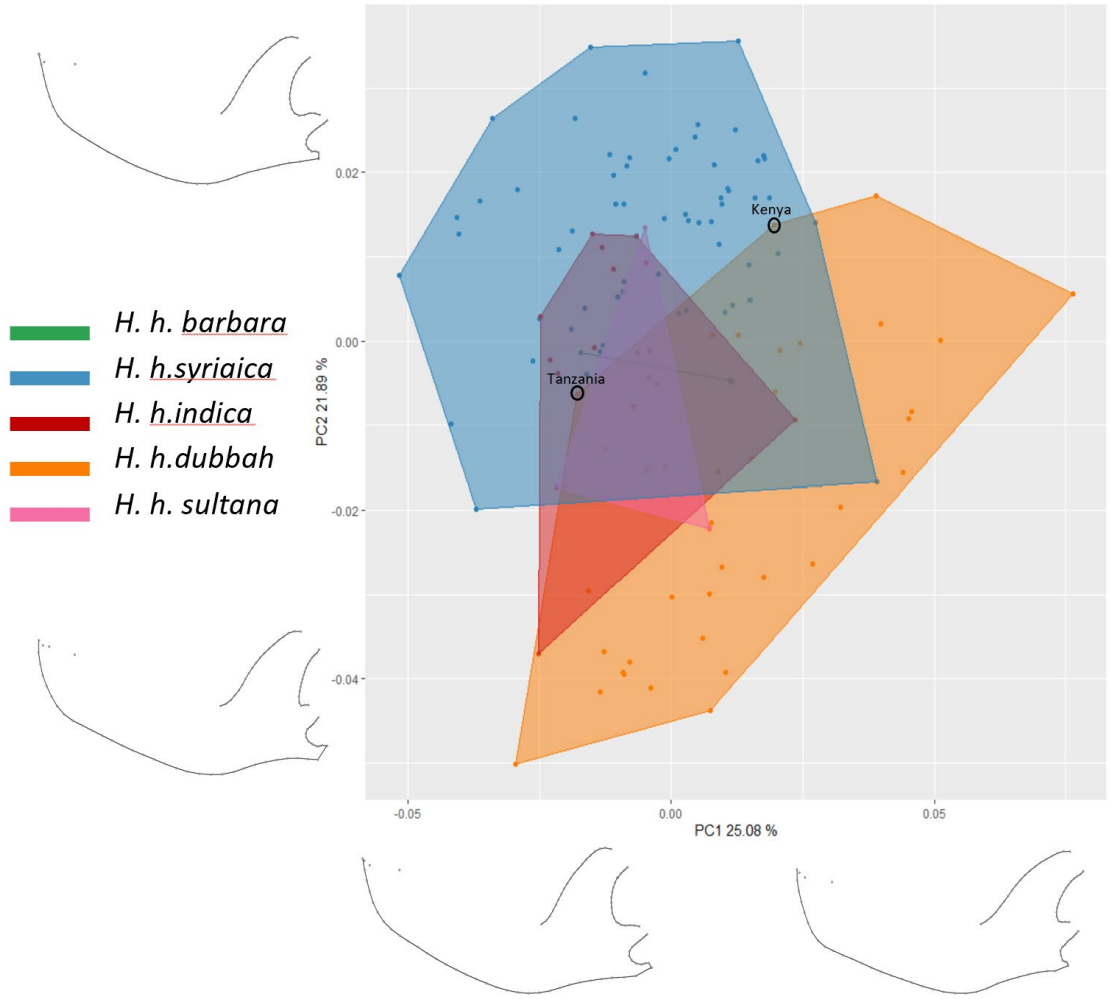

Figure 3.17: Plot of the first two principal components of the PCA based on Procrustes shape coordinates for the mandible of striped hyena (Hyaena hyaena). Point color indicates subspecies designations by Pocock (1932) (*H. h. barbara*,- green, *H. h. syriaca* - blue, *H. h. hyaena* - red, *H. h. dubbah* - orange, and *H. h. sultana* – pink. The areas are the convex hulls of the subspecies. The wireframe figures illustrate shape at the minimum and maximum PC scores.

Table 3.17: Procrustes ANOVAs of shape and sex for the ventral cranium, lateral cranium, and mandible views of *Hyaena hyaena*. The fit of the linear model was evaluated using RRPP. df, degrees of freedom; SS, sums of squares; MS mean square; R2, coefficient of determination; F, F statistic; Z, effect sizes; p, associated probability level. Significance was based on 999 permutations. Significant values indicated with an asterisk, 0 '***' 0.001 '**' 0.01 '*' 0.05 '.' 0.1 ' ' 1.

View	Covariate	Df	SS	MS	R^2	F	Z	p
Ventral	Sex	1	0.001	0.001	0.011	1.121	0.488	0.309
	Residuals	97	0.105	0.001	0.989			
	Total	98	0.107					
Lateral	Sex	1	0.001	0.001	0.007	0.597	-0.608	0.717
	Residuals	90	0.145	0.002	0.993			
	Total	91	0.146					
Mandible	Sex	1	0.003	0.003	0.015	1.467	1.038	0.157
	Residuals	97	0.171	0.002	0.985			
	Total	98	0.173					

Table 3.18: Procrustes ANOVAs of shape, log size and subspecies for subspecies of *Hyaena hyaena* described by Pocock (1934) for the ventral cranium, lateral cranium, and mandible views. The fit of the linear model was evaluated using RRPP. The two fixed factors (log size and subspecies) were allowed to interact with each other. df, degrees of freedom; SS, sums of squares; MS mean square; R2, coefficient of determination; F, F statistic; Z, effect sizes; p, associated probability level. Significance was based on 999 permutations. Significant values indicated with an asterisk, 0 '***' 0.001 '**' 0.01 '*' 0.05 '.' 0.1 ' ' 1.

View	factor	df	SS	MS	R^2	F	Z	p	
Ventral	Log centroid size	1	0.016	0.016	0.115	18.310	6.402	**0.001**	**
	Pocock	4	0.016	0.004	0.119	4.707	7.352	**0.001**	**
	Log centroid size x Pocock	3	0.004	0.001	0.029	1.528	1.699	**0.041**	*
	Residuals	117	0.101	0.001	0.737				
	Total	125	0.137						
Lateral	Log centroid size	1	0.067	0.067	0.219	39.788	5.546	**0.001**	**
	Pocock	4	0.057	0.014	0.189	8.573	7.932	**0.001**	**
	Log centroid size x Pocock	4	0.006	0.001	0.018	0.829	-0.499	0.687	
	Residuals	104	0.174	0.002	0.573				
	Total	113	0.304						
Mandible	Log size	1	0.011	0.011	0.052	7.845	4.244	**0.001**	**
	Pocock	4	0.035	0.009	0.169	6.436	7.045	**0.001**	**
	Log centroid size x Pocock	4	0.009	0.002	0.043	1.635	1.891	**0.029**	*
	Residuals	112	0.154	0.001	0.736				
	Total	121	0.209						

Table 3.19: Cross validation results and overall classification accuracy as percentages for the between group principal component analysis for subspecies of *Hyaena hyaena* described by Pocock (1934).

Ventral overall classification accuracy 84.13%

	barbara	dubbah	indica	sultana	syriaca	total
barbara	100.00	0.00	0.00	0.00	0.00	100
dubbah	0.00	77.50	12.50	2.50	7.50	100
indica	0.00	7.69	92.31	0.00	0.00	100
sultana	0.00	0.00	0.00	100.00	0.00	100
syriaca	0.00	7.02	8.77	0.00	84.21	100

Lateral overall classification accuracy: 72.80%

	barbara	dubbah	indica	sultana	syriaca	total
barbara	0.00	50.00	50.00	0.00	0.00	100
dubbah	10.81	67.57	2.70	13.51	5.41	100
indica	0.00	18.75	81.25	0.00	0.00	100
sultana	0.00	25.00	25.00	50.00	0.00	100
syriaca	0.00	1.82	7.27	12.73	78.18	100

Mandible overall classification accuracy 69.92%

	barbara	dubbah	indica	sultana	syriaca	total
barbara	0.00	0.00	50.00	50.00	0.00	100
dubbah	5.26	71.05	5.26	15.79	2.63	100
indica	12.50	6.25	68.75	6.25	6.25	100
sultana	25.00	25.00	0.00	25.00	25.00	100
syriaca	4.76	3.17	17.46	0.00	74.60	100

APPENDIX B

SPECIMENS LIST

Table 3.20: *Hyaena hyaena* specimens ventral cranium

Hyaena hyaena specimens ventral cranium	
Museum	Catalog Number
OSU	5261
OSU	5585
OSU	5586
OSU	5712
OSU	5758
USNM	163110
USNM	172923
USNM	182034
USNM	182040
USNM	182045
USNM	182047
USNM	182079
USNM	182080
USNM	182086
USNM	182100
USNM	182134
USNM	182135
USNM	182136
USNM	318112
USNM	329351
USNM	523000
TAU	9930
TAU	11821
TAU	11945
TAU	276
TAU	9418
TAU	6640
TAU	594
TAU	7644
TAU	7216
TAU	7238
TAU	7256
TAU	7455
TAU	8666
TAU	9010
TAU	7480
TAU	8294
TAU	7898

Table 3.4 (cont'd)

TAU	7645
TAU	7672
TAU	7217
BMNH	34112814
TAU	9811
TAU	7737
TAU	6140
TAU	7119
TAU	5127
TAU	6510
TAU	10616
TAU	7962
TAU	10617
TAU	11249
TAU	11515
TAU	11130
BMNH	34112813
TAU	11248
NMK	4628
NMK	8297
TAU	10236
TAU	10683
TAU	11533
TAU	11099
TAU	6804
FMNH	140216
FMNH	140218
TAU	11687
BMNH	34112812
BMNH	311210
NMK	3474
TAU	6895
BMNH	39439
BMNH	58624125
TAU	7
TAU	9743
BMNH	3411288
TAU	3316
BMNH	3831388
BMNH	3411283
BMNH	55282

Table 3.4 (cont'd)

BMNH	58209
BMNH	34112810
TAU	2814
BMNH	3411284
BMNH	518251
BMNH	39440
BMNH	3411285
TAU	3597
BMNH	3411286
TAU	12128
TAU	7839
BMNH	23349
BMNH	05121
BMNH	34112811
BMNH	2610873
TAU	9160
MSU	13003
MSU	11143
BMNH	92282
BMNH	2721427
BMNH	521483
BMNH	34847
BMNH	34112818
BMNH	565650
BMNH	34112816
TAU	9739
TAU	6202
TAU	4746
BMNH	2610872
RCSOM	13731
TAU	7813
BMNH [not on tag]	241055
TAU	4376
BMNH	1938101848
BMNH	872412
TAU	8295
FMNH	103991
FMNH	103992
BMNH	2010271
BMNH	231178
TAU	4035

Table 3.4 (cont'd)

BMNH	2010272
BMNH	231179
BMNH	6543
TAU	7618
BMNH	231180
TAU	22
TAU	11846

Table 3.21: *Hyaena hyaena* specimens lateral cranium

Hyaena hyaena specimens lateral cranium	
Museum	Catalog Number
OSU	5261
OSU	5585
OSU	5586
OSU	5712
OSU	5758
USNM	163110
USNM	172923
USNM	182034
USNM	182040
USNM	182045
USNM	182047
USNM	182079
USNM	182080
USNM	182086
USNM	182100
USNM	182134
USNM	182135
USNM	182136
USNM	318112
USNM	329351
USNM	523000
TAU	11821
TAU	11945
TAU	276
TAU	5106
TAU	9418
TAU	6640
TAU	594
TAU	7644
TAU	7216
TAU	7238
TAU	7256
TAU	7455
TAU	8666
TAU	9010
TAU	7480
TAU	8294
TAU	7672

Table 3.5 (cont'd)

TAU	9811
TAU	7217
TAU	7645
TAU	7737
TAU	6140
TAU	7119
TAU	5127
TAU	6510
TAU	10616
TAU	7962
TAU	10617
TAU	11249
TAU	111302
BMNH	34112813
TAU	6677
TAU	11248
NMK	4628
NMK	8297
TAU	10236
TAU	10683
TAU	11533
TAU	11099
FMNH	140216
FMNH	140218
TAU	11687
BMNH	34112812
BMNH	311210
NMK	3474
TAU	6895
BMNH	211225
TAU	71457
TAU	3316
BMNH	34112810
TAU	2814
BMNH	58209
BMNH	518251
BMNH	39440
BMNH	3411285
TAU	3597
BMNH	3411286
TAU	12128

Table 3.5 (cont'd)

BMNH	21142
TAU	7839
BMNH	05121
BMNH	34112811
TAU	9160
TAU	9423
MSU	13003
MSU	11143
BMNH	34846
BMNH	92282
BMNH	2721427
BMNH	521483
BMNH	34847
BMNH	34112818
BMNH	565650
BMNH	34112816
TAU	9739
TAU	6202
TAU	4746
BMNH	2610872
TAU	4376
BMNH	1938101848
BMNH	872412
TAU	8295
FMNH	103991
TAU	103992
BMNH	231178
TAU	4035
BMNH	231179
BMNH	6543
TAU	7618
BMNH	231180
TAU	22
TAU	11846
TAU	6804

Table 3.22: *Hyaena hyaena* specimens mandible

Hyaena hyaena specimens mandible	
Museum	Catalog
OSU	5261
OSU	5585
OSU	5586
OSU	5712
OSU	5757
OSU	5758
USNM	163110
USNM	172923
USNM	182034
USNM	182040
USNM	182045
USNM	182047
USNM	182079
USNM	182080
USNM	182086
USNM	182100
USNM	182134
USNM	182135
USNM	182136
USNM	318112
USNM	329351
USNM	523000
TAU	9930
TAU	11821
TAU	11945
TAU	276
TAU	5106
TAU	9418
TAU	6640
TAU	594
TAU	7644
TAU	7216
TAU	7238
TAU	7256
TAU	7455
TAU	8666
TAU	9010
TAU	7480

Table 3.6 (cont'd)

TAU	7672
TAU	8294
TAU	7898
TAU	7217
TAU	7645
TAU	9811
TAU	7737
TAU	6140
TAU	7119
TAU	5127
TAU	6510
TAU	10616
TAU	7962
TAU	11249
TAU	11515
TAU	11130
BMNH	34112813
TAU	6677
TAU	11248
NMK	4628
TAU	10236
TAU	10683
TAU	11533
TAU	11099
TAU	6804
FMNH	140216
FMNH	140218
TAU	11687
BMNH	34112812
BMNH	311210
NMK	3474
TAU	6895
TAU	8037
TAU	9715
BMNH	153618
BMNH	211225
BMNH	39439
BMNH	58624125
TAU	71457
TAU	3316

Table 3.6 (cont'd)

BMNH	518251
BMNH	55282
BMNH	34112810
TAU	2814
BMNH	58209
BMNH	39440
BMNH	3411285
TAU	3597
BMNH	3411286
TAU	12128
TAU	7839
BMNH	23349
BMNH	05121
BMNH	34112811
BMNH	21142
TAU	9160
TAU	9423
MSU	13003
BMNH	34846
BMNH	92282
BMNH	2721427
BMNH	521483
BMNH	34847
BMNH	34112818
BMNH	565650
BMNH	34112816
TAU	9739
TAU	6202
TAU	4746
BMNH	2610872
RCSOM	13731
TAU	7813
TAU	4376
BMNH	1938101848
BMNH	872412
TAU	8295
FMNH	103991
BMNH	231178
TAU	4035
BMNH	231179
BMNH	6543

Table 3.6 (cont'd)

TAU	22
TAU	7618
BMNH	231180
TAU	11846

APPENDIX C

LANDMARK DEFINITIONS

Table 3.23: Ventral landmarks definitions

Landmark	Definition
1	Juncture between the incisors on the premaxilla
2	Premaxilla-maxilla suture intersection with the medial edge of the left canine
3	Most posterior point of the left incisive foramen
4	Most posterior point of the right incisive foramen
5	Premaxilla-maxilla suture intersection with the medial edge of the right canine
6	Posterior edge of premaxilla-maxilla suture on the palate
7	Center of Maxilla-palatine midline suture
8	Center of left fourth premolar
9	Center of right fourth premolar
10	Posterior edge of the midline suture between the left and right palatine.
11	Most posterior edge of the left maxilla-jugal suture
12	Most posterior edge of the right maxilla-jugal suture
13	Most posterior edge of the left jugal-squamosal suture
14	Most posterior edge of the right jugal-squamosal suture
15	Most anterior point of the foramen magnum
16	Posterior end of the left maxilla-palatine suture
17	Posterior end of the right maxilla-palatine suture
18	Center of left, jugular canal
19	Center of right, jugular canal
20	Most anterior point of left retroarticular process
21	Most anterior point of right retroarticular process
22	Posterior edge of left second premolar
23	Posterior edge of right second premolar
24	Most distal point of the left external auditory meatus
25	Most distal point of the right external auditory meatus

Table 3.24: Lateral Landmarks definations

Landmark	Definition
1	Anterior edge of the third incisor
2	Anterior edge of canine
3	Posterior edge of canine
4	The most posterior part of the infraorbital foramen
5	The intersection of the maxilla, lacrimal and jugal
6	The most lateral projection of post-orbital process
7	Most dorsal anterior part of the squamosal
8	Most ventral posterior part of the jugal
9	The most ventral-posterior point of the jugal-maxilla suture
10	The most posterior edge of the suture of palatine and pterygoid process
11	Suture of the squamosal and occipital inside the auditory meatus
12	Anterior upper edge of the occipital condyle
13	Posterior most edge of the sagittal crest
14	Anterior edge of the nasal-premaxilla suture

32 Semi-landmarks along curve of dorsal cranium, 14 to 13

Table 3.25: Mandible landmarks definitions

Landmark	Definition
1	Anterior edge of third incisor
2	Anterior edge of canine
3	Posterior edge of canine
4	Dorsal apex of the coronoid process
5	Most posterior projection of the coronoid process
6	Anterior edge of the mandibular condyle, distal to the vertical plane of the coronoid
7	Posterior most edge of the mandibular condyle
8	Posterior most point of the articular process
9	Intersection of the mandibular body and ramus
10	Intersection of anterior margin of first incisor with the dentary

32 Semi-landmarks along ventral curve of the mandible, 10 to 8

11 Semi-landmarks along posterior curve between articular process and mandibular condyle, 8 to 7

16 Semi-landmarks along posterior curve between mandibular condyle and coronoid process, 6 to 5

17 Semi-landmarks along anterior curve of ramus, 4 to 9

WORKS CITED

WORKS CITED

Adams, D., Collyer, M., Kaliontzopoulou, A., & Sherratt, E. (2021). Geometric morphometric analyses of 2D/3D landmark data.

Adams, D. C., Collyer, M. L., & Sherratt, E. (2015). Geomorph: Software for geometric morphometric analyses. R package version 2.1.

Adams, D. C., & Otárola-Castillo, E. (2013). geomorph: an R package for the collection and analysis of geometric morphometric shape data. *Methods in Ecology and Evolution, 4*(4), 393-399.

Bausani, A. (1971). The Persians from the earliest days to the twentieth century. St. Martin's Press, New York City, New York.

Bookstein, F. L. (1997). Landmark methods for forms without landmarks: morphometrics of group differences in outline shape. *Medical image analysis, 1*(3), 225-243.

Campbell, K. M., & Santana, S. E. (2017). Do differences in skull morphology and bite performance explain dietary specialization in sea otters? *Journal of Mammalogy, 98*(5), 1408-1416.

Cardini, A. (2019). Craniofacial Allometry is a Rule in Evolutionary Radiations of Placentals. *Evolutionary Biology*.

Cardini, A., & Polly, P. D. (2013). Larger mammals have longer faces because of size-related constraints on skull form. *Nature communications, 4*(1), 1-7.

Cardini, A., & Polly, P. D. (2020). Cross-validated between group PCA scatterplots: A solution to spurious group separation? *Evolutionary Biology, 47*(1), 85-95.

Christiansen, P., & Harris, J. M. (2012). Variation in craniomandibular morphology and sexual dimorphism in pantherines and the sabercat Smilodon fatalis. *PloS one, 7*(10), e48352.

Düring, B. S. (2010). *The prehistory of Asia Minor: from complex hunter-gatherers to early urban societies*: Cambridge University Press.

Esri. (2018). ArcMap: Release 10.6. 1.

Green, W. (1996). *The thin-plate spline and images with curving features.* Paper presented at the Proceedings in image fusion and shape variability techniques.

Haig, S. M., Beever, E. A., Chambers, S. M., Draheim, H. M., Dugger, B. D., Dunham, S., Elliott-smith, E., Fontaine, J. B., Kesler, D. C., Knaus, B. J., & Knaus, B. J. (2006). Taxonomic considerations in listing subspecies under the US Endangered Species Act. *Conservation Biology, 20*(6), 1584-1594.

Hassan, M. G., Kaler, H., Zhang, B., Cox, T. C., Young, N., & Jheon, A. H. (2020). Effects of multi-generational soft diet consumption on mouse craniofacial morphology. *Frontiers in physiology, 11*, 783.

Hollister, N. (1918). East African mammals in the United States National Museum pt. 1: Insectivora, Chiroptera, and Carnivora. *Bulletin of the United States National Museum*, 1–194.

Hoshi, H. (1971). Comparative morphology of the mammalian mandible in relation to food habit. *Okajimas folia anatomica Japonica, 48*(5), 333-345.

Kia, M. (2016). *The Persian Empire: A Historical Encyclopedia [2 volumes]: A Historical Encyclopedia*: ABC-CLIO. Santa Barbara, California.

Klingenberg, C. P. (2016). Size, shape, and form: concepts of allometry in geometric morphometrics. *Development genes and evolution, 226*(3), 113-137.

Klingenberg, C. P., Barluenga, M., & Meyer, A. (2002). Shape analysis of symmetric structures: quantifying variation among individuals and asymmetry. *Evolution, 56*(10), 1909-1920.

Larsson, E., Øgaard, B., Lindsten, R., Holmgren, N., Brattberg, M., & Brattberg, L. (2005). Craniofacial and dentofacial development in pigs fed soft and hard diets. *American journal of orthodontics and dentofacial orthopedics, 128*(6), 731-739.

Law, C. J., & Mehta, R. S. (2018). Carnivory maintains cranial dimorphism between males and females: evidence for niche divergence in extant Musteloidea. *Evolution, 72*(9), 1950-1961.

Machado, F. A., & Teta, P. (2020). Morphometric analysis of skull shape reveals unprecedented diversity of African Canidae. *Journal of Mammalogy*.

MacLeod, N., & Horwitz, L. K. (2020). Machine-learning strategies for testing patterns of morphological variation in small samples: sexual dimorphism in gray wolf (*Canis lupus*) crania. *BMC biology, 18*(1), 1-26.

Mavropoulos, A., Ödman, A., Ammann, P., & Kiliaridis, S. (2010). Rehabilitation of masticatory function improves the alveolar bone architecture of the mandible in adult rats. *Bone, 47*(3), 687-692.

Mayr, E. (1942). Systematics and the origin of species–Columbia Univ. *Press, New York*.

Mills, M., & Hofer, H. (1998). Status survey and conservation action plan. Hyaenas. *IUCN/SSC Hyaena Specialist Group, IUCN, Switzerland*.

Mitteroecker, P., & Bookstein, F. (2011). Linear discrimination, ordination, and the visualization of selection gradients in modern morphometrics. *Evolutionary Biology, 38*(1), 100-114.

Mitteroecker, P., Gunz, P., Windhager, S., & Schaefer, K. J. H., the Italian Journal of Mammalogy. (2013). A brief review of shape, form, and allometry in geometric morphometrics, with applications to human facial morphology. *Hystrix, the Italian Journal of Mammalogy, 24*(1), 59-66.

Morris, J. S., & Brandt, E. K. (2014). Specialization for aggression in sexually dimorphic skeletal morphology in grey wolves (C anis lupus). *Journal of Anatomy, 225*(1), 1-11.

Morris, J. S., & Carrier, D. R. (2016). Sexual selection on skeletal shape in Carnivora. *Evolution, 70*(4), 767-780.

Pocock, R. I. (1934). The Races of the Striped and Brown Hyænas. *Proceedings of the Zoological Society of London, 104*(4), 799-825.

Radinsky, L. (1985). Patterns in the evolution of ungulate jaw shape. *American Zoologist, 25*(2), 303-314.

Radinsky, L. B. (1981). Evolution of skull shape in carnivores: 1. Representative modern carnivores. *Biological Journal of the Linnean Society, 15*(4), 369-388.

Rezić, A., Bošković, I., Lubinu, P., Piria, M., Florijančić, T., Scandura, M., & Šprem, N. (2017). Dimorphism in the Skull Form of Golden Jackals (*Canis aureus* Linnaeus, 1758) in the Western Balkans: A Geometric Morphometric Approach. *Pakistan Journal of Zoology, 49*(3).

Rieger, I. (1979). A review of the biology of striped hyaenas, Hyaena hyaena (Linne, 1758). *Sugetierkundliche Mitteilungen, 27*, 81-95.

Rohlf, F. J. (2015). The tps series of software. *Hystrix, 26*(1), 9-12.

Shine, R. (1989). Ecological Causes for the Evolution of Sexual Dimorphism: A Review of the Evidence. *The Quarterly Review of Biology, 64*(4), 419-461.

Suzuki, S., Abe, M., & Motokawa, M. (2012). Integrative study on static skull variation in the J apanese weasel (Carnivora: Mustelidae). *Journal of Zoology, 288*(1), 57-65.

Tanner, J. B., Zelditch, M. L., Lundrigan, B. L., & Holekamp, K. E. (2010). Ontogenetic change in skull morphology and mechanical advantage in the spotted hyena (*Crocuta crocuta*). *J Morphol, 271*(3), 353-365.

Tsolakis, I. A., Verikokos, C., Perrea, D., Bitsanis, E., & Tsolakis, A. I. (2019). Effects of diet consistency on mandibular growth. A review. *Journal of the Hellenic Veterinary Medical Society, 70*(3), 1603-1610.

Ungar, P. S. (2010). Mammal teeth: origin, evolution, and diversity: Johns Hopkins University Press. Baltimore, Maryland.

Van Valkenburgh, B. (1996). Feeding behavior in free-ranging, large African carnivores. *Journal of Mammalogy, 77*(1), 240-254.

Van Valkenburgh, B. (2007). Déjà vu: the evolution of feeding morphologies in the Carnivora. *Integrative and Comparative Biology, 47*(1), 147-163.

Wilson, E. O., & Brown Jr, W. L. (1953). The subspecies concept and its taxonomic application. *Systematic zoology, 2*(3), 97-111.

Zelditch, M. L., Swiderski, D. L., & Sheets, H. D. (2012). Geometric morphometrics for biologists: a primer. academic press.